

# **Dysregulation of Cationic Channels in Chronic Kidney Diseases**

---

A Dissertation

Presented to

the Faculty of the Department of Biology and Biochemistry

University of Houston

---

In Partial Fulfillment

of the Requirements for the Degree

Doctor of Philosophy

---

By

Hila Roshanravan

May 2016

# **Dysregulation of Cationic Channels in Chronic Kidney Diseases**

---

**Hila Roshanravan**

APPROVED:

---

**Dr. Stuart Dryer, Vice Chair**

---

**Dr. Brigitte Dauwalder**

---

**Dr. Gregg Roman**

---

**Dr. Yanlin Wang**  
**Division of Nephrology – Baylor College of**  
**Medicine**

---

**Dr. Jason Eriksen**  
**College of Pharmacy – University of Houston**

---

**Dean, College of Natural Sciences and**  
**Mathematics**

## ACKNOWLEDGEMENTS

I would like to express sincere gratitude to my mentor Dr. Stuart Dryer for his support and guidance during my stay at his laboratory. His extraordinary ability to think of new ideas and design experiments was fundamental for this dissertation. I also thank Dr. Eunyoung Kim and Dr. Marc Anderson in his laboratory for useful discussions and technical advice. Dr. Eunyoung Kim generated significant portion of data that made much of this dissertation possible. Our meetings and informal discussions were critical for the development of the projects. I would also like to express gratitude to Dr. Brigitte Dauwalder, Dr. Gregg Roman, Dr. Jason Eriksen and Dr. Yanlin Wang for their enthusiasm, love for science, and friendship provided a great atmosphere in the Department of Biology and Biochemistry at the University of Houston and the Division of Nephrology at the Baylor College of Medicine. I would like to thank the members of my committee for providing helpful ideas and constructive comments for this dissertation.

I am enormously grateful with my parents and siblings: Dr. Kambiz Roshanravan, Azar Afrooz, Hooman, Hiva and Ali for their love and encouragement, and my lovely husband Dr. Ali Kahirdeh for his unconditional support.

# Dysregulation of Cationic Channels in Chronic Kidney Diseases

---

An Abstract of a Dissertation

Presented to

the Faculty of the Department of Biology and Biochemistry

University of Houston

---

In Partial Fulfillment

of the Requirements for the Degree

Doctor of Philosophy

---

By

Hila Roshanravan

May 2016

## ABSTRACT

According to the Centers for Disease Control and Prevention, one in 10 American adults, has some level of chronic kidney disease (CKD), a condition characterized by reduced kidney function over time. Although recent research has uncovered many pathways and mechanisms involved in the pathophysiology of kidney diseases, this has not yet led to development of new drugs for the treatment of patients with these conditions. In this dissertation, we introduce two potential therapeutic targets for different forms of CKD. First, we discuss gating properties of the transient receptor potential cationic-6 (TRPC6) channel, then we show dysregulation of this channel in models of focal segmental glomerulosclerosis (FSGS). In a separate chapter, we introduce another channel protein, the N-methyl-D-aspartate (NMDA) receptor, as a potential therapeutic target for treatment of diabetic nephropathy.

Much of this work entailed making whole-cell recordings from highly specialized kidney cells called podocytes. This technique was used to measure TRPC6 channel activity in cells *in vitro*, as well as in *ex vivo* preparations in which podocytes are still attached to the isolated glomerular capillary. Serum samples from a variety of primary FSGS patient groups were obtained from collaborators. We used the sera to treat our cells *in vitro* and investigate the effect of soluble factors in the patients' serum on the activity and expression levels of TRPC6 channels. Regarding the other target, we studied the effect of NMDA inhibitors in alleviating the development of diabetic nephropathy *in vivo*.

I concluded that TRPC6 channels are dysregulated in FSGS. This suggested that further development of TRPC6 inhibitors might be warranted as potential therapeutic

agents. We observed that diabetes caused a marked increase in the expression of renal NMDA receptors, and that sustained treatment with NMDA antagonists reduces the progression of nephropathy in two mouse models of type-1 diabetes. Consequently, it is possible that this class of drugs can be useful for reducing the progression of nephropathy.

# TABLE OF CONTENTS

<b>1. INTRODUCTION .....</b>	<b>1</b>
1.1 Kidney .....	1
1.1.1 Glomerulus .....	2
1.1.2 Podocyte .....	2
1.2 Chronic kidney diseases (CKD).....	3
1.2.1 Focal Segmental Glomerulosclerosis .....	4
1.2.1.1 Pathogenesis/ available treatments .....	5
1.2.1.2 Genetic forms of FSGS.....	6
1.2.1.2.1 <i>Nephrotic Syndrome 2 (NPHS2)</i> gene mutation.....	7
1.2.1.2.2 <i>Transient Receptor Potential Cation-6 (TRPC6)</i> gene mutation .....	7
1.2.2 Diabetic Nephropathy (DN) .....	8
1.2.2.1 Histopathology.....	9
1.2.2.2 Pathophysiologic pathways and available treatments.....	9
1.3 Summary of objectives.....	10
<b>2. MATERIALS AND METHOD .....</b>	<b>12</b>
2.1 Cell Culture protocols .....	12
2.2 Primary isolation of rat glomeruli .....	12
2.3 siRNA knockdown protocol.....	13
2.4 Electrophysiology.....	13
2.5 Immunoblot/cell surface biotinylation assay.....	14
2.6 RNA isolation, reverse transcription, and RT-PCR .....	15
2.7 Histology, immunohistochemistry, and electron microscopy .....	15
2.8 Patient serum and plasma samples .....	18
2.9 Mouse models of type-1 diabetes.....	18
2.10 Chronic puromycin aminonucleoside (PAN) nephrosis.....	19
2.11 Surgical implantation of Alzet minipumps .....	20
2.12 Assessment of diabetic nephropathy .....	20
2.13 Reagents .....	21
2.14 Statistical analysis .....	22
<b>3. ATP ACTING THROUGH P2Y RECEPTORS CAUSES ACTIVATION OF PODOCYTE TRPC6 CHANNELS: ROLE OF PODOCIN AND REACTIVE OXYGEN SPECIES .....</b>	<b>24</b>

3.1	Introduction .....	24
3.2	Results .....	26
3.3	Discussion .....	37
<b>4.</b>	<b>20-HETE ACTIVATES PODOCYTE TRPC6 CHANNELS: POSSIBLE PATHWAY FOR GLOMERULAR INJURY.....</b>	<b>41</b>
4.1	Introduction .....	41
4.2	Results .....	43
4.3	Discussion .....	50
<b>5.</b>	<b>DYSFUNCTION OF PODOCYTE TRPC6 CHANNELS IN <i>IN VIVO</i> AND <i>IN VITRO</i> MODELS OF FSGS: A ROLE FOR MULTIPLE INTERACTING CIRCULATING FACTORS?.....</b>	<b>53</b>
5.1	Introduction .....	53
5.2	Results .....	56
5.3	Discussion .....	71
<b>6.</b>	<b>THE NMDA RECEPTORS AS POTENTIAL THERAPEUTIC TARGETS IN DIABETIC NEPHROPATHY: INCREASED RENAL NMDA RECEPTOR SUBUNIT EXPRESSION IN AKITA MICE AND REDUCED NEPHROPATHY FOLLOWING SUSTAINED TREATMENT WITH MEMANTINE OR MK-801. 79</b>	
6.1	Introduction .....	79
6.2	Results .....	81
6.3	Discussion .....	93
<b>7.</b>	<b>CONCLUSIONS.....</b>	<b>98</b>
	<b>REFERENCES.....</b>	<b>101</b>

# 1. INTRODUCTION

## 1.1 Kidney

Kidneys are the organs primarily responsible for the removal of metabolic waste from our bodies [1]. Although this is true, our kidneys do much more than that. The kidneys are responsible for regulation of water, electrolyte, and acid-base balance, excretion of bioactive substances (hormones and many foreign substances); regulation of systemic arterial blood pressure; regulation of red blood cell production; regulation of vitamin D production; and gluconeogenesis [1]. Our kidneys are largely responsible for implementing the “balance” concept, which states that our bodies are in balance for any substance when the input and output of that substance are matched [1]. The kidneys respond to intake and consumption by varying the output of water and other substances such as sodium, potassium, phosphate, bicarbonate, and magnesium in the urine, thereby maintaining balance for water and substances (constant total body water and metabolites content). Kidneys excrete the end products of metabolic processes such as urea (from protein), uric acid (from nucleic acid), creatinine (from muscle creatine) the products of hemoglobin breakdown, and hundreds of other metabolic end products [1]. These end products have no function in our body and many are harmful when they accumulate. Kidneys regulate the arterial blood pressure, which is largely determined by blood volume over long time scales [1]. Kidneys regulate blood volume by maintaining salt and water balance, in particular by a process called pressure natriuresis, in which elevated arterial pressures lead to increased excretion of sodium and water. Kidneys also release vasoactive substances that regulate myogenic tone in smooth muscles [1]. Kidneys release factors that regulate red blood cell

production and they metabolize vitamin D, which contribute to regulation of blood chemistry and physical properties related to blood pressure [1]. Also, during a prolonged fast, when our body requires glucose production and consumption, our kidneys serve as a site for gluconeogenesis to synthesize new glucose from non-carbohydrate sources [1].

### **1.1.1 Glomerulus**

Each kidney is comprised of approximately 1 million nephrons, which are made up of a spherical filtering component, called the renal corpuscle, and a tubule extending from the renal corpuscle [1]. The renal corpuscle allows formation of an initial ultrafiltrate of blood that is subjected to further processing in the tubules. The corpuscle consists of a dense tuft of interconnected capillary loops, called the glomerulus, surrounded by a balloon like hollow layer of parietal epithelial cells called Bowman's capsule. At one side of the renal corpuscle, blood enters and leaves Bowman's capsule through afferent and efferent arterioles, respectively. On the opposite side, Bowman's capsule has an opening that leads the filtered fluid into the first portion of the tubule.

The glomerular filtration barrier is composed of three layers. The first layer is the capillary endothelium of the glomerular capillaries, which is perforated by many large fenestrae, allowing most of the acellular components of the blood to permeate. The second layer is the glomerular basement membrane (GBM) formed by glycoproteins and proteoglycans. The last filtration layer is a monolayer of epithelial cells called podocytes that cover the GBM and face Bowman's space [1].

### **1.1.2 Podocyte**

Podocytes are highly specialized cells with finger-like processes called pedicels (or

foot processes) that extend from major processes, which in turn emanate from podocyte cell bodies. The foot processes cover the GBM. These processes interdigitate with the pedicels from adjacent podocytes, forming thin bridges of adhesion proteins in structures called glomerular slit diaphragms. Podocyte foot processes with slit diaphragms cover the outer part of the GBM and form a selective filtration barrier [1]. Podocyte injury or loss of podocytes are a hallmark of progressive glomerular diseases such as focal segmental glomerulosclerosis (FSGS), minimal change disease, diabetic nephropathy (DN), lupus nephritis and membranous glomerulopathy [2, 3]. This dissertation focuses on two of these chronic kidney diseases, DN and FSGS.

## **1.2 Chronic kidney diseases (CKD)**

According to the Kidney Disease Outcomes Quality Initiative (KIGO), chronic kidney disease (CKD) is present when kidney damage persists for three months and longer, as expressed by structural or functional abnormalities of the kidney, with or without decreased glomerular filtration rate (GFR) [4]. CKD is also diagnosed when a patient has a GFR of less than 60 ml/min (normally  $\geq 90$ ) per 1.73 m<sup>2</sup> for three months or more, with or without histological kidney damage [4]. During the progression of CKD, some nephrons are lost and the ones that survive must compensate for the loss of other nephrons to maintain overall renal capacity.

Glomerular hyperfiltration (increased pressure and flow through individual glomeruli) has initial adaptive effects by maintaining overall GFR, but in the long run, this situation results in maladaptive consequences. The pathophysiologic mechanisms and conditions such as endothelial injury, foot process effacement and detachment of

podocytes, and stimulation of cytokines and inflammatory substances, can further lead to glomerular hypertrophy, proteinuria and infiltration of immune cells leading to tubulointerstitial disease [5-10]. The risk of CKD is determined by many factors, including genetic susceptibility, metabolic status including hyperlipidemia, hyperglycemia or inadequate glucose control, hypertension, and smoking [11-22]. According to the US Renal Data System 2015 (USRD), two-third of CKD cases are caused by diabetes [23].

### **1.2.1 Focal Segmental Glomerulosclerosis**

One of the most common causes of the nephrotic syndrome is Focal Segmental Glomerulosclerosis (FSGS). FSGS has been increasing in incidence in both African Americans and Hispanics (both adults and children) in United States [24, 25]. In FSGS, scarring (sclerosis) is observed in some glomeruli (focal) but only in a portion of the glomerular capillary tuft (segmental). FSGS represents a syndrome that has multiple pathogenic mechanisms and histologic patterns of injury. FSGS can be a primary renal disease or a secondary disease caused by a variety of other conditions. The universal clinical feature of FSGS is proteinuria, and the ubiquitous pathologic feature is the focal segmental glomerular scarring and obliteration. The lesions occur in various distinctive patterns sometimes referred to as perihilar, collapsing, cellular, tip lesion, and not-otherwise-specified, depending on the appearance and location within the glomerulus [26]. In terms of etiology, FSGS can be classified as primary or idiopathic FSGS, secondary FSGS, and familial forms [27, 28]. There does not appear to be a direct relationship between the pathological mechanisms and the histological variant observed in renal biopsies. The primary (idiopathic) forms of FSGS are sometimes associated with

alterations in circulating permeability factors such as serum-soluble urokinase plasminogen activator receptor (suPAR), cardiotrophin-like cytokine-1 (CLC-1) and tumor necrosis factor (TNF $\alpha$ ) [29-36]. This is especially true in patients that do not respond to therapy with glucocorticoids (steroid-resistant forms). Secondary forms of FSGS are associated with drug toxicity, metabolic diseases such as sickle cell disease, HIV and other viral infections, chronic hypertension, and toxins [37-41]. FSGS lesions are often seen in later stages of other forms of CKD, as renal function declines. Familial forms typically are caused by mutations in certain genes expressed in podocytes, and can occur in autosomal dominant and autosomal recessive forms [42].

#### **1.2.1.1 Pathogenesis/ available treatments**

Glomerular hypertrophy is typically observed in primary FSGS and often precedes overt glomerulosclerosis in FSGS [43]. There is an increased risk for FSGS progression if the glomerular area gets larger than 50% of the glomerular area of a normal age-matched control [44]. Almost 1,000 FSGS patients each year receive kidney transplants; however, within hours to weeks after kidney transplantation, FSGS recurs in approximately 30% to 40% of adult patients and up to 80% in children with steroid-resistant forms of the disease [45]. During FSGS recurrence, foot process effacement precedes the development of overt sclerosis. The presence of serum-soluble circulating permeability factors in the serum of patients with primary FSGS, which induces increased glomerular permeability and proteinuria, was suggested by cases of recurrence of FSGS after kidney transplantation [29-36].

Podocytes are considered to be the originating site of FSGS pathogenesis. Changes

in podocyte structure, such as the effacement of foot processes, precede proteinuria [46]. This early stage podocyte damage is reversible; however, if the stimuli is sustained, it may become the basis for further aggravating injury resulting in proliferation, cell cycle arrest, apoptosis, and necrosis [46]. Significant loss of podocytes (~25%) ultimately leads to the irreversible loss of the entire nephron.

There are very few effective drug treatments for primary FSGS. In recurrent forms, plasmapheresis or protein absorption strategies are used to remove circulating factors. Also, angiotensin converting enzyme (ACE) inhibitors or angiotensin receptor blockers (ARB) may provide a substantial reduction in proteinuria, and a wide range of immunosuppressive therapies are typically used, although the drugs used are toxic and are not well tolerated.

#### **1.2.1.2 Genetic forms of FSGS**

Genetic analyses of familial FSGS have identified several mutations in genes encoding podocyte proteins that have shed light on the functions of the glomerular filtration barrier. For instance, mutation in a gene that encodes a podocyte actin-binding protein called  $\alpha$ -actin 4 (*ACTN4*) causes an autosomal dominant FSGS [42]. Patients with *ACTN4* mutations typically require dialysis or transplantation by age of 30, and rare recurrence will happen for some of these patients who go through transplantation [42]. An autosomal recessive congenital nephrotic syndrome is caused by a mutation in the *NPHS1* gene, which encodes for a protein called nephrin [47]. Nephrin is one of the main adhesion proteins of the slit diaphragm and is also widely used as a podocyte marker. Nephrin mutations lead to severe congenital nephrotic syndromes even prior to birth.

#### **1.2.1.2.1 *Nephrotic Syndrome 2 (NPHS2) gene mutation***

Podocin, the product of *NPHS2* gene, is nonfunctional in many autosomal recessive forms of FSGS. This typically results in early childhood onset of proteinuria, rapid progression to end-stage renal disease, and no recurrence after renal transplantation [48]. Podocin belongs to the stomatin protein family. It is a cholesterol-binding hairpin loop protein, and it is selectively expressed at the inner membrane leaflet of the slit diaphragm domains of podocyte foot processes [49-51]. Podocin is expressed in the podocytes of fetal and mature kidney glomeruli, and has a crucial role in the glomerular filtration barrier [52].

#### **1.2.1.2.2 *Transient Receptor Potential Cation-6 (TRPC6) gene mutation***

TRPC6 channels are  $\text{Ca}^{2+}$ -permeable cationic channels that are expressed in many cells and tissues. Mutations in the *TRPC6* gene have been implicated in the pathophysiology of glomerular diseases. TRPC6 is a member of the TRP superfamily of ion channels, and a member of TRPC subfamily [53-55]. The initial reports described a series of autosomal-dominant mutations in *TRPC6* gene causing the familial forms FSGS [56, 57]. Most of the mutant TRPC6 channels identified in FSGS patients show a gain of function when they are heterologously expressed in human embryonic kidney (HEK-293) cells [56-58]. In those studies, TRPC6 channels were usually activated in response to stimulation of G protein-coupled receptors coupled to phospholipase C (PLC) signaling cascades [56, 57, 59]. In addition, TRPC6 expression in podocytes is increased in certain acquired (non-genetic) glomerular diseases such as membranous glomerulonephritis [60]. It has been reported that podocyte-specific overexpression of wild-type and mutant TRPC6 channels in mice results in foot process effacement, glomerulosclerosis, and albuminuria [61].

Moreover, acute glomerular toxicity evoked by puromycin aminonucleoside is driven in part by upregulation of TRPC6 secondary to generation of reactive oxygen species (ROS) [62]. Abnormal TRPC6 channel activation has been shown to play a significant role in the pathophysiology of glomerular disease. The canonical pathway for TRPC6 activation is through PLC, which leads to formation of diacylglycerol (DAG) from inner leaflet plasma membrane phospholipids. DAG causes robust activation of heterologously expressed TRPC6 channels [63]. Application of membrane-permeable DAG analogs such as 1-oleoyl-2-acetyl-*sn*-glycerol (OAG) can also evoke robust activation of native TRPC6 channels in podocytes [64, 65]. Importantly, our group has also observed that ROS contribute significantly to activation of TRPC6 channels evoked by insulin [65], N-methyl-D-aspartate (NMDA) receptor agonists, including metabolites of homocysteine [66], and by application of angiotensin II (Ang II) [67], ATP [68], and 20-HETE (unpublished data). Other groups observed ROS-dependent activation of podocyte TRPC6 channels in response to elevated glucose [69] and puromycin aminonucleoside [62]. Last but not least, our lab showed that podocyte TRPC6 channels can be activated by mechanical stimuli, as well as chemical stimuli [64]. Importantly, the mechanical activation of TRPC6 channels in podocytes is not mediated by G protein signaling cascades in contrast to the situation in vascular smooth muscle [70, 71].

### **1.2.2 Diabetic Nephropathy (DN)**

Throughout the world, the number of people diagnosed with diabetes is increasing. The increased prevalence of diabetes has also caused an increase in the number of macro- and microvascular complications of diabetes such as stroke, coronary heart disease, DN,

and end stage renal disease. DN is diagnosed when diabetic patients have albuminuria (ratio of albumin/creatinine  $\geq 30$  mg/g), impaired glomerular filtration rate ( $< 60$  mL/min/1.73m<sup>2</sup>), or both [72].

### **1.2.2.1 Histopathology**

The histopathologic changes of DN have been well documented. The glomeruli of DN patients show an increase in matrix secretion (mesangial expansion) and cell enlargement. Also, a thickened GBM and podocyte foot process effacement are visible by electron microscopy [72]. When podocytes are enlarged, or start losing their attachment to GBM because of their foot process effacement, the filtration barrier fails, leading to an increase in urine albumin excretion [72, 73]. In the vessels, the initial hyaline thickening progresses to arterial hyalinosis of the afferent and efferent arterioles; this eventually leads to glomerular hyperfiltration in the remaining nephrons [73, 74]. Diffuse diabetic glomerulosclerosis and characteristic Kimmelstiel-Wilson nodules (nodular glomerulosclerosis) are often observed later in the disease [75].

### **1.2.2.2 Pathophysiologic pathways and available treatments**

There are several pathophysiologic pathways that lead to DN. These include hemodynamic mechanisms, often attributed to vasoconstriction of the efferent arteriole by angiotensin and endothelin [73, 76-78]. However, elevations in blood glucose by itself can increase transmural pressures across glomerular capillaries owing to water and glucose uptake in proximal tubules, and changes in tubuloglomerular feedback. Hyperglycemia causes an increased glycolysis, which then upregulates four distinct mechanisms: the polyol pathway [79-81], the hexosamine pathway [79], the production pathway of

advanced glycation end products (AGEs) [73, 82, 83], and activation of protein kinase C (PKC) [84-87]. Last but not least, DN may be a consequence of inflammatory pathways. Inflammatory pathways induce a chronically activated innate immune system and a low-grade inflammatory state in patients with diabetes [88, 89]. Therapeutic options are still limited. Glycemic control and renin-angiotensin-aldosterone system (RAAS) inhibition with angiotensin converting enzyme (ACE) inhibitors and angiotensin receptor blockers (ARBs) are used to reduce albuminuria in patients with diabetic kidney disease. The rationale for RAAS inhibition is to reduce efferent arteriolar vasoconstriction that occurs in response to RAAS, thereby reducing hyperfiltration. Sustained RAAS hyper-activation is likely to have deleterious effects on many other renal cell types, including cells in the interstitium.

### **1.3 Summary of objectives**

The first objective of this research is to study physiological mediators and transduction cascades that cause activation of TRPC6 channels. In this dissertation, I focus on the effects of chemical stimuli such as ATP and 20-hydroxyeicosatetraenoic acid (20-HETE) on the gating properties of TRPC6 channels in immortalized mouse podocyte cell line (*in vitro*) and in intact podocytes covering the glomerulus from the *ex vivo* preparation of isolated rat glomeruli. Following the material and methods section in chapter two of this dissertation, I discuss the effects of ATP and 20-HETE on the activity of podocyte TRPC6 channels in the third and fourth chapter, respectively.

The second objective of this dissertation is to study the dysfunction of podocyte TRPC6 channels in *in vivo* and *in vitro* models of a syndrome called focal segmental

glomerulosclerosis (FSGS). Since mutations in the *TRPC6* gene have been shown to cause FSGS, I examine whether the gating properties of podocytes TRPC6 channels are altered in these models in response to chemical and mechanical stimuli. Also, I examine the role of multiple interacting circulating factors such as suPAR and TNF on the TRPC6 channel activity. For this study, I use a secondary FSGS model in rats, the effects of sera from patients with primary FSGS on cultured podocytes, and the effects of recombinant suPAR and TNF on cultured podocytes.

The third objective of this research is to validate NMDA receptors as potential therapeutic targets in diabetic nephropathy. Using two different type-1 diabetic mouse model, I show that renal NMDA receptor subunit expression is increased, and sustained treatment with NMDA receptor antagonists such as memantine and MK-801 reduces nephropathy.

## **2. MATERIALS AND METHOD**

### **2.1 Cell Culture protocols**

An immortalized mouse podocyte cell line (MPC-5) was obtained from Dr. Peter Mundel of Harvard Medical School and maintained as described previously [90]. Podocyte differentiation and expression of podocyte markers were induced by removal of  $\gamma$ -interferon and temperature switch to 37°C for 14 days.

### **2.2 Primary isolation of rat glomeruli**

For glomerular isolation, male Sprague-Dawley rats (150–200 g from Charles River Laboratories) were anesthetized with isoflurane and euthanized according to NIH guidelines as approved by the University of Houston Institutional Animal Care and Use Committee. Glomeruli were immediately isolated using a sieving procedure described previously [64, 67, 91]. Isolated glomeruli were plated for 24 h at 37°C in RPMI-1640 medium supplemented with 10% fetal bovine serum (FBS) and 100 U/ml penicillin-streptomycin on collagen-coated glass coverslips. By that time they adhered sufficiently tightly to the substrate to allow analysis by whole cell recordings. To isolate mesangial cells from glomeruli, the glomeruli were then plated onto collagen-coated dishes, maintained in RPMI-1640 medium containing 10% fetal bovine serum, 100 U/ml penicillin and 100  $\mu$ g/ml streptomycin at 37°C for two weeks. At that time, cells that had migrated out of the glomeruli had achieved approximately 80% confluence. The vast majority of those cells had an elongated spindle shape, and expressed the mesangial cell marker  $\alpha$ -smooth muscle actin. In experiments on the effects of high glucose, cultured cells were

exposed for 24 hr to the standard RPMI-1640 medium (which contains 9 mM glucose), supplemented with either 16 mM glucose (for a final glucose concentration of 25 mM) or with 16 mM mannitol (as an osmotic control).

### **2.3 siRNA knockdown protocol**

Protocol is followed using procedures described previously [63, 64, 66]. In brief, the medium of MPC-5 cells or isolated rat glomeruli were changed out to antibiotic and FBS free medium for 24 hours before transfection. The siRNA (either TRPC6 siRNA, podocin siRNA, or control siRNA) was diluted in serum/antibiotic free medium (5  $\mu$ M siRNA into 250  $\mu$ M medium, for 35 mm plate). Lipofectamine was diluted 1:50 in a separate tube. Both tubes were kept at room temperature for 5 minutes. Next, the contents of both tubes were mixed and kept at room temperature for 30 minutes. The mixture was then added to 2 mL of serum/antibiotic free medium in 35 mm plate, or spread onto 5 wells of a 24-well plate for electrophysiology.

### **2.4 Electrophysiology**

Methods for conventional whole cell recordings from podocytes were carried out by standard methods that have been described in detail previously [64-67, 92]. Recordings were made with an Axopatch 1D amplifier (Molecular Devices) and analyzed using pClamp v 10 software (Molecular Devices). The bath solution contained 150 mM NaCl, 5.4 mM CsCl, 0.8 mM MgCl<sub>2</sub>, 5.4 mM CaCl<sub>2</sub>, and 10 mM HEPES, pH 7.4. Pipette solutions in all experiments contained 10 mM NaCl, 125 mM CsCl, 6.2 mM MgCl<sub>2</sub>, 10 mM HEPES, and 10 mM EGTA, pH 7.2. The use of Cs<sup>+</sup> in bath and pipette solutions prevents contamination by current flowing through K<sup>+</sup> channels that are also expressed in

these cells [90]. The relatively high  $\text{Ca}^{2+}$  concentration in the bath solution markedly increases stability of whole cell recordings. In some experiments, the pipette solution also contained guanosine 5'-O-(2-thiodiphosphate) (GDP- $\beta$ S), a GDP analog resistant to hydrolysis and phosphorylation that competitively inhibits G protein activation by GTP [93]. Activators and inhibitors in the absence or presence of other agents were applied by gravity feed through the recording chamber. Tempol was applied to cell line or glomeruli 30 min prior to electrophysiological analyses. To monitor TRPC6, currents were periodically evoked by 2.5-s ramp voltage commands (-80 to +80 mV) from a holding potential of -40 mV. Whole cell currents were quantified at +80 mV. It is possible to compensate up to 80% of series resistance without introducing oscillations into the current output of the amplifier. Data are presented as means  $\pm$  SE, and quantitative comparisons were analyzed using ANOVA followed by Tukey's post hoc test with  $P < 0.05$  considered significant.

## **2.5 Immunoblot/cell surface biotinylation assay**

Methods used for immunoblot analysis from podocyte lysates have been described in detail previously [65, 92, 94]. Filters were probed using primary antibodies, washed, incubated with horseradish peroxidase-conjugated secondary antibodies, and visualized using chemiluminescence. Methods for cell-surface biotinylation assays to measure steady-state surface expression of TRPC6 channels were also described previously [65, 92, 94]. Briefly, after exposure to putative permeability factors or patient sera, cells were treated with a membrane-impermeable biotinylation reagent (Pierce Biotechnology, Rockford, IL) to selectively label proteins on the cell surface. The reaction was stopped, cells were lysed,

and surface proteins were captured using immobilized streptavidin-agarose beads. A sample of the initial lysate used to measure the total protein abundance.

## **2.6 RNA isolation, reverse transcription, and PCR**

Total RNA from mouse renal cortex, immortalized mouse podocytes (MPC-5 cells) and primary cultures of rat mesangial cells was isolated using the QIA™ shredder and RNeasy™ mini kit (Qiagen Inc., Valencia, CA). RNA was stored at -80°C before being reverse transcribed into cDNA. Aliquots of total RNA (1.0 µg) from each sample were transcribed into the first strand cDNA using the ThermoScript™ RT-PCR System (Invitrogen, Carlsbad, CA) according to the manufacturer's description. The primer sequences used in PCR were:

*NR1*: fd ACTCCCAACGACCACTTCAC, reverse GTAGACGCGCATCATCTCAA

*NR2A*: fd AGACCTTAGCAGGCCCTCTC, reverse CTCTTGCTGTCCTCCAGACC

*NR2B*: fd CCGCAGCACTATTGAGAACA, reverse ATCCATGTGTAGCCGTAGCC

*NR2C*: fd GCAGAACTTCCTGGACTTGC, reverse CACAGCAGAACCTCCACTGA

*NR2D*: fd CAGCTGCAGGTCATTTTTGA, reverse GGATCTGCGCACTGACACTA

*NR3A*: fd CAGAGGGATGAGCCAGAGTC, reverse CTTCCACACGGTTCAGGTTT

*β-actin*: fd AGCCATGTACGTAGCCATCC, reverse CTCTCAGCTGTGGTGGTGAA

Cycling parameters for PCR were 94° for 5 min, 30 cycles of 94° for 30 sec, 55° for 30 sec, 72° for 30 sec: and a final extension at 72° for 10 min. PCR products were separated on agarose gels and visualized using ethidium bromide. The signals obtained for each transcript were quantified using Image J™ software (Bethesda, MD). All experiments were performed in triplicate.

## **2.7 Histology, immunohistochemistry, and electron microscopy**

In each experiment, rat or mouse kidneys was immersion-fixed in 4% paraformaldehyde in phosphate-buffered saline (PBS) solution, embedded in paraffin, and 2  $\mu$ m sections prepared for staining by periodic acid-Schiff's (PAS). In addition, some paraffin sections were immunostained with antibodies against various NMDA receptor subunits (anti-NR1 from Abcam, Cambridge MA), anti-NR2A and anti-NR2B (Thermo Fisher Scientific, Waltham MA), and anti-NR2C (Alomone Labs). Antigens were retrieved using a citrate-based antigen unmasking solution (H-3300 Vector Laboratories, San Mateo, CA). Slides were then quenched and blocked using manufacture's protocol, and incubated with primary antibody overnight at 4°C. Immunostaining was produced using the Vectastain Elite ABC Kit™ (Vector Laboratories) and the DAB Peroxidase (HRP) Substrate Kit™ (Vector Laboratories). Mesangial matrix expansion in PAS-stained sections was calculated from fractional volume of the mesangium on all of the glomeruli in a section using Adobe Creative Cloud-Ps CC on PAS-stained slides, and analyzed using similar to those reported previously (34). The percentage of mesangial matrix occupying each glomerulus was then rated on a scale from 0, 0%; 1, 25%; 2, 50%; 3, 75%; and 4, 100%. For each mouse, glomerular matrix expansion was evaluated in 15 glomeruli and averaged to obtain a value for that animal. Statistical analysis was carried out on the mean values from each group of animals, with N = 4 mice per group.

The other kidney was fixed by immersion in 3% glutaraldehyde plus 3% paraformaldehyde in 0.1 M sodium cacodylate buffer pH 7.3 for ultrastructural analysis using transmission and scanning electron microscopy (EM) at the High Resolution Electron Microscopy Facility at the M. D. Anderson Cancer Center in Houston, TX. For transmission EM, the samples were post-fixed with 1% cacodylate buffered osmium

tetroxide for 30 min, and stained *en bloc* with 1% uranyl acetate. The samples were dehydrated by passing through graded ethanol, embedded in LX-112 resin, and allowed to polymerize at 60° for three days. Ultrathin sections (50-70 nm thick) were cut using a Leica Ultracut microtome (Leica, Deerfield USA), stained with uranyl acetate and lead citrate in a Leica EM Stainer, and examined in a JEM 1010 transmission electron microscope (JEOL USA Inc., Peabody, MA) at an accelerating voltage of 80 kV. Digital images were obtained using an AMT Imaging System (Danvers, MA). The thickness of the glomerular basement membrane (GBM) was measured from the digital images using Adobe Creative Cloud-Ps CC. For each mouse, 15 glomeruli were selected and 3-4 different points of GBM from the same glomerulus were used for measurements to calculate a mean GBM thickness for that animal. Statistical analyses of GBM thickness on groups of animals was then carried out with N = 4 mice per group. For scanning EM, fixed samples were washed with 0.1 M sodium cacodylate buffer pH 7.3, post-fixed with 1% cacodylate-buffered osmium tetroxide, washed in 0.1 M sodium cacodylate buffer, and then with distilled water. The samples were then treated sequentially with filtered 1% aqueous tannic acid, distilled water, filtered 1% aqueous uranyl acetate, and then rinsed thoroughly with distilled water. Samples were dehydrated by passing through graded ethanol, transferred through a graded series of hexamethyldisilazane (Electron Microscopy Sciences, Hatfield, PA), and then air dried overnight. Samples were mounted onto double-stick carbon tabs (Ted Pella Inc., Redding, CA) attached to glass slides, and coated under vacuum using a Balzer MED 010 evaporator (Technograde International, Manchester, NH) with platinum alloy to a thickness of 25 nm, and immediately flash carbon-coated under vacuum. Samples were imaged in a JSM-5910 scanning electron microscope (JEOL USA

Inc.) at an accelerating voltage of 5 kV.

## **2.8 Patient serum and plasma samples**

Studies with serum and plasma samples were done following a protocol approved by the University of Houston Committee for the Protection of Human Subjects. Serum or plasma samples were taken from patients with biopsy proven FSGS that recurred after transplantation following ethical review by panels at the institutions where the patients were seen. Plasma samples from patients 001 and 006 were collected from patients seen at the University of Bristol, UK. Those samples were collected during relapse and after treatment with plasma exchange. Sera from patients 002 and 003 were collected from patients at the Rush University Medical Center during a relapse. Sera from patients 004 and 005 were collected at the Department of Medicine II at the University of Cologne, Germany. The samples from patient 004 were collected during relapse and after this patient achieved a remission as a result of intensive LDL apheresis therapy using a Miltenyi TheraSorb™ column (Miltenyi Biotec, Gladbach, Germany) with preadsorbed sheep antibody against the B-100 component of LDL. These samples have been stored at -80°. In most experiments, immortalized mouse podocytes were cultured with media containing plasma or serum at 10% (replacing fetal bovine serum) for 24 hr. Controls in those cases consisted of sera from healthy humans replacing fetal bovine serum. Serum from healthy controls never produced changes compared to cells cultured in fetal bovine serum. However, the plasma from patient 001 was applied to podocytes at 2% because higher concentrations tended to be toxic.

## **2.9 Mouse models of type-1 diabetes**

All animal experiments were conducted according to protocols approved by the Institutional Animal Care and Use Committee of the University of Houston. Male DBA/2J mice (strain 000671) and D2.B6-*Ins2*<sup>Akita/MatbJ</sup> mice (Akita, strain 007562) of 5-6 weeks age were purchased from the Jackson Laboratory, and were given free access to food and water during the time of the experiments. In a subset of experiments, 10-week old DBA/2J mice were administered five injections of streptozotocin (STZ) (40 mg/kg i.p in 0.1 ml of 0.1 M Na-citrate buffer, pH 4.5) or with the Na-citrate vehicle at 24-hr intervals. Treatment with NMDA antagonists in low-dose STZ-induced diabetic mice began 15 weeks after the completion of STZ treatment.

### **2.10 Chronic puromycin aminonucleoside (PAN) nephrosis**

These experiments were carried out according to a protocol approved by the University of Houston Institutional Animal Care and Use Committee. Sprague-Dawley rats (100-150 g) were purchased from Charles River, and were given three injections of a sterile solution of PAN (200 mg/kg i.p.) dissolved in 0.9% saline. Controls received the saline vehicle. Injections were made at 30 day intervals. Periodically, animals were placed in metabolic cages for 24 hr to collect urine for analysis of albumin excretion using a commercial ELISA (Exocell Inc. Philadelphia, PA). At 10-14 days after the third injection, animals were sacrificed by CO<sub>2</sub> inhalation followed by cervical dislocation and both kidneys were immediately excised. A portion of renal cortex of one kidney was removed and fixed by immersion in paraformaldehyde overnight. Then sample was dehydrated, embedded in paraffin, and 2 µm sections were stained using the periodic acid-Schiff's method (PAS). The rest of the kidneys were used for isolation of glomeruli by sieving for

use in electrophysiology and for analysis of podocyte proteins by immunoblot, as described below. Calculation of mesangial score was done by analysis of PAS-stained sections as described by [95] using Adobe Photoshop CC.

### **2.11 Surgical implantation of Alzet minipumps**

All the following procedures carried out according to a protocol approved by the University of Houston Institutional Animal Care and Use Committee. The least invasive method of drug delivery was used in our Akita mice and low-dose STZ induced diabetic mice, and control groups. The subcutaneous implantation of Alzet minipumps filled with either drug or vehicle were performed. Mice were anesthetized, shaved and prepared for surgical implantation using 70% ethanol and Lidocaine. A mid-scapular incision was made in the skin and a hemostat was used to create a pocket for the pump. Finally, the filled pump carrying either drug or vehicle was inserted in the pocket, exit port first. The incision was closed with wound clips or sutures. NMDA antagonists or saline vehicle were delivered continuously using Alzet™ model 1004 osmotic minipumps (Durect Corporation, Cupertino, CA) implanted subcutaneously in the mid-scapular area under isoflurane anesthesia. These pumps were filled with sterile-filtered solutions containing memantine HCl, or (5S,10R)-(+)-5-Methyl-10,11-dihydro-5H-dibenzo[a,d]cyclohepten-5,10-imine maleate (MK-801), or 0.9% saline vehicle. Memantine was delivered at a dose of 0.2 mg/kg/day, whereas MK-801 was delivered at 0.5 mg/kg/day.

### **2.12 Assessment of diabetic nephropathy**

Just prior to initiation of treatment with NMDA antagonists or vehicle, mice were weighed and mean arterial blood pressure was measured using a non-invasive tail cuff

plethysmographic procedure (Kent Scientific Corporation, Torrington, CT). Mice were then placed in metabolic cages for 24 hr and urine was collected and albumin analyzed using the Albuwell M™ ELISA assay (Exocell, Philadelphia, PA). Animals were weighed every 7 days during the course of drug treatment. After 28 days of drug or vehicle treatment, a final 24-hr urine sample was collected for albumin excretion analysis, and animals were sacrificed by CO<sub>2</sub> inhalation. Kidneys were excised and a portion of renal cortex was reserved for biochemical analysis. The rest of the kidney was used for histological and ultrastructural analysis. Data on 24-hr albumin excretion were obtained from *N* = 9-10 animals in each experimental group.

### **2.13 Reagents**

The pan-TRP channel inhibitor 1-[2-(4-methoxyphenyl)]-2-[3-(4-methoxyphenyl)propoxy]ethyl-1H-imidazole hydrochloride (SKF-96365) was obtained from Sigma. ATP, UTP, UDP, ADP, GDP-βS, tempol, suramin, and D-609 were also obtained from Sigma. 20-hydroxyeicosatetraenoic acid (20-HETE) was purchased from Cayman Chemical Inc. TRPC6 siRNA, podocin siRNA and control siRNA were purchased from Santa Cruz Biotechnology. The P2Y<sub>2</sub>-selective agonist 4-thiouridine-5'-O-(β,γ-difluoromethylene) triphosphate used in one set of experiments was obtained from Tocris (catalog no. 4333). Rabbit antibodies against TRPC6 were obtained from Alomone Labs (Jerusalem, Israel), antibodies against podocin and β3-integrin were obtained from Santa Cruz (Santa Cruz, CA).

Recombinant TNF was obtained from R&D Systems (Minneapolis, MN). A large recombinant form of suPAR containing domains 1, 2 and 3 was obtained from R&S

Systems. A smaller form of suPAR containing domains 2 and 3 was expressed in *Drosophila* SF2 cells and purified from the conditioned medium by affinity chromatography using the amino-terminal fragment of full-length urokinase (ATF; residues 1–143) followed by reversed-phase HPLC using a C4 column on a Waters HPLC system. The organic solvents were evaporated by Speedvac and the pure recombinant protein was lyophilized, resuspended in water, and frozen for subsequent use. Cilengitide was obtained from Seleck Chem (Houston, TX, USA).

Antigen unmasking solution, Vectastain Elite ABC Kit, M.O.M Kit, and VectaMount were all purchased from Vector Laboratories. Anti-NR3A antibody and Anti-NR1 antibody were purchased from Abcam. Anti-NR2A and Anti-NR2B antibodies were from Zymed-ThermoFisher. Anti-NR2C was from Alomone Labs. MK-801 and memantine were obtained from Sigma.

## **2.14 Statistical analysis**

All experiments on immunoblot or cell surface biotinylation assays were performed in triplicate and analyzed by densitometry using Image J<sup>TM</sup> software (Bethesda, MD). The data are presented as fold changes relative to the lowest value observed in a control group. These data are presented graphically as mean  $\pm$  SD. Unpaired student t-test used for statistical analysis. Electrophysiological data on TRPC6 current amplitudes are presented as fold changes of current observed at +80 mV relative to the current measured at a stable baseline, prior to application of hypoosmotic stretch, OAG, or other agonists or blockers. Those data are presented graphically as mean  $\pm$  S.E.M. and were analyzed using Student's unpaired t-test. There were always at least 10 cells in each group. Data from animal

experiments are presented graphically as mean  $\pm$  S.E.M. Quantitative data on renal phenotypes were analyzed using weighted measures two-way ANOVA followed by Tukey's *post hoc* test. In these analyses the two independent variables were genotype (Akita vs. DBA/2J) and drug treatment (NMDA antagonist vs. saline vehicle). A statistically positive result was inferred when F values for the interaction between drug effects and genotype, or for drug effects alone, indicated  $P < 0.05$ . Data from immunoblot and RT-PCR are presented as mean  $\pm$  SD from triplicate measures. The analysis of the fold increase in podocyte TRPC6 channel activity induced by 20-HETE were presented as two-tailed unpaired T-test, one-way ANOVA and Tukey HSD test.

### **3. ATP ACTING THROUGH P2Y RECEPTORS CAUSES ACTIVATION OF PODOCYTE TRPC6 CHANNELS: ROLE OF PODOCIN AND REACTIVE OXYGEN SPECIES**

#### **3.1 Introduction**

Podocytes are highly polarized cells that cover the external surface of the glomerular capillary. Podocyte foot processes attach to the capillary basement membrane and are connected to each other through specialized junctions known as slit diaphragms [96]. The extracellular portions of slit diaphragms are formed from the interacting ectodomains of adhesion molecules such as nephrin and Neph1, which collectively comprise a porous matrix through which water and small solutes pass as a result of hydrodynamic and diffusive driving forces. The permselective properties of slit diaphragms normally prevent significant movement of albumin and comparably sized macromolecules into the urinary space inside Bowman's capsule. While slit diaphragms and foot processes are often depicted as static structures, there is evidence that dynamic processes within foot processes can alter the passage of solutes through slit diaphragms [97, 98] and may in this way contribute to regulation of GFR. Even more dramatic changes in the shape of podocytes may allow for a stronger attachment to the glomerular capillary in the face of injury or stress, although this typically occurs at the expense of normal glomerular filtration [99].

GFR is regulated by a number of feedback mechanisms that operate over several time scales [100, 101]. A mechanism of particular importance is tubuloglomerular feedback (TGF), a process in which cells of the macula densa detect changes in distal tubule flow rate and luminal Na<sup>+</sup> content and initiate signals in response that ultimately act on

glomerular cells to control GFR [102, 103]. While a vast body of work on TGF has focused on regulation of vascular smooth muscle in the afferent and efferent arterioles [104-107], recent studies have provided evidence that TGF generates a  $\text{Ca}^{2+}$  wave that propagates from smooth muscle through extra- and intraglomerular mesangial cells, into endothelial cells, and into podocytes [108]. Importantly, the propagation of this  $\text{Ca}^{2+}$  wave is suppressed by extracellular ATP scavengers, and by blockade of P2 purinergic receptors [108]. In recent years it has become clear that connexin and pannexin hemichannels can allow for regulated ATP release from a wide variety of cells [109, 110]. It is notable that glomerular endothelial cells (GEnCs) express connexin 40, which mediates release of ATP and propagation of  $\text{Ca}^{2+}$  waves, in part by extracellular diffusion of ATP [111]. Since only a short diffusion distance would be required for ATP secreted from endothelial cells to act on podocytes, this provides a potential mechanism for propagation of the final phase of the glomerular  $\text{Ca}^{2+}$  wave observed in TGF. Something like this would appear to be necessary, since podocytes and GEnCs lie on opposite sides of the GBM and therefore cannot be connected by gap junctions. The purpose of the present study is to examine the actions of ATP on canonical transient receptor potential-6 (TRPC6) channels in podocytes.

TRPC6 channels are  $\text{Ca}^{2+}$ -permeable cationic channels that play a role in G protein-mediated signaling in a wide variety of cell types [112]. Podocyte TRPC6 channels in podocytes are expressed in foot processes in a complex with other slit diaphragm proteins, including podocin and nephrin [51, 56, 64, 113]. However, TRPC6 is also detected in the major processes and in the podocyte cell body [113], where it exists in different macromolecular complexes [52, 64, 92, 113]. TRPC6 is of particular interest because mutations in these channels result in familial nephrotic syndromes [56-58]. Moreover,

podocyte TRPC6 channels are upregulated in several acquired glomerular diseases [60], and podocyte-specific overexpression of wild-type or mutant TRPC6 channels in mice results in proteinuria and glomerulosclerosis [61]. Therefore there is considerable interest in understanding the physiological mediators and transduction cascades that can cause these channels to become active. ATP is an attractive candidate because of its role in TGF, and because earlier studies have shown that it could evoke an increase in intracellular  $\text{Ca}^{2+}$  in podocytes [114, 115].

We now report that ATP evokes a concentration-dependent increase in current through TRPC6 channels in immortalized mouse podocyte cell lines, and in primary rat podocytes that are still attached to the GBM in explanted decapsulated glomeruli. The effects of ATP are blocked by the pan-P2 antagonist suramin as well as by inhibition of G protein signaling, and mimicked by P2Y agonists such as ADP and UTP. These effects of ATP are also blocked by TRPC6 knockdown using siRNA and by TRPC6 blocking agents. We also report that podocin is required for robust responses to ATP in podocytes, and we present evidence suggesting that reactive oxygen species play a role in the overall signal transduction cascade leading from P2Y receptors to TRPC6.

### **3.2 Results**

Our initial experiments were carried out on the differentiated cells of an immortalized mouse podocyte cell line (MPC-5 cells) that we have used in several previous studies on TRPC6 [64-67]. Cationic currents were evaluated during application of slow duration (2.5 s) ramp voltage commands (-80 mV to +80 mV). Application of ATP by gravity-fed bath superfusion evoked large cationic currents that showed substantial

outward rectification under our recording conditions (Fig. 1A) and which reversed rapidly upon washout (not shown). The effects of ATP were concentration dependent, with half-maximal currents typically occurring at  $\sim 10 \mu\text{M}$  (Fig. 1B), and with maximal responses observed at  $100 \mu\text{M}$  (Fig. 1B). Pretreating podocytes with  $100 \mu\text{M}$  suramin completely eliminated responses to ATP (Fig. 1, C and D), suggesting that they are mediated by  $\text{P}_2$  receptors. The  $\text{P}_2$  receptor can be subdivided into seven forms of ionotropic  $\text{P}_2\text{X}$  receptors, and a family of eight metabotropic receptors, known as  $\text{P}_2\text{Y}_{(1,2,3,4,6,11,12,13,14)}$  [116]. Transcripts encoding  $\text{P}_2\text{Y}_1$ ,  $\text{P}_2\text{Y}_2$  and  $\text{P}_2\text{Y}_6$  have been detected in rodent podocytes [114]. ATP can activate  $\text{P}_2\text{Y}_1$  and  $\text{P}_2\text{Y}_2$  receptors, whereas UTP can activate  $\text{P}_2\text{Y}_2$  and  $\text{P}_2\text{Y}_4$  receptors. Note, however, that the later are not inhibited by suramin. UDP preferentially activates  $\text{P}_2\text{Y}_6$ , whereas ADP preferentially activates  $\text{P}_2\text{Y}_1$  [116]. We observed that cationic currents qualitatively similar but consistently smaller than those evoked by ATP could be activated by  $100 \mu\text{M}$  or  $200 \mu\text{M}$  of ADP, UTP, or UDP (Fig. 1E). Responses were also evoked by the synthetic agonist 4-thiouridine-5'-O-( $\beta,\gamma$ -difluoromethylene) triphosphate at concentrations where it is selective for  $\text{P}_2\text{Y}_2$  receptors [117]. For all of these nucleotides, response amplitudes were similar when they were evoked at  $100$  or  $200 \mu\text{M}$ , suggesting that they comprise the top of the concentration-response curves. These data suggest that the functional  $\text{P}_2\text{Y}_1$ ,  $\text{P}_2\text{Y}_2$ , and  $\text{P}_2\text{Y}_6$  receptors are expressed in mouse podocytes, consistent with earlier investigations on transcript expression [114]. ATP evoked larger responses than any of the other nucleotides, which suggests that its effects are caused by simultaneous activation of multiple subtypes of receptors expressed in these cells, most likely  $\text{P}_2\text{Y}_1$  and  $\text{P}_2\text{Y}_2$  (since it is not able to activate  $\text{P}_2\text{Y}_6$ ).

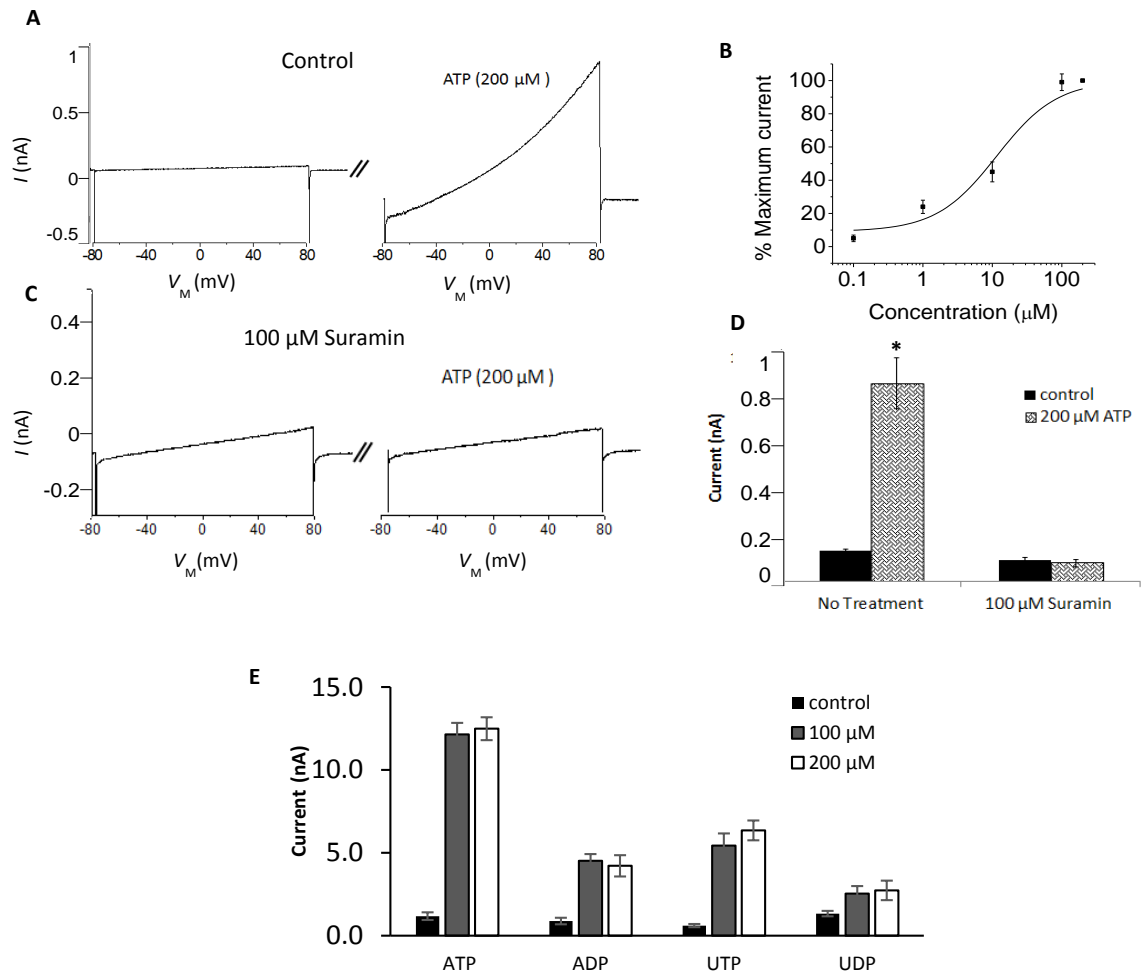


Figure 1. ATP activates cationic currents in immortalized mouse podocyte cell lines. **A**: whole cell currents recorded from a podocyte during ramp voltage commands (-80 to +80 mV in 2.5 s) before (left) and after (right) application of 200  $\mu\text{M}$  ATP. Note marked increase in rectifying cationic current after ATP application. **B**: concentration-response relationship for ATP-evoked currents measured at +80 mV, at the end of ramp voltage commands. Points are fitted with the Hill equation, with EC50 at 9.5  $\mu\text{M}$ . Points are means  $\pm$  SE (N = 3 cells). **C**: cationic currents before and after ATP application in cell pretreated with the P2 antagonist suramin. **D**: currents at +80 mV before and after ATP application in control cells and in cells pretreated with 100  $\mu\text{M}$  suramin (N = 9 cells per group). **E**: several nucleotides can activate cationic currents in immortalized mouse podocyte cell lines. Mean currents  $\pm$  SE recorded at +80 mV are plotted for ATP, ADP, UTP, and UDP at 100 and 200  $\mu\text{M}$ , as indicated (N = 5 cells per group).

Irrespective of the relative contributions of the various subtypes of P2Y receptors, responses to ATP were not seen when recording electrodes contained 50  $\mu\text{M}$  guanosine 5'-O-(2-thiodiphosphate) (GDP- $\beta\text{S}$ ), a GDP analog resistant to hydrolysis and phosphorylation that competitively inhibits G protein activation by GTP [93] (Fig. 2). We have previously shown that this pipette solution also blocks responses to angiotensin II (ANG II), although activation of TRPC6 by hypoosmotic stretch persists under those recording conditions [64]. These data indicate that podocyte responses to ATP are mediated by G protein-coupled metabotropic receptors in the P2Y family [114].

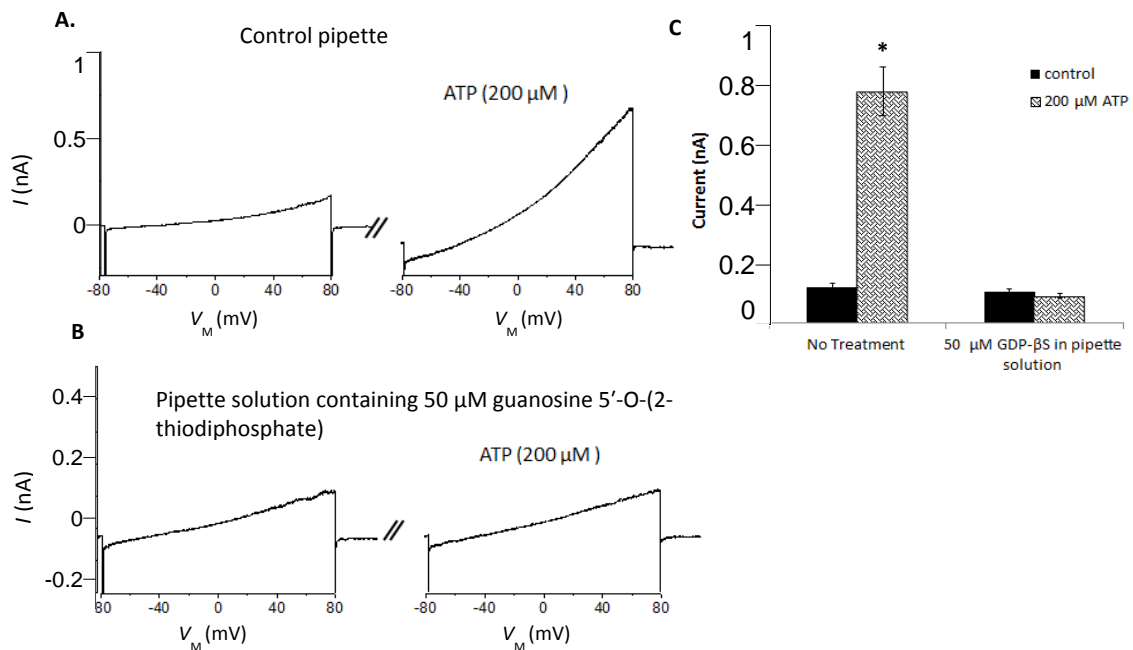


Figure 2. ATP activation of podocyte cationic currents requires G protein signaling. Whole cell recordings of ATP-evoked currents in immortalized mouse podocytes. A: recording made using an electrode filled with normal solution. B: recording made using electrode filled with normal solution supplemented with 50  $\mu\text{M}$  GDP- $\beta\text{S}$ , an agent that prevents GTP binding and thereby abolishes G protein signaling. Bar graph in C shows summary of several repetitions of these experiments (N = 5 cells per group).

The ATP-evoked cationic current appears to flow through endogenously expressed TRPC6 channels. Currents activated by ATP were completely blocked by bath application of 10  $\mu\text{M}$  SKF-96365, a nonselective pan-TRP channel inhibitor (Fig. 3A). Podocytes express TRPC5 and TRPC6 subunits [65, 113, 118], and those two types of channels are both blocked by SKF-96365 [118]. However, they are differentially sensitive to micromolar concentrations of  $\text{La}^{3+}$ , as TRPC6 can be completely inhibited by micromolar  $\text{La}^{3+}$ , whereas TRPC5 is actually activated by  $\text{La}^{3+}$  at that concentration [118, 119]. We observed that 50  $\mu\text{M}$   $\text{La}^{3+}$  rapidly and completely blocked currents evoked by 200  $\mu\text{M}$  ATP, suggesting that they are mediated by channels containing TRPC6 subunits, and indicating that TRPC5 channels cannot be making a significant contribution to the ATP-evoked currents in these cells (Fig. 3B). Consistent with this, we observed that transient siRNA knockdown of TRPC6 using procedures described previously [64, 65, 67] abolished podocyte responses to ATP, whereas cells continued to respond to ATP after treatment with a control siRNA (Fig. 4). The effectiveness of the siRNA was confirmed by immunoblot (Fig. 4D).

Previous studies have shown that P2Y<sub>1</sub>, P2Y<sub>2</sub>, and P2Y<sub>6</sub> receptors are preferentially coupled to Gq [116] and therefore have the potential to activate phospholipases that feed into TRPC6 [63]. The role of phospholipases in TRP channel signaling must be assessed with caution, because several of the most commonly used phospholipase inhibitors, such as U-73102, are direct inhibitors of certain TRP channels, including TRPC6 (unpublished observations). However, we have observed that tricyclodecan-9-yl-xanthogenate (D-609) can be used for experiments on TRPC6 channels, since it does not block responses evoked by diacylglycerol analogs. D-609 inhibits phosphatidylcholine-specific forms of

phospholipase C (PLC) as well as certain forms of phospholipase A2. We observed that pretreatment with 100  $\mu\text{M}$  D-609 for 30 min abolished responses to ATP (Fig. 5), suggesting that signaling from P2Y receptors to TRPC6 channels in podocytes entails activation of phospholipases.

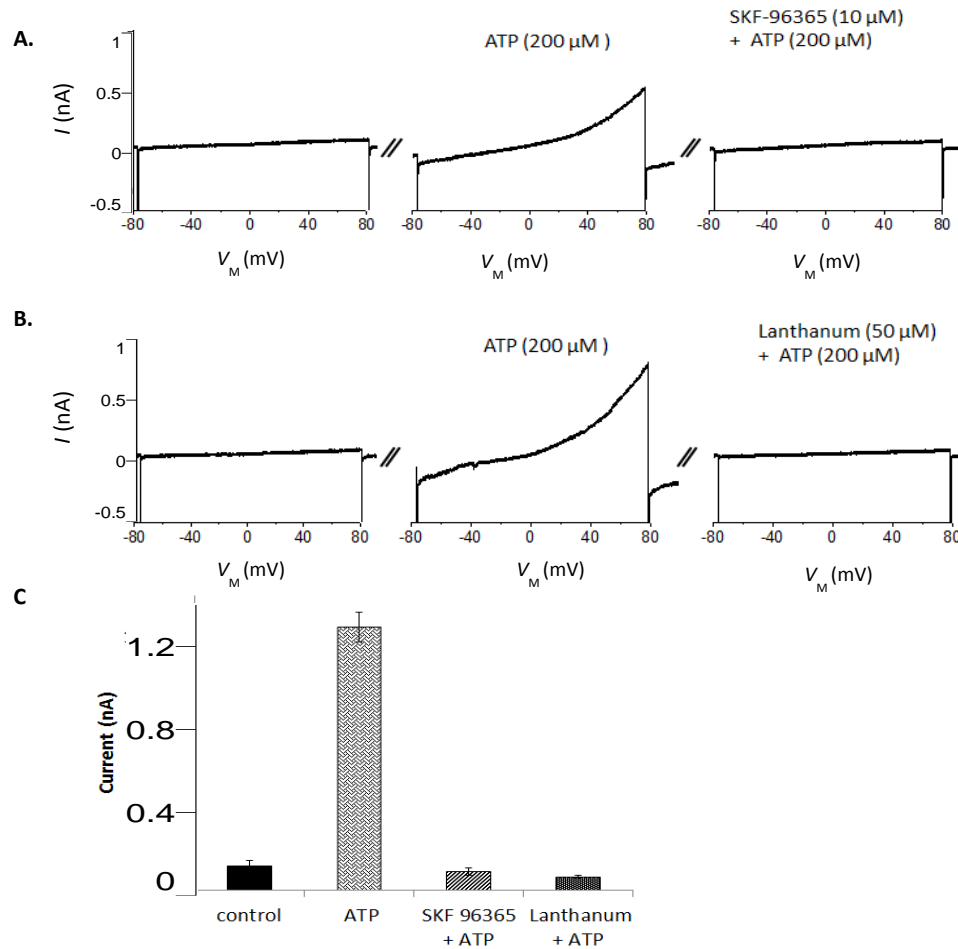


Figure 3. ATP-evoked cationic currents are blocked by TRP inhibitors in immortalized mouse podocyte cell lines. A: cationic currents evoked by 200  $\mu\text{M}$  ATP are blocked by 10  $\mu\text{M}$  SKF-96365, a nonselective inhibitor of TRP family channels, including TRPC6 and TRPC5. B: ATP-evoked cationic currents are completely blocked by 50  $\mu\text{M}$   $\text{La}^{3+}$ , an agent that blocks TRPC6 but not TRPC5. C: summary of several repetitions of this experiment (N = 5).

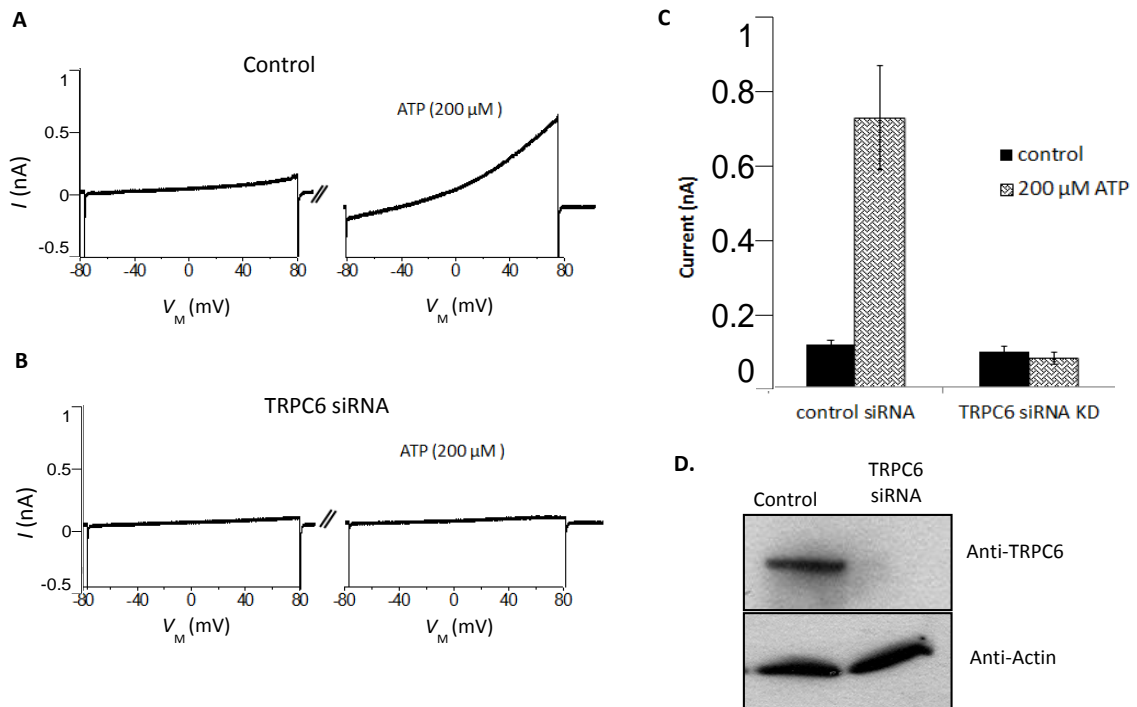


Figure 4. TRPC6 knockdown using siRNA eliminates ATP-evoked cationic currents in podocytes. A: ATP effects in a podocyte 24 h after transient transfection with a control siRNA. B: ATP response in podocyte 24 h after transient transfection with siRNA targeting TRPC6. C: summary (N = 6). D: immunoblot analysis of TRPC6 expression showing effectiveness of the siRNA knockdown.

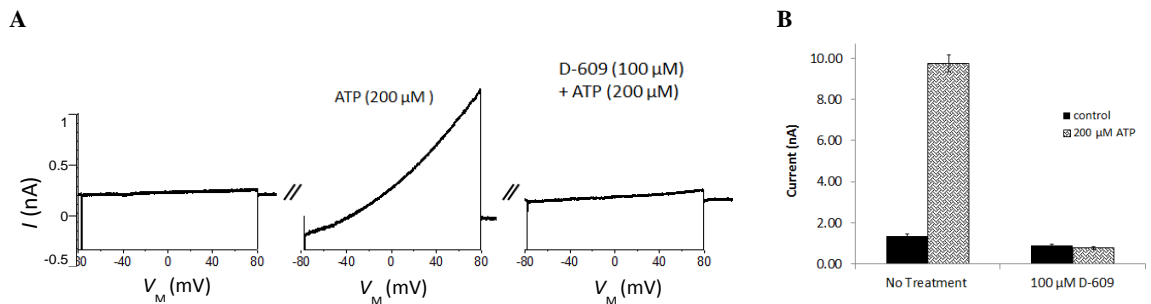


Figure 5. Phospholipase signaling is required for ATP activation of TRPC6 channels in immortalized mouse podocytes. A: after establishing a response to ATP, bath application of 100  $\mu$ M D-609 reversed activation of the currents. In pilot experiments we have shown that D-609 does not block TRPC6 activation by diacylglycerol analogs. B: cells were pretreated with control solution or 100  $\mu$ M D-609 for 30 min prior to testing of response to ATP by whole cell recording (N = 6).

Previous studies have shown that TRPC6 channels of podocytes become active in response to signals that increase generation of reactive oxygen species [65-67], including rapidly acting signals such as Ang II [67]. We observed that 30 min pretreatment with 10 mM tempol, a membrane-permeable superoxide dismutase mimetic, abolished responses to ATP (Fig. 6), suggesting a pathway similar to the one we previously described for Ang II [67]. In a more recent study we observed that podocyte TRPC6 channels reside in multiprotein complexes that include the NADPH oxidase NOX2, which can generate ROS locally to facilitate TRPC6 activation in podocytes [92]. The interaction between TRPC6 and NOX2 is indirect, and coimmunoprecipitation of these proteins requires the hairpin-loop inner membrane protein podocin [92]. As with our previous studies on Ang II [67], we observed that podocin knockdown using a panel of siRNAs eliminated ATP activation of TRPC6 channels, whereas responses were readily detected in cells transfected with a control siRNA (Fig. 7). Immunoblot analysis showed that podocin siRNA produced strong reductions in podocin expression but had no effect on TRPC6 (Fig. 7D).

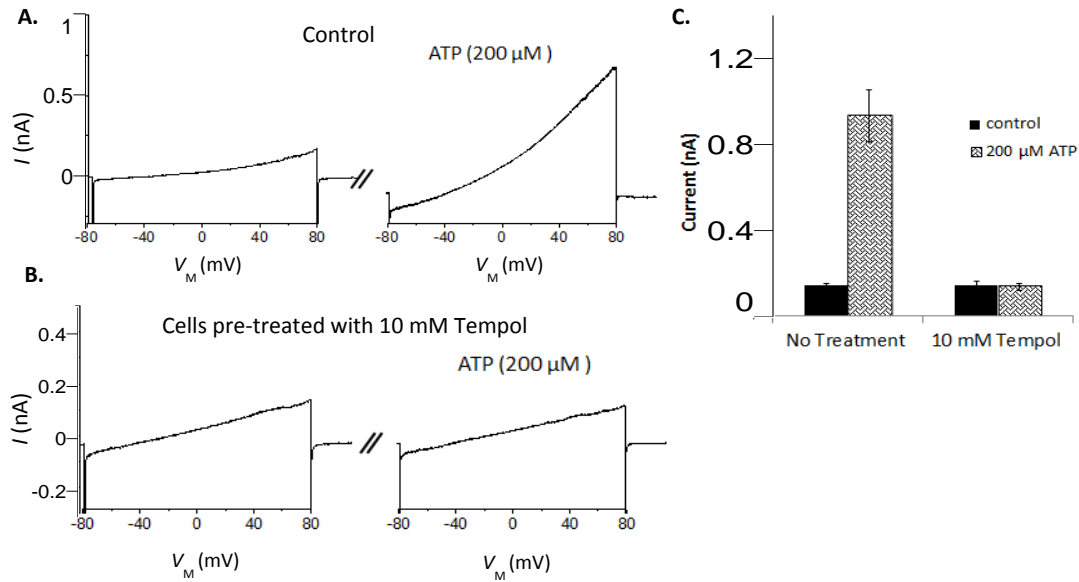


Figure 6. Reactive oxygen species contribute to TRPC6 activation by ATP in immortalized mouse podocytes. A: example of typical robust response to 200 μM ATP. B: ATP does not evoke significant cationic currents in cells pretreated with 10 mM tempol for 30 min. C: summary of results of this experiment (N = 6 cells).

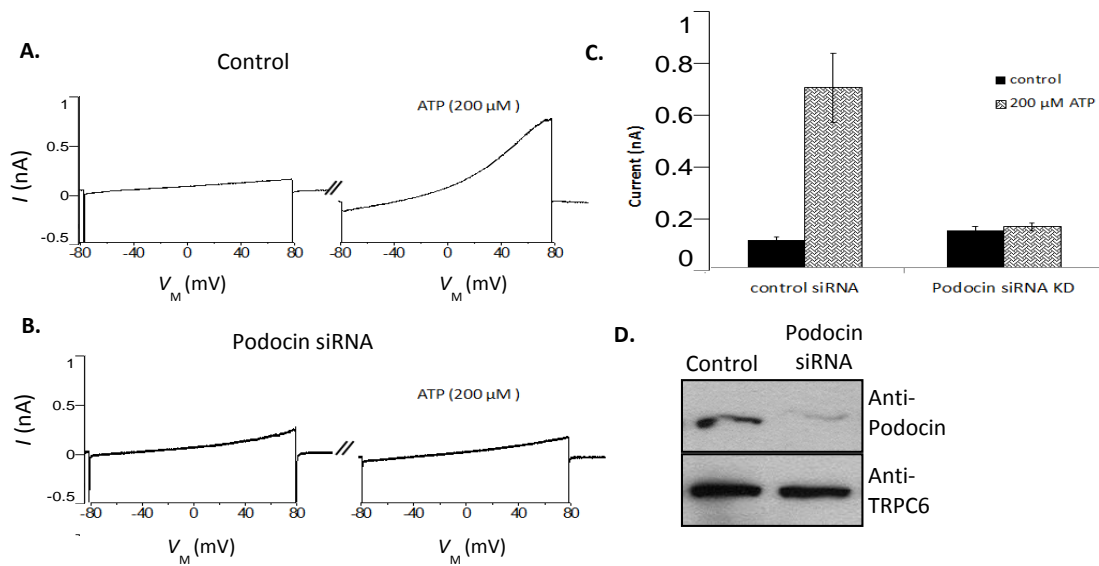


Figure 7. Podocin is required for ATP activation of TRPC6 in podocytes. A: response to 200 μM ATP recorded 24 h after transient transfection with a control siRNA. B: response to 200 μM ATP recorded 24 after transfection with an siRNA that targets podocin. C: summary (N = 6 cells). D: immunoblot analysis of podocin and TRPC6 expression showing effectiveness of the siRNA knockdown.

It is possible that changes in gene expression and cell physiology occur when podocytes are immortalized and propagated as a cell line. If the response to ATP is physiologically relevant, one would expect to see it in primary podocytes. To this end, we have employed an isolated decapsulated rat glomerulus preparation in which podocytes remain attached to the underlying glomerular basement membrane. This preparation does not require enzymatic digestion, and the podocytes on the external surface of the preparation can be readily seen using Hoffman modulation contrast optics. They are readily accessible to the recording electrode (Fig. 8A), the bath solution, and any agents that we may include in external culture media or recording solutions. We observed that bath application of ATP evoked robust increases in cationic current in this preparation, and these currents were completely blocked by subsequent exposure to 50  $\mu\text{M}$   $\text{La}^{3+}$  (Fig. 8, B and C). Treating the isolated glomerulus preparation for 24 h with the same TRPC6 siRNAs that we used on the immortalized cell lines resulted in a loss of ATP responses of podocytes located along the outer margin of the preparation, whereas glomeruli treated with control siRNA continued to show robust responses to ATP (Fig. 9). Immunoblot analysis confirmed reduction in TRPC6 expression by siRNA (data not shown). Collectively these data indicate that channel complexes containing TRPC6 subunits are required for ATP-evoked cationic currents in primary rat podocytes, as in the immortalized podocyte cell line.

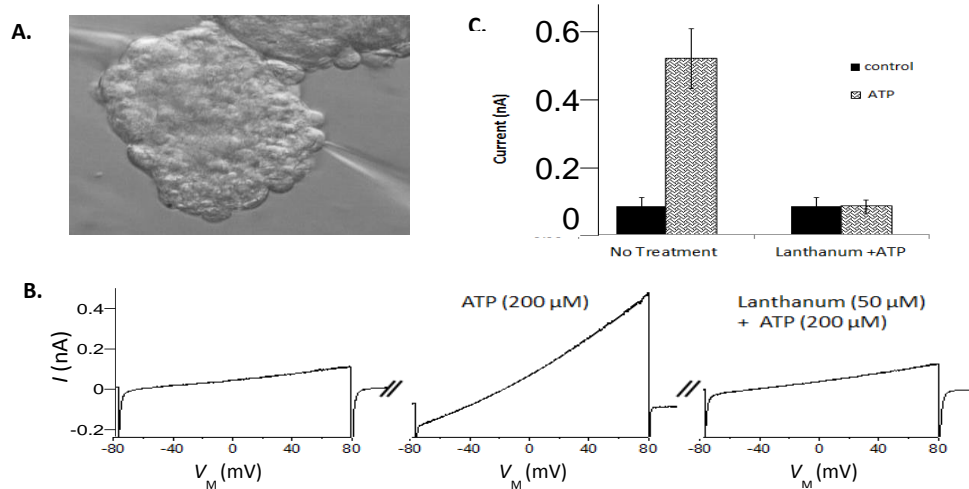


Figure 8. ATP evokes cationic currents in podocytes in isolated rat glomeruli. A: modulation contrast optics view of isolated decapsulated rat glomerulus with patch electrode attached to a podocyte located on the outer margin of the preparation. B: example of typical ATP-evoked current, and complete blockade of this response by 50  $\mu\text{M}$   $\text{La}^{3+}$  in the continued presence of ATP. C: summary of this experiment (N = 5 cells per group).

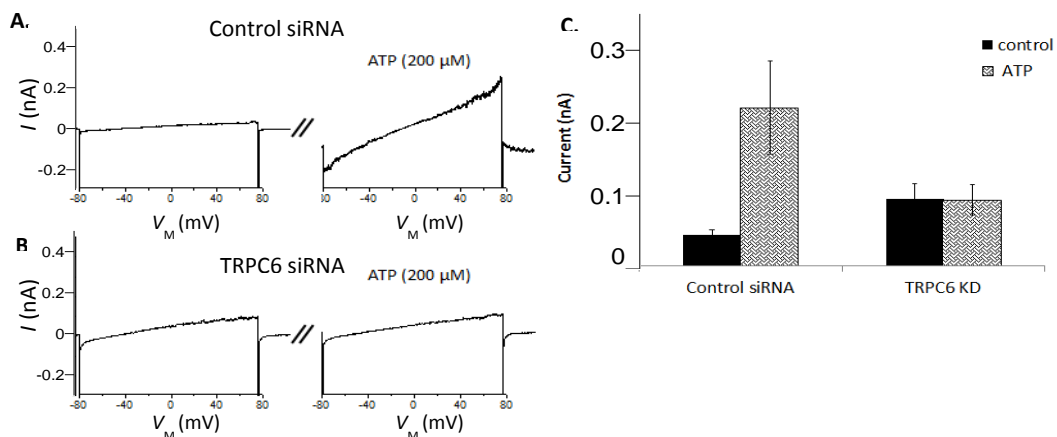


Figure 9. TRPC6 knockdown completely inhibits ATP responses in podocytes in isolated rat glomeruli. Glomeruli in this ex vivo preparation were transfected with control siRNA (A) or siRNA targeting TRPC6 (B) for 24 h. Cell culture medium was changed several times, and glomeruli were then transferred to recording chamber, where whole cell recordings were made from podocytes on the outer margin of the preparation. C: summary of the results of this experiment (N = 5 cells per group).

### 3.3 Discussion

In this study we have shown that ATP evokes robust activation of TRPC6 channels in immortalized mouse podocyte cell lines and in primary rat podocytes still attached to the glomerular basement membrane in *ex vivo* glomeruli. The effects of ATP are mediated by a G protein-coupled pathway from P2Y receptors, through a phospholipase, to the TRPC6 channels. At some point, most likely downstream of phospholipases [92], the transduction cascade generates ROS, which contribute to TRPC6 activation. In addition, the cascade requires podocin, which appears to function as a scaffold to allow for spatial co-localization of the various transduction components within cholesterol-rich membrane proteins [51, 64, 92]. In short, the transduction cascade is qualitatively similar to the one used in these cells by Ang II and AT1R receptors, which we have described recently [67].

Responses to ATP are generally larger than responses to Ang II at concentrations that evoke maximum responses [67]. The robustness of the response to ATP may occur because its signals are simultaneously transduced through multiple forms of P2Y receptors (especially P2Y<sub>1</sub> and P2Y<sub>2</sub>) [114], whereas Ang II signals to TRPC6 are only transduced by ATR1. Responses to UTP, UDP, and ADP suggest the presence of multiple functional P2Y receptors in these cells, which is largely consistent with a recent study [115]. It should bear noting, however, that this last study did not detect Ca<sup>2+</sup> influx in response to UDP. Collectively these observations also suggest that treatments that reduce ATP-evoked Ca<sup>2+</sup> overload into foot processes through this pathway could be especially effective therapeutic strategies. In this regard, a previous study has shown that sustained exposure to ATP can cause cell death in podocytes [114].

In principle, Ca<sup>2+</sup> overload in foot processes could be reduced by agents that inhibit

TRPC6 channels, or possibly by agents that inhibit ROS generation by NADPH oxidases [62]. The present results raise the possibility that P2Y antagonists might also reduce  $\text{Ca}^{2+}$  overload, assuming they could be tolerated. In this regard, P2Y<sub>1</sub> receptors expressed in podocytes have been shown to mediate  $\text{Ca}^{2+}$  influx [115] and are also expressed in proximal tubules where they have been proposed to play a role in regulation of bicarbonate transport [120]. P2Y<sub>1</sub> knockout mice are viable, but kidney function has not been assessed in these animals. P2Y<sub>2</sub> receptors are expressed in podocytes and in several different nephron segments and play a complex role in regulation of renal electrolyte and water transport [121]. P2Y<sub>6</sub> is also expressed in renal vasculature, although it is not responsive to ATP [122]. There is evidence suggesting that locally released ATP may modulate gating and steady-state surface expression of the epithelial sodium channel ENaC in the distal nephron [123-127] and may also regulate collecting duct aquaporin channels [128]. As a result, there is a net salt-resistant increase in mean arterial pressure in P2Y<sub>2</sub> knockout mice that appears to be associated with changes in multiple homeostatic systems [121] and which is consistent with the idea that global P2Y<sub>2</sub> activation results in a steady diuresis [129]. In addition, P2Y<sub>2</sub> knockout mice actually appeared to be more susceptible to various indexes of kidney damage by 8 weeks after subtotal (5/6) nephrectomy, including an increase in albuminuria compared with wild-type mice subjected to the same stress, although there was no increase in glomerulosclerosis in these experiments in the knockout mice [130]. These results would tend to suggest that P2Y<sub>1</sub> or P2Y<sub>2</sub> might be the most promising therapeutic targets for glomerular disease, with the caveat that the P2Y<sub>2</sub> knockout mice used in the studies cited above are complete, global (in every tissue) and constitutive (including during embryonic development) [131]. Therefore it may not be straightforward

to compare the physiology of those mice to what might occur with subtotal pharmacological blockade in a system that developed normally.

One unanswered question from these studies is the the source of ATP that might activate podocyte P2Y receptors during normal physiology. Glomerular endothelial cells are able to secrete ATP through connexin and/or pannexin hemichannels [111], and we favor this as a mechanism for propagation of  $\text{Ca}^{2+}$  waves to podocytes during TGF. The question of whether it is adenosine or ATP that carries the initial signals from the macula densa to the afferent arteriole [106, 107] is immaterial as to how the  $\text{Ca}^{2+}$  wave is subsequently propagated into the rest of the glomerulus. We know from Lucifer yellow dye-filling experiments that podocytes are not connected to other cells by gap junctions (unpublished data) and therefore orthograde signals must pass into podocytes, and possibly from one podocyte to another, by means of diffusible messengers. ATP is a prime candidate for this, based on previous studies on the effects of suramin and ATP scavengers on propagation of  $\text{Ca}^{2+}$  waves through the glomerulus during TGF [108]. Obviously, ATP is also freely filtered, and there would be minimal diffusional barriers for ATP released from glomerular endothelial cells to podocytes. ATP can also be modified by extracellular nucleotidases once it is secreted and can thereby produce ADP, which is also an effective agonist in podocytes.

We note that podocin knockdown abolished the ability of ATP to evoke cationic currents in podocytes. This observation is consistent with previous studies showing that podocin potentiates chemical activation of TRPC6 by diacylglycerol analogs [51, 64]. We have recently reported that podocin is required for co-localization of TRPC6 channels and NOX2 in podocytes [92], which can allow for a locally generated source of ROS to

modulate TRPC6 gating as part of a physiological transduction cascade without the need for toxic increases in cytosolic ROS. Thus our observations with podocin knockdown are consistent with the observation that tempol (a ROS quencher) also blocks ATP activation of TRPC6 in podocytes. However, if local ATP concentrations were sustained for a long period of time, for example during inflammation, it might result in oxidative damage to the foot process.

In summary we have demonstrated that ATP evokes activation of TRPC6 channels in podocytes through P2Y receptors, G protein signaling, and generation of reactive oxygen species. ATP-evoked cationic currents are abolished by treatments that inhibit or knockdown TRPC6, and ATP causes the largest activation of TRPC6 of any stimulus that we have examined. Ectonucleotide signaling to podocytes may therefore play a role in normal glomerular filtration or in the pathophysiology of glomerular disease.

## **4. 20-HETE ACTIVATES PODOCYTE TRPC6 CHANNELS: POSSIBLE PATHWAY FOR GLOMERULAR INJURY**

### **4.1 Introduction**

Podocytes are highly specialized terminally differentiated cells that cover the glomerular capillary and form the final barrier for glomerular filtration. Changes in podocyte ultrastructure often occur in response to glomerular injuries or disease processes. If these insults are sustained, podocytes will detach or die, which above a threshold leads to loss of the entire nephron [99]. Primary podocyte diseases can occur as a result of mutations to key genes expressed in podocytes, for example gain-of-function mutations in the gene encoding TRPC6 channels [56, 57] or mutations in the NPHS2 gene encoding podocin [52].

TRPC6 channels are  $\text{Ca}^{2+}$ -permeable cationic channels that play a role in G protein-mediated signaling in many cell types. Within the kidney, TRPC6 channels are expressed in mesangial cells and podocytes, and possibly in other cell types including vascular myocytes [112]. Within podocytes, TRPC6 channels are located in the slit diaphragm domains of foot processes, as well as in major processes, and in the cell body [51, 56, 57, 113]. TRPC6 channels in foot processes are components of larger complexes that include podocin, nephrin, NADPH oxidases, and phospholipases [64]. Additionally, over-expression of wild-type or mutant podocyte TRPC6 channels in mice results in proteinuria [61] and increased expression of glomerular TRPC6 is observed in acquired glomerular diseases [58, 60, 61].

In the past decade, a growing body of evidence has suggested a role for 20-

hydroxyeicosatetraenoic acid (20-HETE) in glomerular function and dysfunction. 20-HETE is the  $\omega$ -hydroxylated metabolite of arachidonic acid produced by a family of cytochrome P450 variants known as CYP4A, typically in transduction cascades that include phospholipase A activation [132]. CYP4A is expressed in the renal cortex and outer medulla, in the proximal tubule, the thick ascending loop, and within renal arterioles [132-137]. 20-HETE is a potent vasoconstrictor of renal arteries [138-140], and it is known to increase  $\text{Ca}^{2+}$  influx in vascular smooth muscle cells [141], and to cause activation of protein kinase C [141, 142], mitogen-activated protein kinases [143], tyrosine kinases [144], and the Rho kinase pathway [145]. There is evidence that 20-HETE is part of the transduction cascades used by vasoconstrictors such as ANG II, vasopressin, endothelin and norepinephrine [146-148].

In vascular smooth muscle, 20-HETE has been reported to cause activation of TRPC6 channels, and to act synergistically with exogenous DAG, the canonical lipid activator of TRPC6 [70]. In the present study we test the hypothesis that 20-HETE activates TRPC6 channels in immortalized mouse podocytes (MPC-5 cells) *in vitro*, and in primary rat podocytes that are still attached to the glomerular basement membrane of isolated glomeruli. We now report that 20-HETE exposure increases the steady-state surface expression of TRPC6 and increases cationic currents through TRPC6 channels in podocytes. We also show that 20-HETE and a DAG analog cause at least additive activation of podocyte TRPC6 channels, and that the ROS are required for 20-HETE modulation of TRPC6 channels. Finally we show that podocin is required for endogenous podocyte TRPC6 channels to respond to 20-HETE.

## 4.2 Results

In the kidneys, 20-HETE is stored in tissue lipids, representing a significant reservoir in these tissues, and are released in response to hormonal stimuli such as angiotensin II- and receptor-mediated hydrolysis of phospholipids [149]. Therefore, during glomerular injury, the concentration of renal 20-HETE increases in the vicinity of podocyte. Here we observed that 1  $\mu$ M 20-HETE increased steady-state cell surface expression of TRPC6 channels in MPC-5 cells (Fig. 1A), and the increase was more than 2 fold (Fig. 1B). As a result, the abundance of TRPC6 channels on the cell surface of the podocytes are doubled in response to 20-HETE.

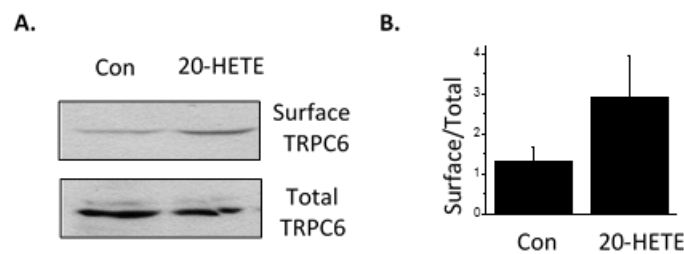


Figure 1. 20-HETE increases steady-state cell surface expression of TRPC6 channels in MPC-5 cells. A: Immunoblot analysis depicting increased expression of TRPC6 channels in MPC-5 cells in response to 1  $\mu$ M 20-HETE. B: Densitometric analysis of three repetitions of the experiment shown in A.

Next, we exposed MPC-5 cells or isolated rat glomeruli to 1  $\mu$ M 20-HETE by gravity-fed bath superfusion, and performed the whole-cell recordings on podocytes. Application of 1  $\mu$ M 20-HETE to immortalized mouse podocytes evoked a cationic current (Fig. 2A and 2B), which were further abolished by addition of 10  $\mu$ M SKF 96365, a

nonselective pan-TRP channel blocker, or 50  $\mu\text{M}$   $\text{La}^{3+}$  as a TRPC6 channel inhibitor. We observed the same pattern in intact podocytes attached to the freshly isolated rat glomeruli (data not shown). TRPC6 channels are completely blocked by micromolar concentrations of  $\text{La}^{3+}$ , however, TRPC5 which is another subunit expressed in podocytes are instead, activated by micromolar concentrations of  $\text{La}^{3+}$  [118, 119]. This observation suggest that the cationic currents evoked by 20-HETE are mediated by TRPC6 channels in a concentration dependent manner (Fig. 2C). To further confirm whether 20-HETE-induced cationic currents require TRPC6 channels, we used siRNA protocol to knockdown TRPC6 channel transcripts and observed that 20-HETE did not activate TRPC6 channels in the podocytes that were treated with TRPC6 siRNA; whereas, 20-HETE continued activating these channels in the control set (Fig. 2D and 2E). To validate our siRNA knockdown assay, we performed an immunoblot showing effectiveness of the siRNA knockdown (Fig. 2F). Overall, our data suggest that the 20-HETE-evoked cationic currents in immortalized mouse podocytes are mediated by channels containing TRPC6 subunits.

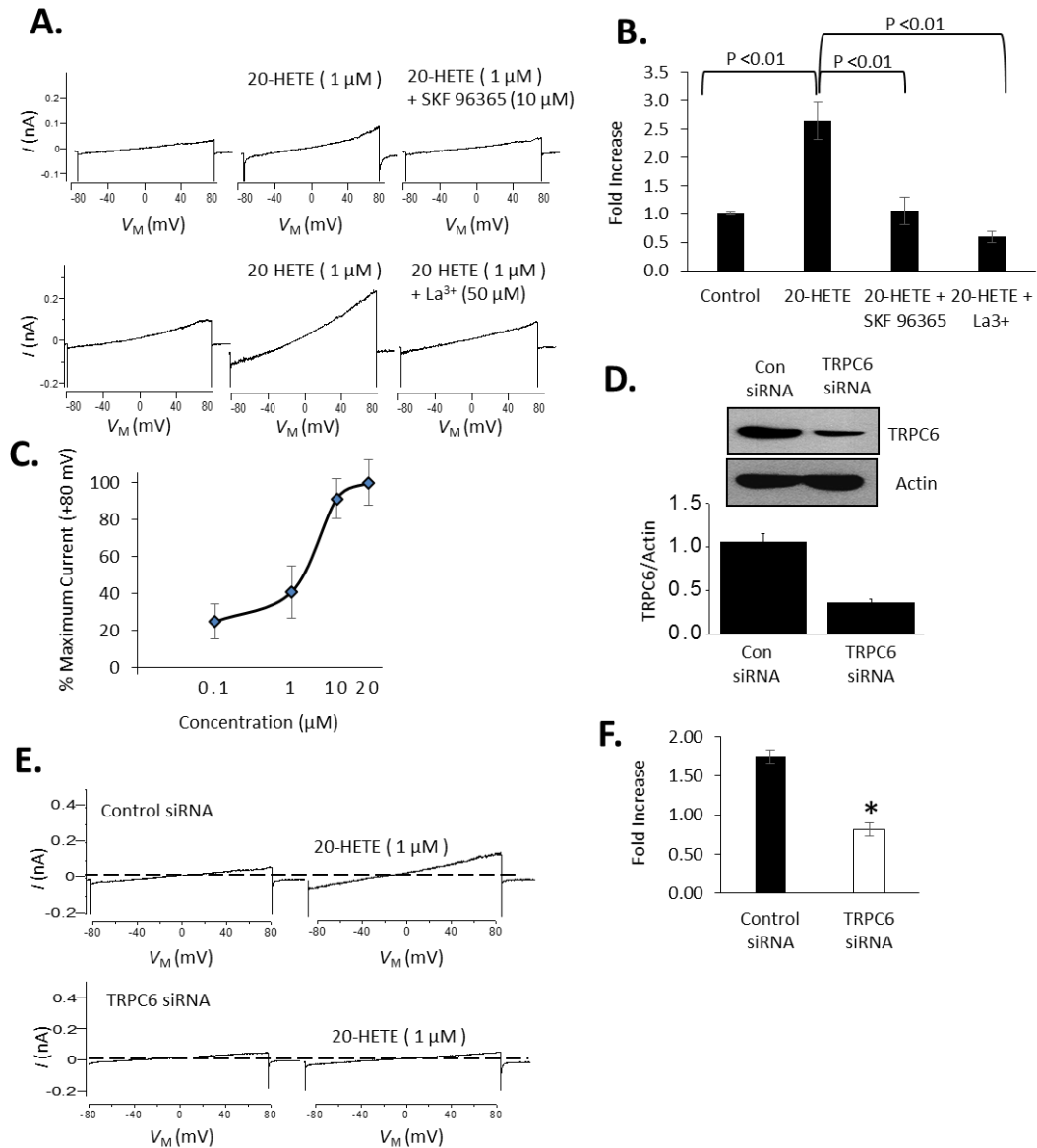


Figure 2. 20-HETE evokes TRPC6 channel currents in MPC-5 cells. A: Immortalized mouse podocytes exposed to 20-HETE showed an increase in cationic currents that are blocked by non-specific pan-TRP channel inhibitor SKF 96365 (10 μM), and TRPC6 channel blocker Lanthanum (50 μM). B: Currents at +80 mV in cells with no treatment (control), treated with only 20-HETE, mixture of 20-HETE and SKF 96365, or mixture of 20-HETE and Lanthanum (La<sup>3+</sup>) (N = 10). Tukey HSD test P < 0.01 and one-way Anova P < 0.0001. C: Percentage maximum TRPC6 current in response to 20-HETE concentrations. D: Immunoblot analysis of TRPC6 expression showing effectiveness of the siRNA knockdown. E: Example of 20-HETE effects in a podocyte 24 h after transient transfection with a control (nontargeting) and siRNA targeting TRPC6. siRNA TRPC6 knockdown eliminates 20-HETE-evoked cationic currents in MPC-5 cells. F: Summary of several repetitions of this experiment (N = 6), with two-tailed P = 0.0001.

20-HETE effects on TRPC6 channel currents in podocyte cell line require podocin and ROS. A recent work by our group showed that TRPC6 channels are located in a multiprotein complex, where NADPH oxidase NOX2 exists and can locally generate ROS to assist in activation of TRPC6 channels in podocytes [92]. TRPC6 channel and NOX2 interact via a hairpin-loop inner membrane protein called podocin [92]. We had previously reported that podocin knockdown eliminated angiotensin II- and ATP-induced TRPC6 channel activation in podocytes [67, 150]. Here we observed that application of 20-HETE to cells treated with podocin siRNA did not activate TRPC6 channels (Fig. 3A and 3B), and podocin siRNA is effective in abolishing the protein expression of TRPC6 channels (Fig. 3C). Moreover, consistent with our previous findings where we observed that TRPC6 channels become active in response to signals that increase production of ROS [65-67, 150], in this study we showed that 20-HETE increased the intracellular ROS levels in podocytes (Fig. 4A). To further confirm whether ROS are required for 20-HETE modulation of TRPC6 channels, we pretreated podocytes for 30 minutes with 10 mM tempol, a membrane-permeable superoxide dismutase mimetic, and performed whole-cell recording from podocytes. Results indicated that pre-treatment of cells with tempol abolished TRPC6 channel activation in the presence of 20-HETE (Fig. 4B, 4C). In brief, 20-HETE effects on TRPC6 channels in podocytes required podocin and ROS.

20-HETE and OAG have synergistic effects on TRPC6 channels. The canonical pathway of TRPC6 channels activation includes involvement of DAG. OAG is a diacylglycerol analog and is widely used to activate TRPC6 channels in podocytes. To test the hypothesis that 20-HETE and OAG have additive effects on TRPC6 channels, we first applied 100  $\mu$ M OAG to the bath solution and activated TRPC6 channels, while OAG was

running, we then introduced 1  $\mu\text{M}$  20-HETE as well in the presence of OAG. We observed that 20-HETE and OAG caused synergistic activation of TRPC6 channels in podocytes (Fig. 5A and 5B). Also, it is observed that the order of activation does not matter (Fig. 5C and 5D). This simply suggests that 20-HETE and OAG activate TRPC6 channels through different pathways, and therefore, the presence of both molecules in the running bath solution have additive effect on TRPC6 activation.

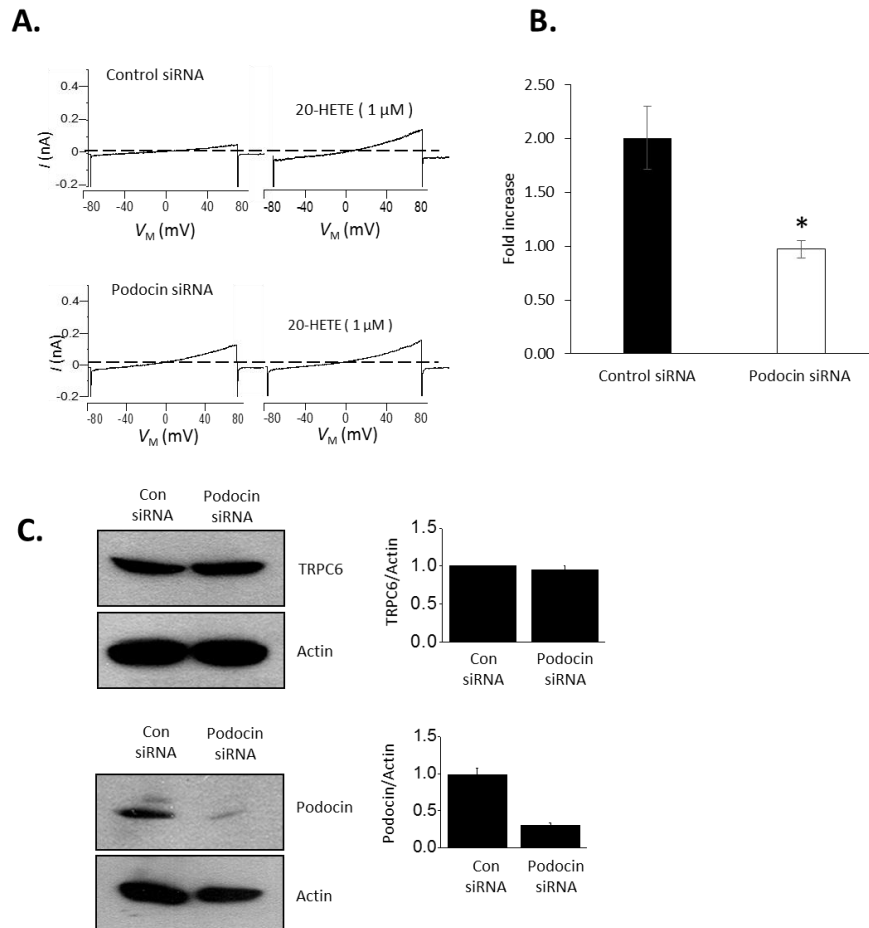


Figure 3. Podocin siRNA knockdown eliminates 20-HETE-induced TRPC6 channel currents in MPC-5 cells. A: Example of 20-HETE effects in a podocyte 24 h after transient transfection with a control (nontargeting) and siRNA targeting podocin. siRNA podocin knockdown abolished 20-HETE-evoked cationic currents in MPC-5 cells. B: Summary of several repetitions of this experiment ( $N = 6$ ), two-tailed  $P = 0.0009$ . C: Immunoblot analysis of TRPC6 expression in podocin knockdown cells and showing the effectiveness of the siRNA knockdown.

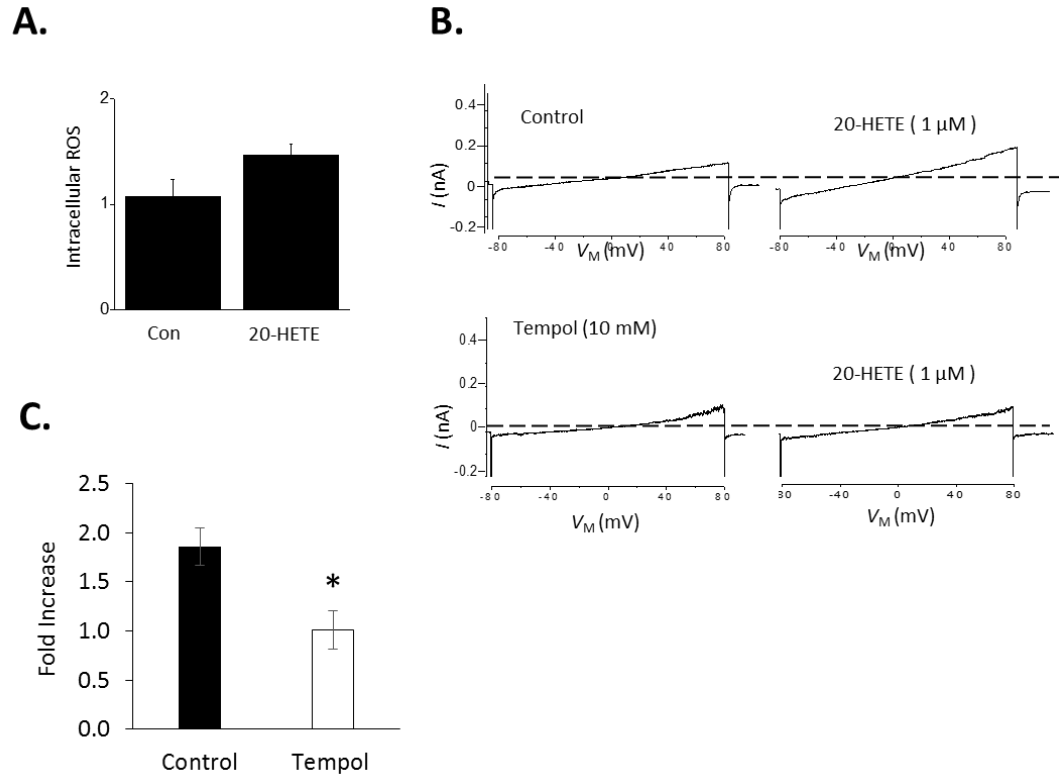


Figure 4. 20-HETE evoked TRPC6 channel activation requires ROS. A: 20-HETE increases the intracellular ROS levels in immortalized mouse podocytes. B: 20-HETE does not evoke significant cationic currents in cells pretreated with 10 mM tempol for 30 min. C: Summary of results of this experiment (N = 6 cells), two-tailed P < 0.0001.

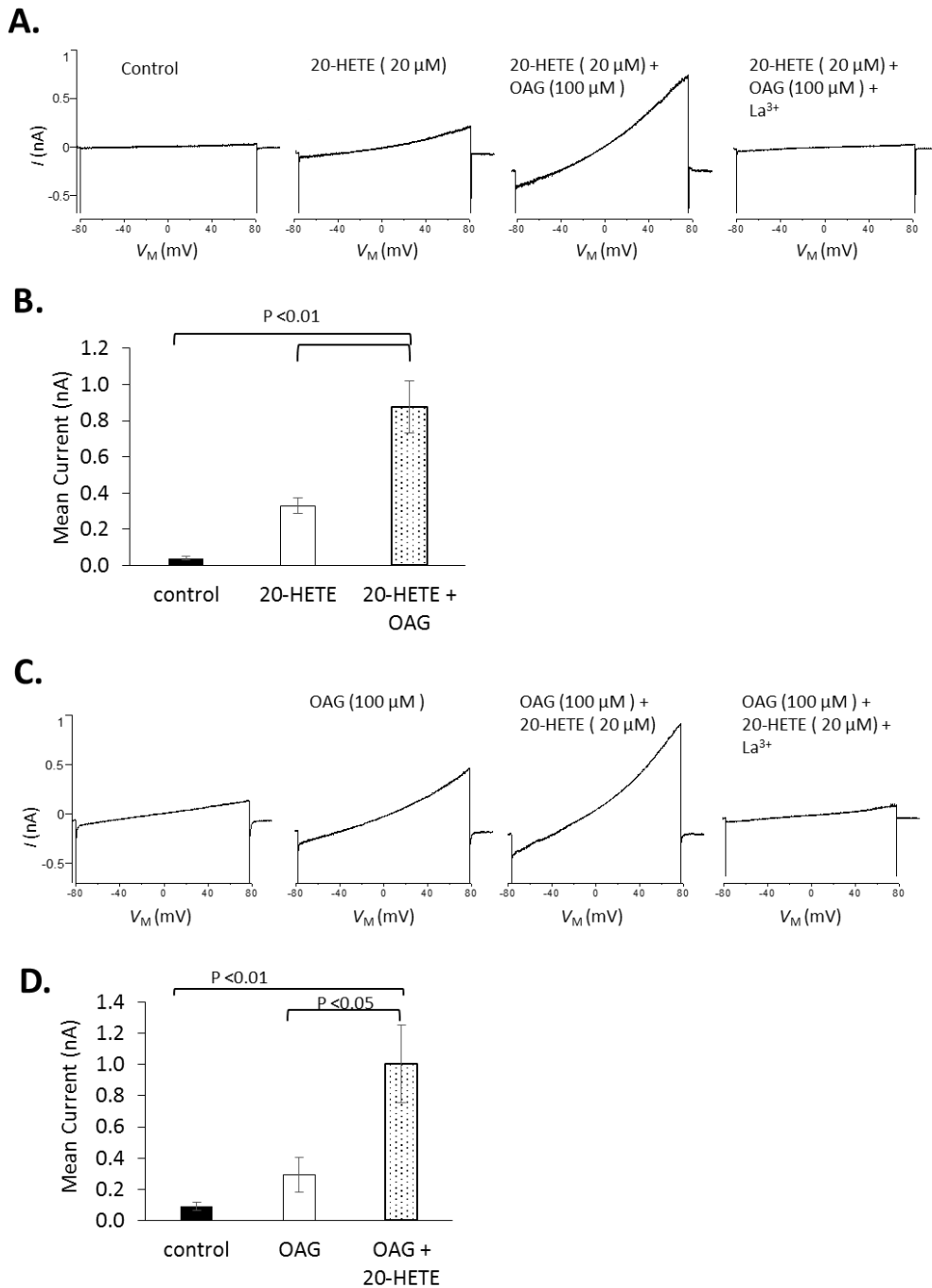


Figure 5. 20-HETE and OAG cause synergistic activation of TRPC6 channels. A: Example of synergistic effects of OAG and 20-HETE in MPC-5 cells. B: Summary of several repetitions of this experiment (N = 4), Tukey HSD Test  $P < 0.01$ , and one-way Anova  $P = 0.0013$ . C: Reverse order of the same experiment in A. D: Summary of several repetitions of C (N = 4), Tukey HSD Test  $P < 0.01$ ,  $P < 0.05$ , and one-way Anova  $P = 0.003993$ .

### 4.3 Discussion

Here we report that 20-HETE-evoked cationic currents in immortalized mouse podocytes *in vitro* and in intact podocytes on the freshly isolated rat glomeruli (*ex vivo*) are mediated by channels containing Ca<sup>2+</sup>-permeable TRPC6 subunits. Over-expression of podocyte TRPC6 channels in mice results in proteinuria [61]; also, an increased expression of glomerular TRPC6 is observed in acquired glomerular diseases [58, 60, 61]. Proteinuria and glomerular diseases are characterized by pathologic alterations in normal glomerular structure and function, primarily in podocytes that form the filtration barrier. An increase in intracellular Ca<sup>2+</sup> levels in podocytes, apoptosis, and podocyte loss are some key features occurring in glomerular diseases. Therefore, increase in steady-state cell surface expression of Ca<sup>2+</sup>-permeable TRPC6 channels and their increased activation could very well be the primary pathway leading to glomerular diseases.

The podocin protein, TRPC6 channels, and NADPH oxidase NOX2 are present in a complex found in the cholesterol-rich regions of the cell membrane [92]. NOX2 generates ROS, which can immediately upregulate TRPC6 channels in its vicinity [92]. In this study, we observed that exposing immortalized mouse podocytes to 20-HETE causes an increase in the intracellular ROS levels. We also showed that 20-HETE induced activation of TRPC6 channels in podocytes requires ROS. Podocin is a hairpin-loop inner membrane protein that brings TRPC6 channels and NOX2 together. Podocin is also one of the key proteins in the slit diaphragm. Mutations in the gene encoding podocin leads to primary podocyte diseases [52].

We tested the hypothesis that podocin is required for the 20-HETE induced TRPC6 channels activation, and we observed that podocin is necessary for this TRPC6 activation

mode. We also noticed that 20-HETE and OAG caused synergistic activation of TRPC6 channels in podocytes. This observation suggests that the pathway by which 20-HETE activates TRPC6 channels is separate from the canonical activation pathway of these channels. Hence, OAG and 20-HETE have an additive effect on activation of TRPC6 channels.

In the past decade, several studies imply that 20-HETE plays a key role in the renal pathologies. 20-HETE is shown to regulate tubuloglomerular feedback, blood pressure, chronic kidney disease, diabetic nephropathy (DN), and polycystic kidney disease (PKD) [151-156]. Therefore, it is most likely that 20-HETE leads to an increase in intracellular  $\text{Ca}^{2+}$  levels in podocytes through activation of TRPC6 channels in pathological conditions, which then leads to other downstream effects such as podocyte foot process effacement, apoptosis, and podocyte loss. The role of 20-HETE in kidney pathology is controversial. However, depending on the location of its synthesis and the target cell type, it may play a protective or deleterious role in glomerular injury. Some studies showed that 20-HETE is elevated in the serum of autosomal dominant PKD patients [155] and also in *in vitro* and *in vivo* models of DN [157, 158]. Other studies showed that 20-HETE levels in renal circulation are decreased in both type I and type II diabetic animal models with hyperfiltration and glomerular disease [159, 160]. There are supporting data on a protective role of 20-HETE against renal injury by ischemia-reperfusion injury [161], whereas, another set of data supports the fact that antagonists of 20-HETE play protective roles in IRI, and not 20-HETE [162].

Here we report that 20-HETE activates TRPC6 channels in podocytes, which allows for  $\text{Ca}^{2+}$  influx. Our results are consistent with previously published data on vascular

smooth muscle cells [70]. In our study we report that 20-HETE causes an increase in ROS levels that would further upregulate steady-state cell surface expression of TRPC6 channels in podocytes. The increase in  $\text{Ca}^{2+}$  influx make podocytes contract, which could very well be part of a physiological response of podocyte to stimuli, in order to maintain the integrity of the slit diaphragm, preventing podocytes from detaching from GBM, and providing necessary stability to the glomerular capillary wall [163]. Consequently, inhibiting TRPC6 channels or pathways leading to 20-HETE-induced activation of these channels could be a promising therapeutic target for glomerular injuries.

## 5. DYSFUNCTION OF PODOCYTE TRPC6 CHANNELS IN *IN VIVO* AND *IN VITRO* MODELS OF FSGS: A ROLE FOR MULTIPLE INTERACTING CIRCULATING FACTORS?

### 5.1 Introduction

Focal segmental glomerulosclerosis (FSGS) refers to lesions in which portions of a glomerular capillary tuft are obliterated by extracellular matrix in a subset of glomeruli. FSGS lesions can arise from any pathological process that causes a loss of podocytes and denudation of patches of the external surface of a glomerular capillary. This can occur as a consequence of podocyte detachment caused by hyperfiltration, by viral infections that cause de-differentiation of podocytes, by chemically-induced podocyte damage, and as a result of dysfunctions of immune responses [38].

In addition to these “acquired” forms of FSGS, genetic studies have identified several genes that are mutated in familial forms of FSGS, two of which encode proteins central to the current study. Mutations in the *NPHS2* gene encoding the hairpin loop protein podocin give rise to severe nephrotic syndromes that often present in children [52]. The disease caused by *NPHS2* mutations has an autosomal recessive mode of inheritance, and many of the *NPHS2* mutations identified to date give rise to non-functional proteins that are frequently retained in the endoplasmic reticulum [49]. Several gain-of-function mutations in the *TRPC6* gene were subsequently identified in patients with familial FSGS [56-58]. The *TRPC6* gene encodes a  $\text{Ca}^{2+}$ -permeable cation channel expressed in many different cell types, including mesangial cells and podocytes. FSGS associated with *TRPC6* mutations usually presents with an adult onset, and the resulting disease has an autosomal dominant mode of inheritance [56, 57]. *TRPC6* and podocin are expressed at the slit

diaphragm domains of podocytes and there are functionally significant biochemical interactions between these two proteins [49, 51, 56, 64]. Podocin, like other members of the stomatin-prohibitin family, is a cholesterol-binding protein that tends to form higher-order oligomers within lipid rafts. Podocin regulates the dominant mode of TRPC6 gating, facilitating activation of these channels by G protein signaling pathways or by canonical lipid activators such as diacylglycerol, but suppressing activation by as yet unknown mechanotransduction pathways [64, 68, 92].

Many cases of histologically verified FSGS are idiopathic. Patients with nephrotic levels of proteinuria have a high risk of progressive renal failure when they do not respond to glucocorticoids [164]. Moreover, a substantial portion of patients who receive a kidney allograft as a result of steroid-resistant primary FSGS will experience early recurrence of nephrotic range proteinuria [164]. It is now generally accepted that recurrence of FSGS in an allograft recipient is caused by circulating factors that cause changes in the cell physiology of podocytes [32]. In addition, several studies have reported that patients with primary FSGS have elevated glomerular expression of TRPC6 [60] and reduced expression of podocin [165]. A loss of podocin can be recapitulated *in vitro* by exposing cultured podocytes to serum from patients with recurrent FSGS [166, 167].

The identity of the circulating “permeability factor” in primary FSGS has been controversial. One candidate is the soluble urokinase plasminogen activator receptor (suPAR) [31], a term that encompasses a class of 22-50 kD glycoproteins shed from various hematopoietic cells, endothelial cells, fibroblasts, and smooth muscle cells as a result of proteolytic or phospholipase-mediated cleavage of a glycosylphosphatidylinositol-anchored glycoprotein [168]. It was originally reported that total plasma suPAR levels are

elevated in a subset of patients with FSGS, especially patients with recurrent forms of FSGS [31], and this association was subsequently found to be stronger when urine levels of suPAR were measured [169]. However, other studies have not observed a correlation between total plasma suPAR and primary FSGS, and instead have found that suPAR levels increase whenever eGFR levels decline [170, 171]. In addition, while an early study showed that intravenous injection or transient cutaneous over-expression of recombinant suPAR could evoke proteinuria in mice [31], another study failed to detect proteinuria or glomerulosclerosis in a mouse over-expressing a high molecular weight form of suPAR in the liver [170].

Other circulating factors have been proposed to mediate recurrent FSGS. A handful of case reports have observed remissions of recurrent FSGS by anti-TNF therapy in pediatric patients [36, 172, 173]. In addition, there are reports that circulating TNF is elevated in patients with primary nephrotic syndromes [33], and monocytes isolated from these patients secrete TNF at an order of magnitude greater rate than monocytes from healthy controls [34, 174]. Moreover, effects of plasma from patients with recurrent FSGS on podocyte cytoskeletal organization were blocked by antibodies that absorb soluble TNF and by agents that block TNF receptors [36]. Mutations that cause hyperactivation of TNF receptors cause severe nephrosis that can be blocked by etanercept, an inhibitor of TNF receptors [175], and sustained TNF infusion induces glomerular pathology [176]. There is also evidence that TNF increases the albumin permeability of isolated glomeruli [177]. Finally, other circulating factors, such as cardiotrophin-like cytokine 1, which activates transduction cascades that overlap those of TNF, may also contribute to recurrent FSG. On the basis of reported literature, there is reason to suspect that primary FSGS patients, even

the subset whose disease recurs after transplantation, are not homogeneous.

The results in the present study support a model in which a loss of surface podocin and an accompanying change in the dominant mode of TRPC6 gating occurs in several experimental models of FSGS *in vivo* and *in vitro*. They also support a “multiple circulating factor” model of primary FSGS, in which suPAR, TNF, and probably other circulating factors produce distinct but additive or synergistic effects on podocytes that converge on TRPC6. Put another way, the effects of a single factor, for example suPAR, may be conditional. This model suggests that correlations between circulating levels of any one circulating factor and clinical status in primary FSGS may not always be seen, even when that factor contributes to the pathology.

## 5.2 Results

Repeated intraperitoneal (i.p.) injection of puromycin aminonucleoside (PAN) produces sustained proteinuria accompanied by histological changes that resemble FSGS in humans [178]. In the present experiments, Sprague-Dawley rats were given multiple i.p. injections of PAN (200 mg/kg) or saline at 30-day intervals. Urine samples were collected from each rat before this protocol, and 10 days after the first and second PAN injections. This resulted in a marked increase in 24-hr urine albumin excretion (Fig. 1A). Rats were sacrificed 30 days after the last PAN injection. A portion of one kidney was used for histological analysis, which revealed sclerosis of glomeruli in the PAN treated animals (Fig. 1B). We also observed protein casts in tubules accompanied by tubular atrophy and interstitial hypercellularity as described by others (Fig. 1C) [179]. Glomeruli were isolated from the remaining renal cortex using a standard sieving procedure. Using immunoblot

analysis, we observed markedly reduced podocin abundance in glomeruli from PAN-treated rats, whereas total TRPC6 and podocalyxin were increased relative to either actin or total nephrin (Fig. 1D and 1E).

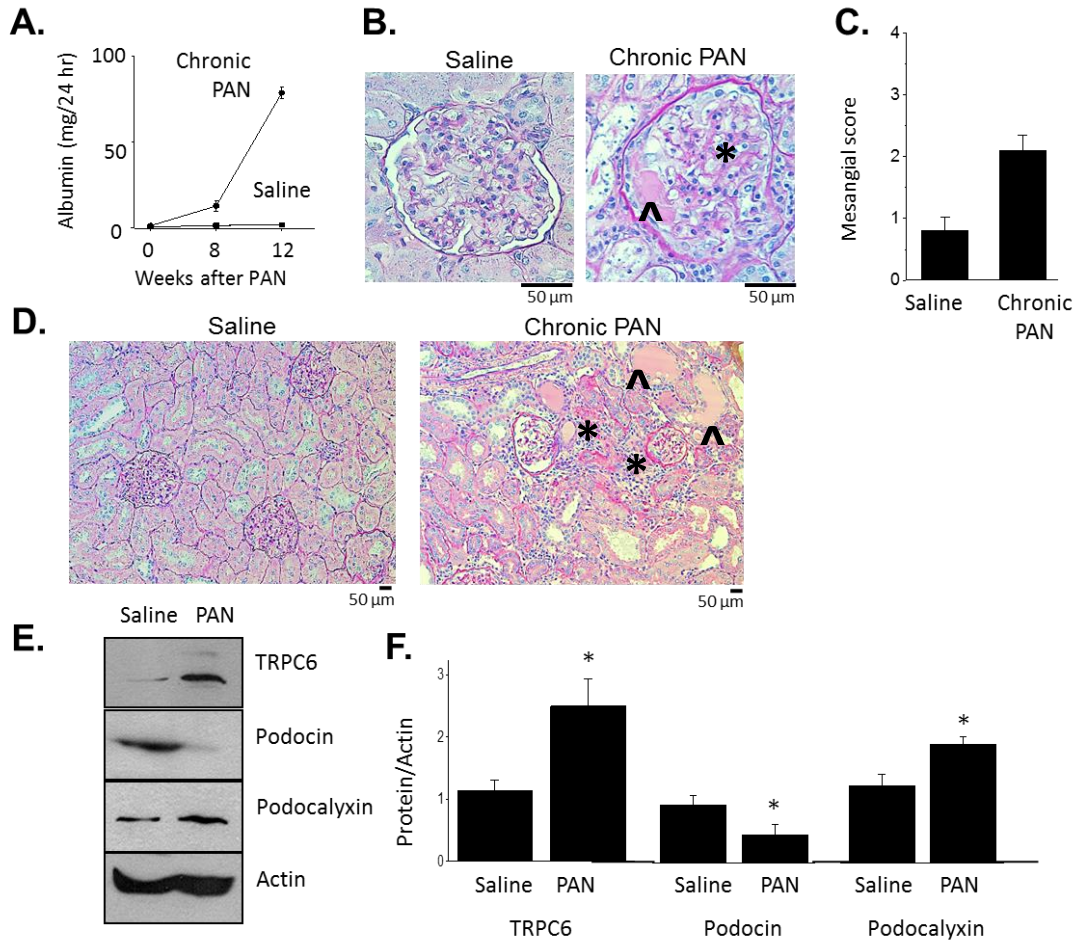


Figure 1. Altered abundance of TRPC6 and podocin in PAN-induced secondary FSGS in adult Sprague-Dawley rats. A: Increased 24-hr albumin excretion in chronic PAN nephrosis, twelve weeks after first injection. B: Periodic acid–Schiff (PAS) staining of FSGS lesions in a PAN-treated rat, compared to normal glomeruli from a saline-treated rat. Glomerulosclerosis (\*) and protein cast (^) are observed in PAN-treated rats. C: Lower magnification of PAS staining showing tubulointerstitial fibrosis and hypercellularity (\*), and tubular protein casts (^) in chronic PAN nephrosis model. D: Immunoblot showing increased TRPC6 channel abundance and decreased podocin abundance in isolated decapsulated glomeruli from a PAN treated rat. E: Densitometric analysis from a total of four rats (D). Unpaired student t-test used for statistical analysis ( $P < 0.05$ ).

Whole-cell recordings were performed from podocytes in decapsulated glomeruli isolated from saline-treated animals and rats with chronic PAN nephrosis (Fig. 2). Currents were monitored during application of 2.5-s voltage ramps (-80 to +80 mV). In glomeruli from saline-treated rats, modest and approximately equivalent increases in cationic currents were evoked by a mechanical stimulus comprised of 70% hypoosmotic stretch as described previously [64] (Fig. 2A) or after application of a membrane-permeable diacylglycerol analog (100  $\mu$ M OAG) (Fig. 2B). In previous electrophysiological studies on podocytes we have shown that these currents are eliminated by TRPC6 knockdown and several agents known to inhibit TRPC6 channels [67]. The currents evoked by mechanical stimulation were typically around 5-10 fold larger in glomeruli isolated from PAN-treated rats (Fig. 2A). By contrast, OAG failed to evoke any increase in current in the majority of recordings from PAN-treated rats, whereas podocytes from saline-treated controls responded consistently (Fig. 2B). Data from many recordings of this type are summarized in Fig. 2C, in which the ordinate represents the fold increase in current at +80 mV evoked by a given stimulus (and thus 1.0 corresponds to the amplitude of the basal current prior to application of stretch or OAG). In brief, chronic PAN nephrosis results in reductions in podocin abundance in glomeruli accompanied by changes in the dominant mode of TRPC6 activation in podocytes that are qualitatively similar to those seen after podocin knockdown [64].

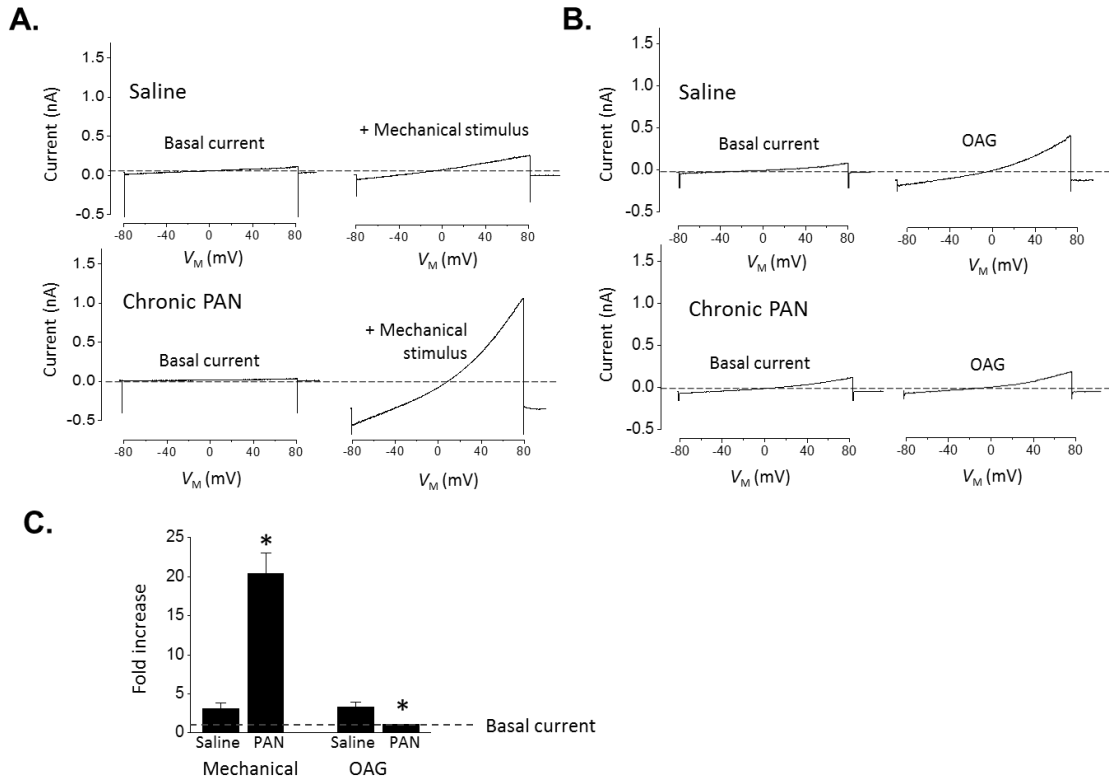


Figure 2. Altered cationic currents in podocytes in isolated decapsulated glomeruli from chronic PAN nephrosis rats. A: Example of hypoosmotic solution effect and B: canonical lipid activation effect on cationic currents during voltage ramp (-80 to +80 mV over 2.5 s). Note large cationic currents observed in the presence of hypoosmotic bath solution (mechanical stimulus) in PAN nephrosis rat compared to currents in saline treated controls. By contrast, cationic currents evoked by membrane-permeable diacylglycerol analog (OAG) were reduced in PAN nephrosis rat compared to those seen in the saline-treated control. C: Summary of the fold increases of cationic currents in response to mechanical stimulus (left) and canonical lipid activation (right) in podocytes of isolated rat glomeruli (N = 10 cells per group). Unpaired student t-test used for statistical analysis (P < 0.05).

The differentiated cells of an immortalized mouse podocyte cell line (MPC-5 cells) were cultured for 24 hr in the presence of plasma samples from an adult male patient (001) with recurrent FSGS taken while he was in relapse (in September of 2007), and a sample taken after this patient had achieved remission as a result of intensive plasmapheresis (in

October of 2007) (Fig. 3). These plasma samples were added to standard culture media at a concentration of 2% and cells were exposed to this plasma for 24 hr. The plasma sample taken while patient 001 was in relapse virtually eliminated podocin detected by immunoblot, whereas a sample taken from the same patient, after remission was achieved, had no effect on podocin abundance compared to cells cultured in fetal bovine serum (Fig. 3A, left). The sample taken in relapse also increased steady-state surface expression of TRPC6 compared to the control, as measured by cell surface biotinylation assays, whereas the sample taken in remission did not have this effect (Fig. 3A, right). We have seen a similar pattern (increase in surface TRPC6 accompanied by loss of podocin) using serum or plasma samples from several other patients with recurrent FSGS. Effects of samples from two of these patients (denoted as 002 and 003) are shown in Fig. 3B). We should note however, that plasma samples from some recurrent FSGS patents do not entirely recapitulate this pattern. For example, plasma from patient 006 at a concentration of 10% induced an increase in the surface abundance of TRPC6 and this effect was greater during a relapse of the disease, but this material had no effect on the abundance of podocin (Fig. 4). In addition, we note that the increase in surface abundance of TRPC6 is not an obligatory consequence of the loss of podocin, since podocin knockdown in this cell line actually caused a modest decrease in steady-state surface levels of TRPC6 (data not shown).

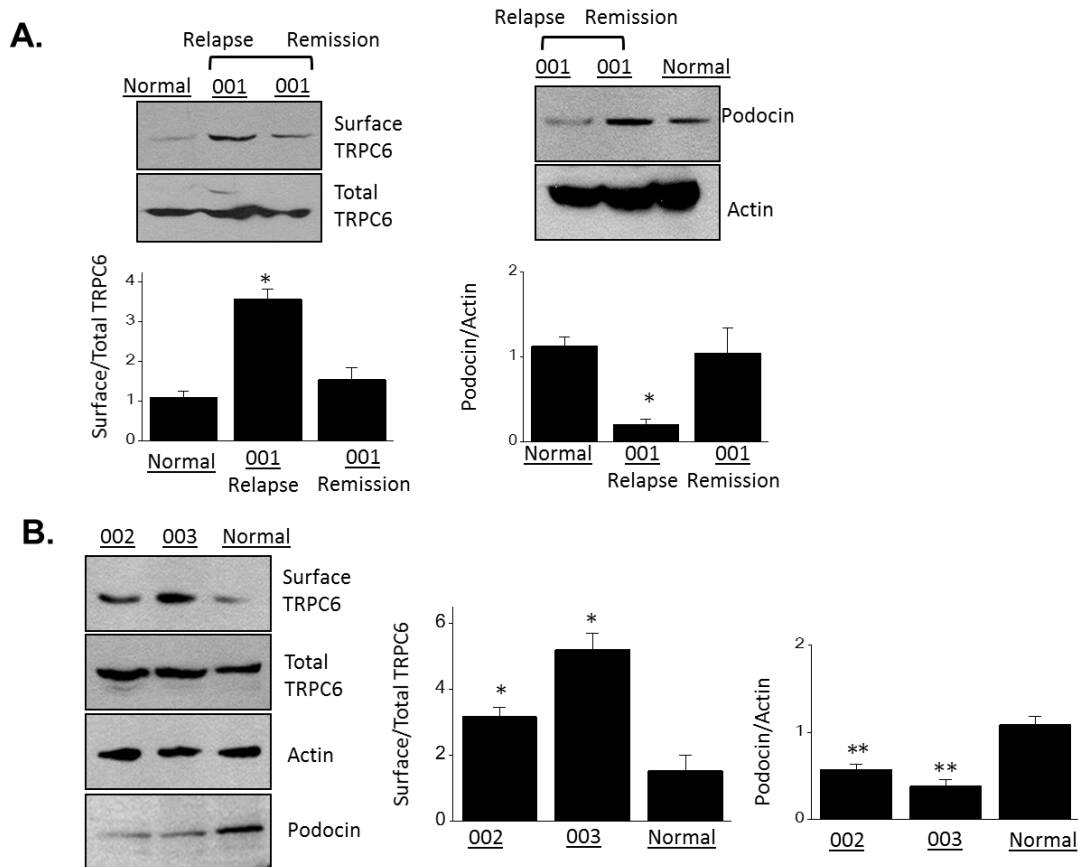


Figure 3. Changes in podocin abundance and TRPC6 channel cell-surface abundance in immortalized mouse podocytes exposed to serum or plasma from patients with primary FSGS for 24 hr. A: MPC-5 cells exposed to a normal serum and the plasma of patient 001 during relapse and remission. Plasma collected during the relapse period caused a loss of podocin abundance, as well as an increase in the abundance of TRPC6 on the cell surface. These effects were markedly reduced with plasma taken from the same patient after remission was achieved. Unpaired student t-test used for statistical analysis ( $P < 0.05$ ). B: Immunoblot analysis of surface TRPC6 and podocin abundance in MPC-5 cells exposed to sera from recurrent FSGS patients 002 and 003. Sera from both patients increased cell surface abundance of TRPC6 channels, but decreased podocin abundance. Unpaired student t-test used for statistical analysis ( $P < 0.05$  and  $P < 0.01$ ).

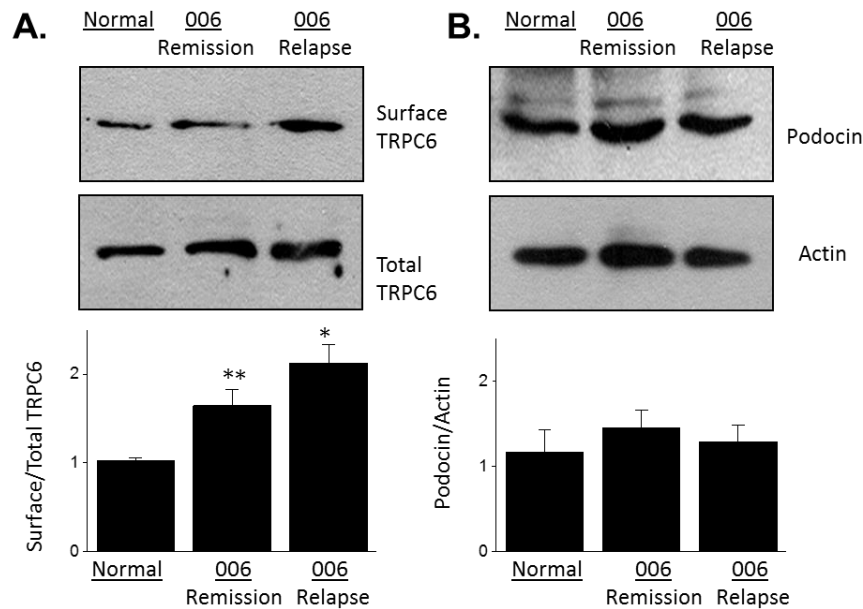


Figure 4. Plasma from recurrent FSGS patient 006 does not change podocin abundance in MPC-5 cells. A: Exposing MPC-5 cells to plasma collected when patient 006 was in relapse increased surface abundance of TRPC6 channels. This effect was reduced but not eliminated with plasma collected during remission. B: Plasma from patient 006 evoked no significant change in podocin levels detected by immunoblot. Unpaired student t-test used for statistical analysis ( $P < 0.05$  and  $P < 0.01$ ).

Electrophysiological experiments were consistent with the biochemical pattern, as we observed that mechanical stimuli evoked much larger cationic currents in cells cultured with plasma from patient 001 in relapse compared to plasma taken from the same patient while in remission (Fig. 5A, B). The mechanically-evoked currents were markedly reduced by  $50 \mu\text{M La}^{3+}$ , but we have noticed that responses in cells exposed 001 serum were not entirely blocked (Fig. 5A, B). This suggests that 001 plasma may have affect multiple podocyte cation channels, and persistence in  $\text{La}^{3+}$  suggests a possible contribution from TRPC5 [118]. While our work in this study focuses on TRPC6, we note that surface expression of TRPC5 is increased by 001 serum (data not shown). This is consistent with

the electrophysiological observations with  $\text{La}^{3+}$ , especially in light of recent studies indicating that TRPC5 can also become active in response to mechanical stimuli [180, 181]. In addition, we observed that podocytes cultured in media containing 2% of patient 001 plasma taken in relapse had markedly reduced responses to 100  $\mu\text{M}$  OAG (Fig. 5C, D). Similar patterns were seen with serum samples taken from other patients with recurrent FSGS (data not shown).

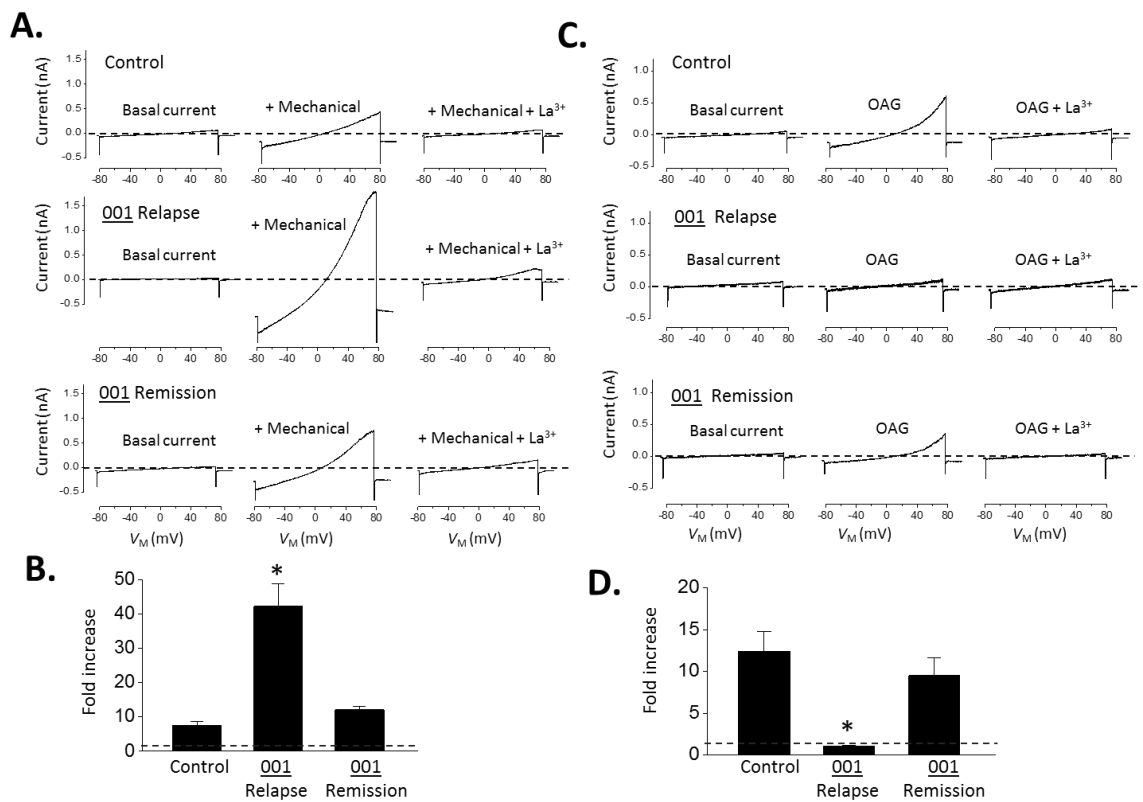


Figure 5. Altered TRPC6 gating properties in MPC-5 podocytes exposed to plasma from patient 001 collected during relapse of recurrent FSGS. A: Hypoosmotic solution effect on TRPC6 currents during voltage ramps. These currents are blocked by  $\text{La}^{3+}$  (50  $\mu\text{M}$ ), an agent that blocks TRPC6 channels but which increases activation of TRPC5. B: Summary of the fold increases of TRPC6 currents in response to mechanical stimulus during relapse and remission (N = 3 cells). C: Example of the diminished TRPC6 currents in response to membrane-permeable diacylglycerol analog, OAG. D: Summary of the fold increases of TRPC6 currents shown in (C) (N = 10 cells). Unpaired student t-test used for statistical analysis (P < 0.05).

The circulating forms of suPAR occur in variety of forms that vary in domain structure and the extent of glycosylation [168]. We have examined two different recombinant forms of suPAR, a smaller form consisting of protein domains 2 and 3, and a larger commercially available form containing domains 1, 2 and 3. These recombinant proteins were prepared in mammalian cells and are therefore likely to be extensively glycosylated. Both forms of recombinant suPAR produced a similar effect on cultured podocytes at 10 ng/ml, and specifically caused a marked increase in steady-state surface expression of TRPC6 accompanied by a marked reduction in total podocin abundance (Fig. 6A). In electrophysiological experiments carried out using the larger D1-D2-D3 form we observed a marked increase in current responses to a hypoosmotic mechanical stimulus (Fig. 6B and 6C) and a loss of responses to 100  $\mu$ M OAG (Fig. 6C), similar to what was seen following treatment with recurrent FSGS plasma samples, or after podocin knockdown [64]. Treating podocytes with 10 ng/ml TNF for 24 hr also caused an increase in surface levels of TRPC6 (Fig. 7). However, in marked contrast to suPAR, exposure to TNF did not produce a robust or consistent effect on podocin abundance (Fig. 7A) and in this respect TNF differs markedly from suPAR. In addition, TNF treatment caused a modest increase in responses to both 100  $\mu$ M OAG or hypoosmotic stretch measured using whole-cell recordings (Fig. 7B).

An earlier study on sera from patients with recurrent FSGS also reported loss of podocin expression in immortalized human podocytes, and those workers reported that this effect required 24 hr of exposure [167]. For comparison, we treated immortalized mouse podocytes with suPAR, TNF, or 001 plasma (in remission) for 3, 6, or 24 hr and then examined podocin abundance. As with that earlier study, loss of podocin evoked by either

suPAR or 001 plasma required 24 hr, whereas podocin was essentially unaffected by TNF (Fig. 7C).

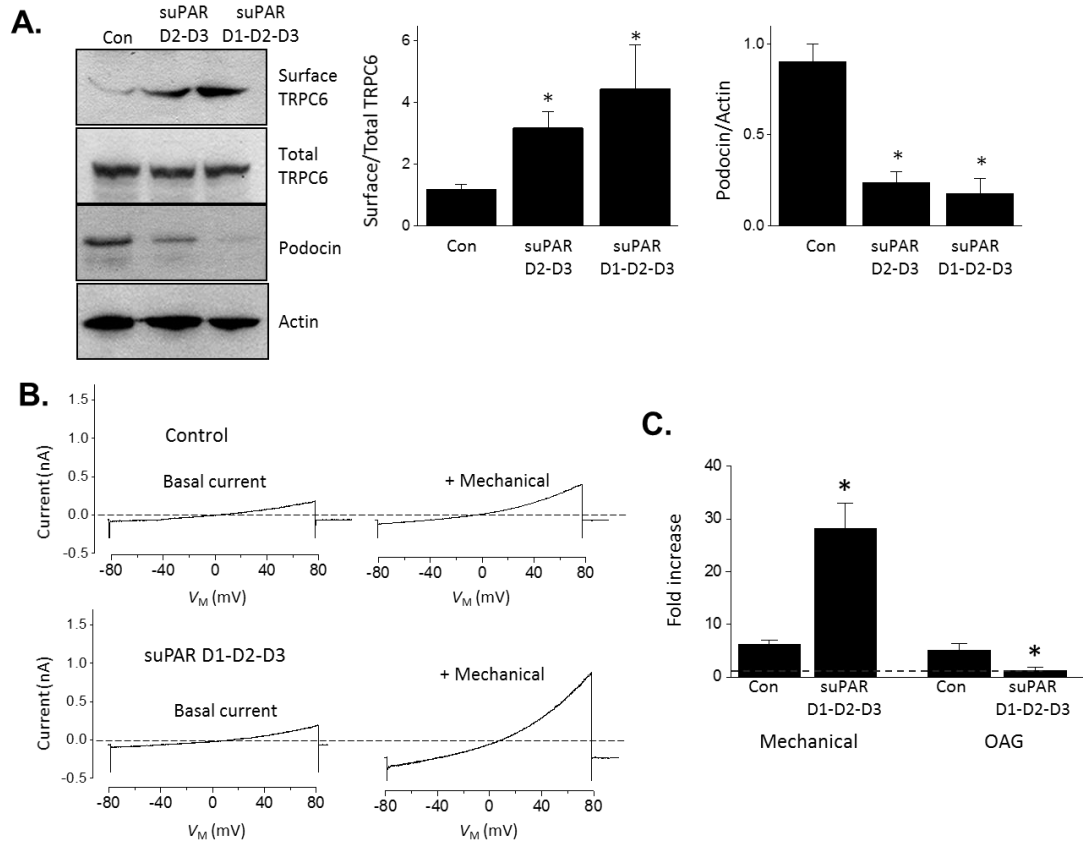


Figure 6. Altered distribution of TRPC6 and podocin evoked by two forms of recombinant suPAR. A: MPC-5 cells exposed to two forms of recombinant suPAR for 24 hr show an increase in cell surface TRPC6 abundance and a reduced total abundance of podocin. B: Examples of TRPC6 currents recorded from cells exposed to full length suPAR or normal medium for 24 hr. Note marked increase in TRPC6 currents evoked by hypoosmotic stretch. C: Summary of the fold increases of TRPC6 currents shown in (B) (N = 5 cells in each group). Unpaired student t-test used for statistical analysis (P < 0.05).

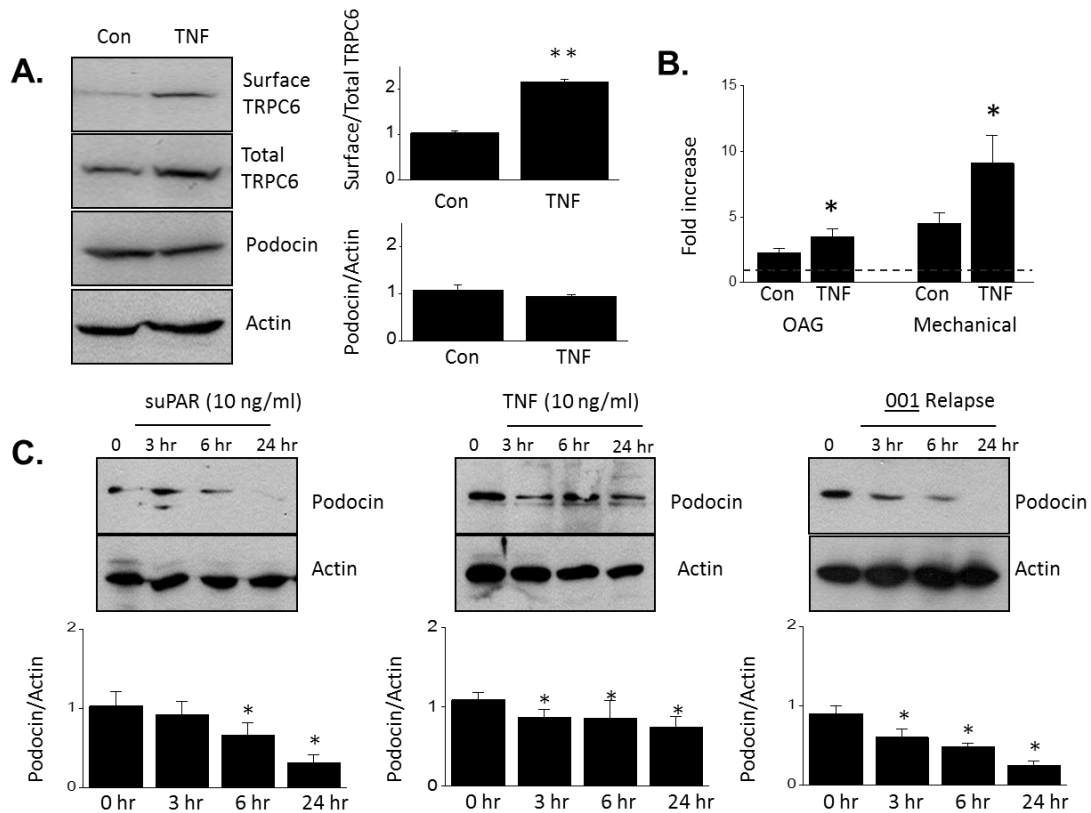


Figure 7. Effects of recombinant TNF on cell surface levels of TRPC6 and total podocin abundance in immortalized mouse podocytes. A: MPC-5 cells exposed to recombinant TNF (10 ng/ml) show an increase in cell surface TRPC6 and no consistent effect on podocin. B: Summary of the fold increases in TRPC6 activity in response to OAG and mechanical stimuli. TRPC6 currents recording during voltage ramps are increased in both conditions compared to untreated controls. Bar graphs represent mean  $\pm$  SEM. C: Immunoblot analysis showing loss of podocin evoked by suPAR or serum from patient 001, but not by TNF. All treatments were for 24 hr. Bar graphs represent mean  $\pm$  SD. Unpaired student t-test used for statistical analysis ( $P < 0.05$ ).

The effects of suPAR and TNF on surface expression of TRPC6 and total abundance of podocin appear to be at the very least additive, and possibly synergistic (Fig. 8A and 8B). To examine this, immortalized podocytes were cultured for 24 hr in presence of 1 ng/ml of either suPAR or TNF or in the presence of both factors, each at 1 ng/ml. At

this low concentration, neither suPAR nor TNF were able to cause a robust or significant effect on surface abundance of TRPC6. However robust increases in surface expression of TRPC6 were consistently observed when both factors were present at 1 ng/ml.

The previous results, including the additive or synergistic effects of TNF and suPAR, suggest that at least in principle the responses of podocytes to one circulating factor could depend on presence and/or concentrations of other circulating factors. Therefore we examined whether a multiple-factor hypothesis based on TNF and suPAR could explain some of the effects of recurrent FSGS sera and plasma on cultured podocytes. Obviously, this does not exclude possible contributions from other circulating factors. In these experiments we used commercial neutralizing antibodies raised against suPAR (anti-suPAR, present at 2  $\mu$ g/ml) and TNF (anti-TNF, present at 0.5  $\mu$ g/ml). In pilot experiments, we observed that these antibodies could completely block the actions of recombinant forms of their target proteins at 10 ng/ml. The experiments in Fig. 8C-F show the effects of these antibodies on actions of plasma from patient 001 while he was in relapse. The effects of this plasma on podocytes were previously shown in Figs. 3 and 5. The plasma was incubated with anti-TNF, anti-suPAR or both for 3 hr at 37°. The mixture was then added to cultured podocytes for 24 hr. As with previous experiments, we observed a marked increase in steady-state surface abundance of TRPC6 (Fig. 8C-D) and a loss of podocin (Fig. 8E-F) when podocytes were exposed to plasma from patient 001. These effects were slightly reduced by anti-suPAR, whereas anti-TNF was more effective. However, the combination of anti-suPAR and anti-TNF abolished the effects of plasma 001 on TRPC6 and markedly reduced effects on podocin. It bears noting that these antibodies had no effect by themselves or in combination on TRPC6 levels in podocytes cultured in control

conditions. We obtained a similar pattern examining podocin expression using serum from patient 005 (data not shown). These data indicate that multiple bioactive factors including suPAR and TNF, and very possibly other factors, may be circulating in patients with recurrent forms of FSGS, resulting in activation of signaling cascades that lead to modulation of TRPC6 and changes in the expression of podocin.

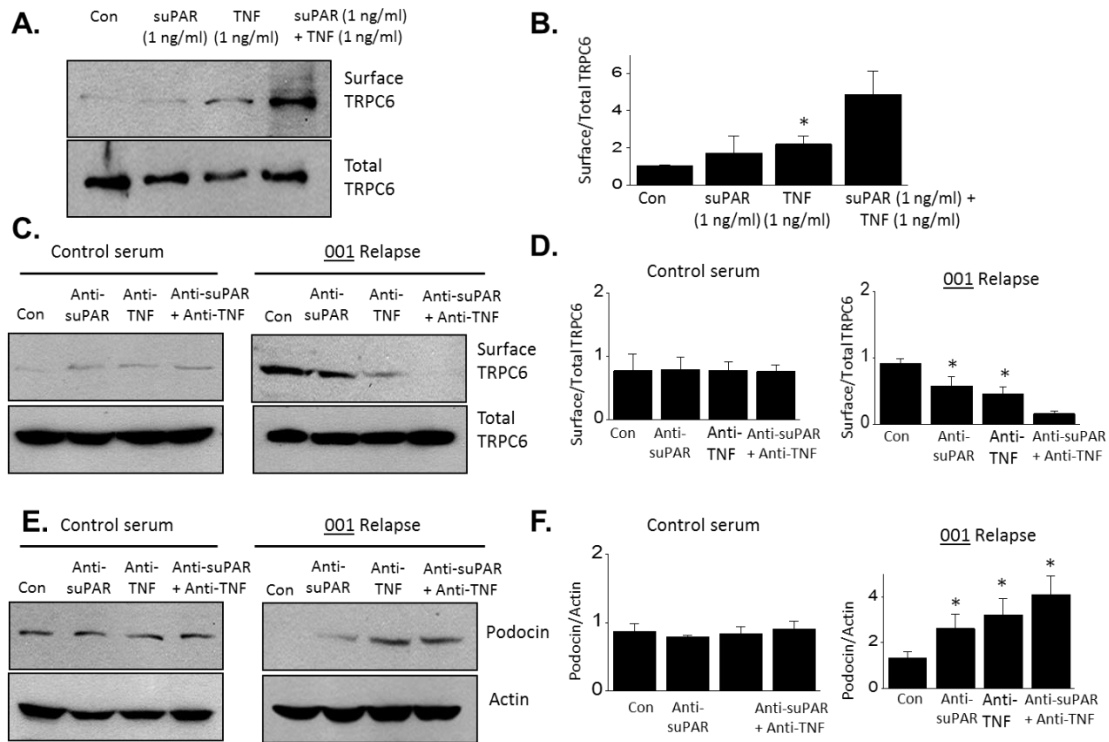


Figure 8. Synergistic effects of suPAR and TNF on surface expression of TRPC6 and total abundance of podocin in MPC-5 cells. A: Low dose of 1 ng/ml of either suPAR or TNF does not induce a significant effect on surface abundance of TRPC6 unless the two factors are applied together. B: Densitometric analysis of three repetitions of the experiment shown in (A). C: The mixture of neutralizing antibodies raised against suPAR (anti-suPAR, 2  $\mu$ g/ml) and TNF (anti-TNF, 0.5  $\mu$ g/ml) abolished the effects of patient 001 relapse plasma on surface abundance of TRPC6. D: Densitometric analysis of three repetitions of the experiment shown in (C). E: The mixture of neutralizing antibodies raised against suPAR and TNF abolished the effects of the 001 patient plasma on total abundance of podocin. F: Densitometric analysis of three repetitions of the experiment shown in (E). Bar graphs represent mean  $\pm$  SD. Unpaired student t-test used for statistical analysis ( $P < 0.05$ ).

Studies of integrin signaling in podocytes formed the original basis for the proposal of suPAR as a circulating glomerular “permeability factor” in nephrotic syndromes [182]. Specifically, it was observed that induction of uPAR, the membrane-anchored form of suPAR, caused activation of  $\alpha$ v $\beta$ 3-integrin, and that this was required for various stimuli to cause foot process effacement *in vivo* or increases in podocyte motility *in vitro*. Moreover, gene delivery of constitutively active  $\beta$ 3-integrin into podocytes was sufficient to cause proteinuria [182]. In the present experiments we examined total expression of  $\beta$ 3-integrin in cultured podocytes, and observed that this was increased after 24 hr exposure to 10 ng/ml TNF or 10 ng/ml suPAR (Fig. 9A, B). The effects of TNF were particularly robust in this respect. At lower concentrations, these two factors appear to exert additive effects on  $\beta$ 3-integrin (Fig. 9C). Moreover, plasma of patient 001 during relapse caused an increase in total abundance of  $\beta$ 3-integrin (Fig. 9D). Plasma from the same patient after remission was achieved was less active. Also, plasma from patient 006 during relapse or remission evokes similar increase in total abundance of  $\beta$ 3-integrin (Fig. 9E). Cilengitide is a cyclic RGD peptide that is known to selectively antagonize outside-in signaling through integrins that contain  $\alpha$ v subunits [183], of which the most abundant in podocytes is  $\alpha$ v $\beta$ 3-integrin [184]. Previous studies have shown that cilengitide can reduce proteinuria evoked by lipopolysaccharide [31] and also blocks several of the effects of recombinant suPAR on podocytes [31]. We observed that 10  $\mu$ M cilengitide inhibited the effects of suPAR, TNF, and plasma from patient 001 and 006 on surface abundance of TRPC6 in cultured podocytes (Fig. 10).

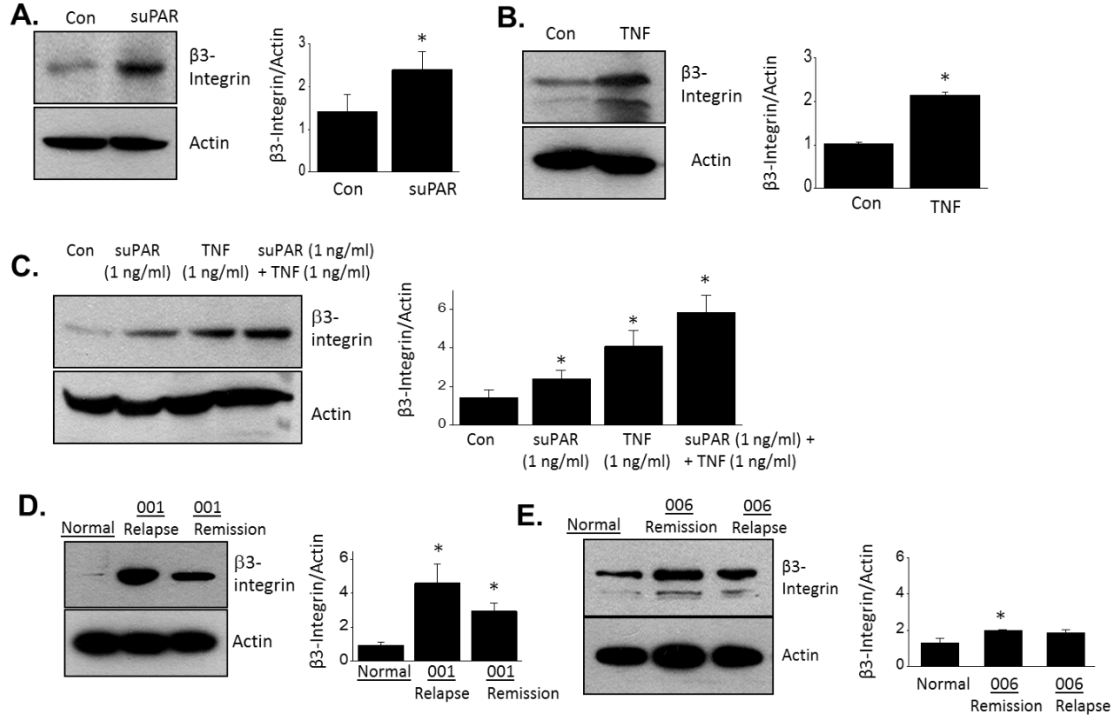


Figure 9. Increased  $\beta 3$ -integrin abundance in cultured podocytes exposed to recombinant suPAR or TNF, or sera of patients with primary FSGS. A: Total abundance of  $\beta 3$ -integrin in cultured podocytes is increased after 24-hr exposure to 10 ng/ml suPAR. B: Total level of  $\beta 3$ -integrin is increased in the presence of 10 ng/ml TNF. C: The mixture of 1 ng/ml suPAR and 1 ng/ml TNF induced additive effects on  $\beta 3$ -integrin abundance. D: Plasma of patient 001 during relapse caused an increase in total abundance of  $\beta 3$ -integrin. Plasma from the same patient after remission was achieved was less active. E: Plasma from patient 006 during relapse or remission evokes similar increase in total abundance of  $\beta 3$ -integrin. Unpaired student t-test used for statistical analysis ( $P < 0.05$ ).

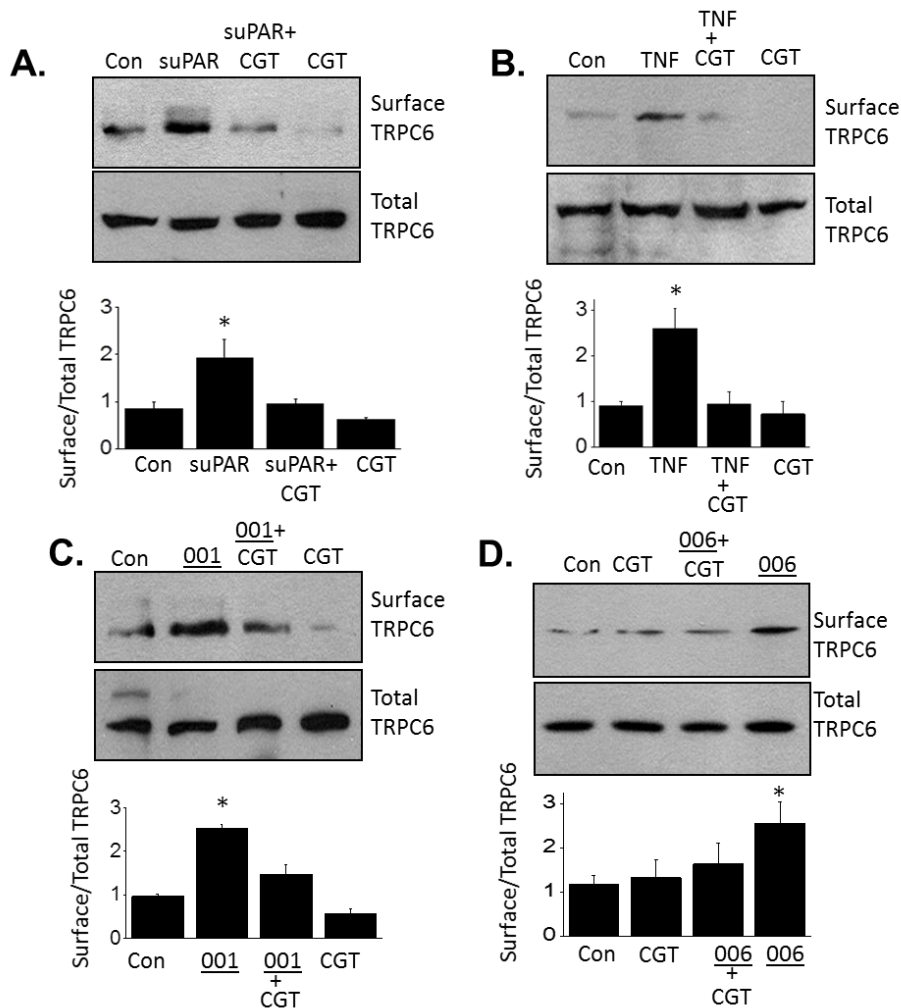


Figure 10. Effect of integrin inhibitor cilengitide (CGT) on surface abundance of TRPC6 in MPC-5 cells exposed to suPAR, TNF, and plasma from patients 001 and 006 with primary FSGS. A: Cilengitide inhibits the effects of suPAR, B: TNF, and plasma from C: patient 001 and D: patient 006 on cell surface abundance of TRPC6 channels in immortalized mouse podocytes. Unpaired student t-test used for statistical analysis ( $P < 0.05$ ).

### 5.3 Discussion

The primary observation of this study is that large qualitative changes in the behavior of podocyte cationic channels with the properties of TRPC6 occur in distinctly different models of acquired nephrotic syndromes. These include the chronic PAN model

of secondary FSGS in rats, and *in vitro* models in which immortalized mouse podocytes were exposed to serum or plasma from patients with relapsed recurrent FSGS, or to recombinant glomerular “permeability factors” implicated in primary FSGS. We also observed that these changes in TRPC6 were reduced in serum or plasma taken from patients who had achieved a remission of their disease.

In most of these models we observed a marked shift in the mode of channel gating in whole-cell recordings, with greatly increased activation by mechanical stimuli accompanied by reduced activation by a diacylglycerol analog and/or activation of G protein-coupled purinergic receptors [68]. A similar change in the dominant mode of TRPC6 activation occurs after podocin knockdown [67, 68, 92] and it is therefore of considerable significance that there was a marked loss of podocin in chronic PAN nephrosis, although it is possible that other proteins also contribute to this effect. A comparable loss of podocin also occurred in cultured podocytes after exposure to suPAR, or after exposure to most of the recurrent FSGS serum or plasma samples tested, and the magnitude of the serum effect again depended on disease severity at the time of sampling. This effect is consistent with two previous reports of a reduction in podocin abundance in cultured human podocytes exposed to serum from FSGS patients for several hours [166, 167].

Podocytes in their normal environment are exposed to large mechanical forces owing to movements of the glomerular capillary caused by the cardiac cycle [185] as well as possible effects of shear forces [186], and possibly distension of the sub-podocyte space [187]. The question as to whether any member of the TRP family of cation channels plays a direct role in normal physiological mechanotransduction is controversial, and it has been

suggested that some if not all TRP family channels are insufficiently mechanosensitive to respond directly to forces encountered in normal physiology [188]. Regardless of how that issue is resolved, it remains possible that pathological changes that alter structure and composition of cell membranes, such as a loss of podocin in foot processes [189], could cause TRPC family channels to activate inappropriately in response to mechanical stimuli, resulting in sustained and excessive Ca<sup>2+</sup> influx. It bears noting that the mechanism of mechanical activation of podocyte TRPC6 channels is not known, and while we favor the hypothesis that the channels are directly mechanosensitive, we certainly cannot exclude that it occurs secondary to effects on some other protein, or only occurs when the channels are part of a specific protein complex.

In addition to changes in the dominant gating mode, the circulating factors examined here caused a large increase in the steady-state surface expression of podocyte TRPC6 subunits. In contrast to changes in the dominant gating mode, we observed that increased TRPC6 surface expression is not an obligatory consequence of loss of podocin. For example, siRNA knockdown of podocin actually led to a modest decrease of steady-state surface abundance of TRPC6 in podocytes. Moreover, exposure to TNF caused a robust increase in surface expression of TRPC6 without affecting podocin.

The sera and plasma samples from recurrent FSGS patients that were tested here contain more than one factor capable of activating cell signaling cascades that converge on podocyte TRPC6 channels, as effects were reduced by neutralizing antibodies against either suPAR or TNF. With respect to TNF, several case reports and small studies over a period of decades have suggested a role for this pro-inflammatory molecule in primary nephrotic syndromes [33-36, 173]. TNF is reported to increase glomerular albumin

permeability owing in part to oxidative stress [190]. In addition, recent studies have proposed a role for circulating suPAR in primary FSGS [30, 31, 191]. On the other hand, several studies have failed to substantiate total serum suPAR concentrations as a specific biomarker for FSGS [192, 193], although suPAR appears to be an independent risk factor for incident kidney disease and future declines in glomerular filtration rate [194]. With respect to FSGS and suPAR, uncertainties remain about the ELISA technology used in many of these studies, lack of knowledge about which forms of circulating suPAR are pathogenic [195], and the possibility that total serum suPAR may simply vary inversely with GFR [171, 193], and patient heterogeneity [196].

However, another possibility is that primary FSGS can result from the net effects of multiple circulating factors, which may vary from one patient to the next. In other words, we propose here that there may be conditions under which suPAR could be pathogenic to glomeruli even when it is present at normal serum concentrations. This proposal is based on two observations. First, we observed that effects of suPAR and TNF on surface abundance of TRPC6 are at least additive and possibly synergistic. In addition, we observed that the actions of plasma or serum from patients with recurrent FSGS in relapse were attenuated by antibodies that neutralize suPAR or TNF, with nearly complete inhibition caused by a combination of these antibodies. We also observed that TNF and suPAR caused marked increases in the abundance of  $\beta$ 3-integrin subunits, and these effects were mimicked by recurrent FSGS serum or plasma. It is thought that  $\alpha$ v $\beta$ 3-integrin functions as a receptor or co-receptor for suPAR [31, 182, 197, 198], and in this regard, cilengitide, an inhibitor of outside-in signaling through  $\alpha$ v $\beta$ 3-integrin [183], completely blocked the increases in surface abundance of TRPC6 evoked by all of these treatments.

Finally, we observed samples, for example the sample from recurrent FSGS patient 006, which did not have any effect on podocin. It is quite likely that there are other circulating factors not tested here that could contribute to recurrent FSGS in at least some patients. One possible factor is cardiotrophin-like cytokine factor-1 (CLCF1), a member of the IL-6 family [199, 200]. The transduction factor used by that cytokine uses several components also used by TNF [199, 200], and might be expected to increase surface TNF without affecting podocin.

There are several potential implications of these observations. The first is that circulating levels of any one putative permeability factor may not always correlate with proteinuria or disease severity but could still be an important factor driving the disease process. A lack of correlation could be due to potentiating actions of a second circulating factor such as TNF or CLCF1. It is also possible that one or more of the key pathogenic factors is produced locally within glomeruli (as with TNF and suPAR) and is therefore not captured in measurements from serum or plasma (but might be captured in urine measurements). In fact, even the original report on circulating suPAR noted a subset of patients with primary and even recurrent FSGS with serum levels well below the cutoff level of 3000 pg/ml [31]. In other words, in a multiple-factor model the sum of the activities of the circulating factors capable of reaching podocytes may be more important than the concentration of any one factor taken in isolation. At this time the number of different factors capable of driving nephrosis is not known. This also suggests that in a generally inflammatory milieu, for example in lupus erythematosus [201] and other secondary glomerulonephritis [202], suPAR signaling may be more deleterious (compared to children or young adults with primary nephrotic syndromes in which inflammation is

generally not present). It is even possible that protective factors exist in the circulation to varying degrees in different patients.

A second implication is that from a therapeutic perspective, the nature of the circulating and/or locally produced factors that drive primary FSGS may not be crucial if they converge onto a small subset of targetable pathways in podocytes. For example, chronic PAN nephrosis and exposure to sera and recombinant factors similarly resulted in a gain of podocyte TRPC6 channel function (and one of these also caused an increase in surface expression of TRPC5). In this regard, an increase in glomerular TRPC6 protein was reported previously in PAN nephrosis [60] and was confirmed here. It has been observed repeatedly that TRPC6 is able to increase its own expression in podocytes through  $\text{Ca}^{2+}$ -calcineurin-NFATc1 signaling pathways [59, 203]. We have observed that 24 hr of exposure to TNF, suPAR, and FSGS patient sera are capable of causing NFATc1 activation in cultured podocytes (unpublished data). As already noted, this suggests that therapeutic approaches based on inhibition of TRPC6 warrant additional investigation.

Another pathway of therapeutic interest is mediated by  $\alpha\text{v}\beta 3$ -integrin. An increase in total levels of  $\beta 3$ -integrin subunits were seen in response to TNF, suPAR, and most of the recurrent FSGS blood samples that we have examined and we observed that the effects of these agents on TRPC6 were reduced by cilengitide. It is thought that  $\alpha\text{v}\beta 3$ -integrin functions as a receptor or co-receptor for suPAR [182] and several other factors [204]. TNF acts primarily on a distinct family of its own receptors but there is evidence that it can cause activation of protein kinases that eventually lead to inside-out activation of integrins [205]. Moreover, by increasing expression of a suPAR receptor, TNF could allow the latter to activate pathogenic signaling pathways at lower circulating concentrations. The

importance of these observations is underscored by a growing number of studies showing efficacy of integrin antagonists in animal models of proteinuric diseases [31]. In this regard, we recently demonstrated that the ectodomain of syndecan-4 (Sdc4) can also cause modulation of podocyte TRPC6 channels through cascades that are blocked by cilengitide [94]. However, as with TNF, application of Sdc4 did not reduce the expression of podocin [94]. In other words, loss of podocin expression is not an inevitable consequence of outside-in signaling through integrins in podocytes. Therefore, it is possible that integrins are necessary but perhaps not sufficient for all of the actions of suPAR on podocytes.

Two well-characterized genetic forms of FSGS occur as a result of mutations that lead to a gain of TRPC6 function [56-58] or a loss of functional podocin and/or sequestration of the protein in the endoplasmic reticulum [49, 52]. Our recent study on TRPC6 gating in podocytes demonstrated direct interactions between cytosolic domains near the carboxy terminals of podocin and TRPC6, and showed that large gains of TRPC6 activation by mechanical stimuli should occur after podocin knockdown [64]. Podocyte foot processes are attached to a mechanically dynamic matrix and are subjected to measurable pulsations driven by the cardiac cycle [185] and slower shear forces associated with feedback regulation of single-nephron GFR [206]. Indeed, the gain of TRPC6 function that occurs following loss of podocin in response to mechanical stimuli [64], is much larger than is seen with the vast majority of TRPC6 mutations described to date [56, 57]. The loss of podocin expression that we observed with most of the experimental manipulations in this study predicts that a substantial gain of TRPC6 will be a hallmark feature of many, if not, most forms of FSGS, including acquired forms associated with circulating factors or as a result of earlier loss of podocytes. Thus it is possible that agents that reduce activation

or expression of podocyte TRPC6 channels might be useful for therapy of many types of nephrotic syndromes, and not just forms caused by gain-of-function TRPC6 mutations. This assumes that inhibition of TRPC6 channels in other cell types would not represent an insurmountable safety issue.

## **6. THE NMDA RECEPTORS AS POTENTIAL THERAPEUTIC TARGETS IN DIABETIC NEPHROPATHY: INCREASED RENAL NMDA RECEPTOR SUBUNIT EXPRESSION IN AKITA MICE AND REDUCED NEPHROPATHY FOLLOWING SUSTAINED TREATMENT WITH MEMANTINE OR MK-801**

### **6.1 Introduction**

More than 40% of end-stage renal disease (ESRD) in the United States can be currently attributed to diabetes mellitus [23]. The pathophysiology of diabetic nephropathy is multifactorial, and includes contributions from dysregulation of metabolic pathways, complex changes in renal hemodynamics, and genetic susceptibility [207-210]. The reasons why only a subset of diabetic patients experience renal complications are not well understood, and therapeutic options remain limited. Current mainstay therapies are based on glycemic and blood pressure control, and reno-protective inhibition of renin-angiotensin signaling systems [209, 210]. While these therapies can slow the progression of diabetic nephropathy, many patients will nevertheless progress to ESRD [209, 210].

NMDA receptors are a class of cation-selective heterotetrameric ionotropic receptors with a high intrinsic  $\text{Ca}^{2+}$  permeability [211, 212]. These receptors are assembled from several different subunits: NR1, NR2A, NR2B, NR2C, NR2D, NR3A and NR3B, which are encoded by seven different genes. Functional NMDA receptors require two NR1 subunits that contain binding sites for the co-agonist glycine. They also require either two NR2 subunits, which bind a number of different endogenous di-acidic agonists, or one NR2 and one NR3 subunit [213]. NMDA receptors were first characterized in the CNS, but NMDA receptors are also expressed in peripheral organs, including the kidney. There is

evidence that renal NMDA receptors play a role in regulation of blood flow, glomerular filtration, proximal tubule reabsorption, and urine concentration in the collecting duct [66, 214-218]. NMDA receptors can be activated by several endogenously occurring di-acidic molecules, including L-glutamate, L-aspartate, L-homocysteic acid (HCA), L-quinolinic acid, and guanidinosuccinic acid, although L-glutamate and L-aspartate are relatively weak agonists for podocyte NMDA receptors [66, 215, 216]. While work in the CNS has predominantly focused on di-acidic agonists such as L-glutamate and L-aspartate, in peripheral tissues it is possible that dynamic changes in glycine may also evoke NMDA receptor activation [216-218]. In the CNS, sustained activation of neuronal NMDA receptors can induce a form of neurodegeneration known as excitotoxicity [219]. Sustained exposure of mouse podocytes to NMDA or HCA evokes a similar phenomenon characterized by increased  $\text{Ca}^{2+}$  influx, oxidative stress, altered expression of slit diaphragm proteins, and apoptosis [66, 220, 221].

A recent study reported that renal NMDA receptor expression is upregulated in the Akita mouse model of type-1 diabetes [222]. In addition, elevated plasma L-homocysteine often occurs in patients with type-1 or type-2 diabetes and is significantly correlated with renal complications [223-225]. Moreover, genes involved in L-homocysteine metabolism are possible susceptibility loci for diabetic nephropathy [226-228]. L-homocysteine spontaneously oxidizes to the NMDA agonist HCA, and albuminuria and glomerular damage in mice with elevated plasma homocysteine can be prevented by treatment with MK-801, a widely-used NMDA receptor antagonist [220]. Here we provide evidence that sustained treatment with either of two structurally dissimilar NMDA receptor antagonists, MK-801 and memantine, reduces nephropathy in a mouse model of type-1 diabetes.

Memantine is already widely used clinically for treatment of Alzheimer's disease, is well tolerated, and currently undergoing a number of clinical investigations in humans, primarily for neurodegenerative disorders [229-232].

## 6.2 Results

Immortalized mouse podocytes were cultured for 24 hr in a medium containing 9 mM glucose supplemented with 16 mM mannitol, or in a medium containing 25 mM glucose. After differentiation, these cells normally express podocyte markers including nephrin, synaptopodin, and podocin [64, 233, 234]. In initial studies we observed that they also express all known NMDA receptor subunits and their transcripts. We focused on NR1 and NR2 subunits required to form functional receptors that respond to NMDA and other di-acidic agonists. With RT-PCR we observed that 24 hr exposure to high glucose medium increased the apparent abundance of NR1, NR2A, NR2B and NR2C subunit transcripts (Fig. 1A, B). The same pattern was observed using immunoblot analysis; namely increased abundance of NR1, NR2A, NR2B and NR2C subunits (Fig. 1C, D). Marked increases in NMDA subunit abundance also occurred in primary rat mesangial cells after 24 hr exposure to high glucose medium. In mesangial cells we observed increased abundance of transcripts encoding NR1, NR2B, and NR2C, but not NR2A or NR2D subunits (Fig. 2A, B). By immunoblot we observed increased abundance of those same subunits (Fig. 2C, D). Thus, elevated glucose is sufficient to increase the expression of multiple NR1 and NR2 subunits in two different glomerular cell types.

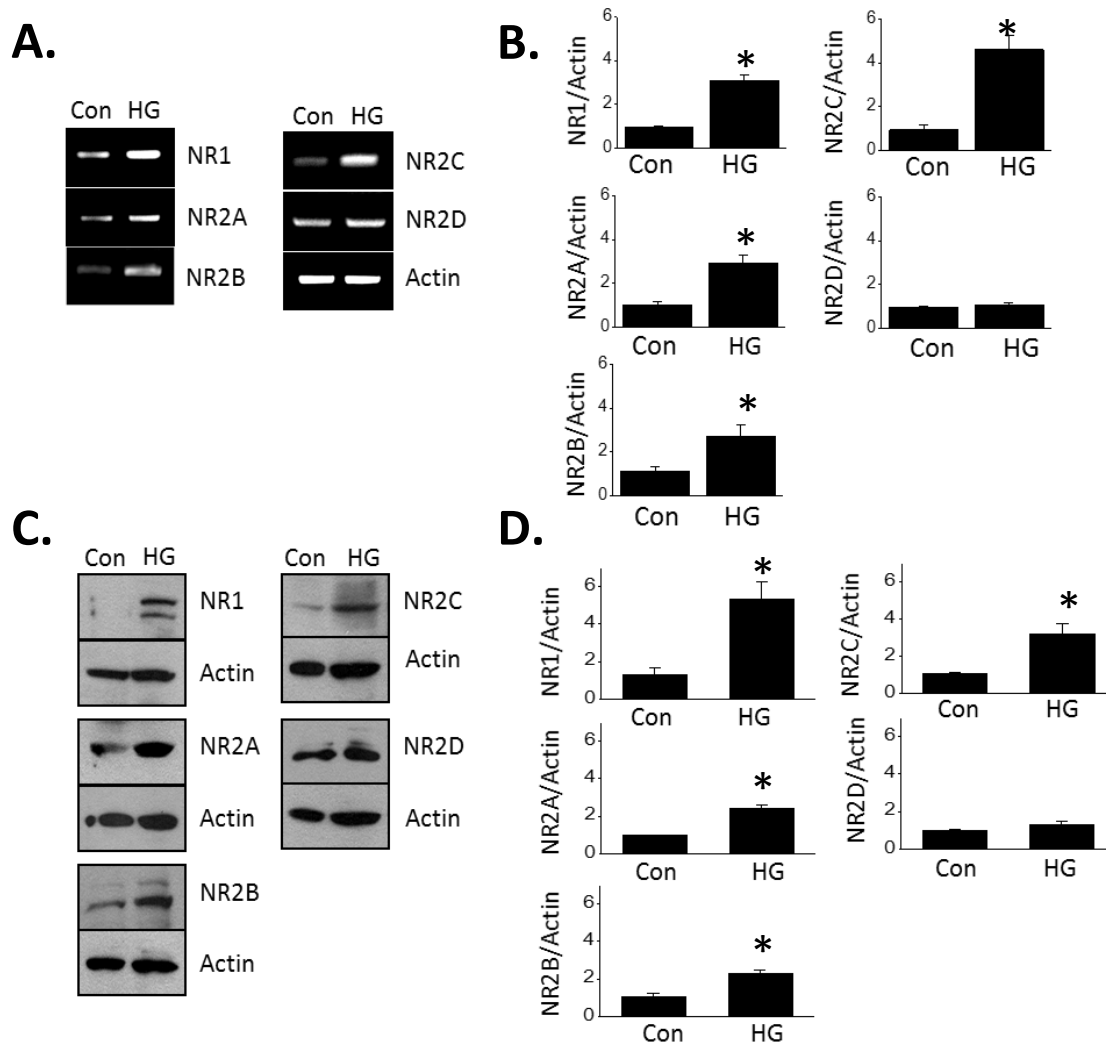


Figure 1. Exposure to high glucose increases expression of NMDA receptor subunits in cultured mouse podocytes (MPC-5 cells). A: Representative results of RT-PCR showing increased abundance of transcripts encoding NR1, NR2A, NR2B and NR2C subunits in cells cultured for 24 hr in a medium containing 25 mM glucose (HG). Control cells (Con) were cultured in medium containing 9 mM with 16 mM mannitol as an osmotic control. B: Densitometric analysis of three repetitions of the experiments shown in (A). Bar graphs represent mean  $\pm$  SD. Unpaired student t-test used for statistical analysis ( $P < 0.01$ ). C: Immunoblot analysis showing increased abundance of NMDA receptor subunits in podocytes cultured in HG compared to control (Con). D: Densitometric analysis of three repetitions of the experiments shown in (C). Bar graphs represent mean  $\pm$  SD. Unpaired student t-test used for statistical analysis ( $P < 0.05$ ).

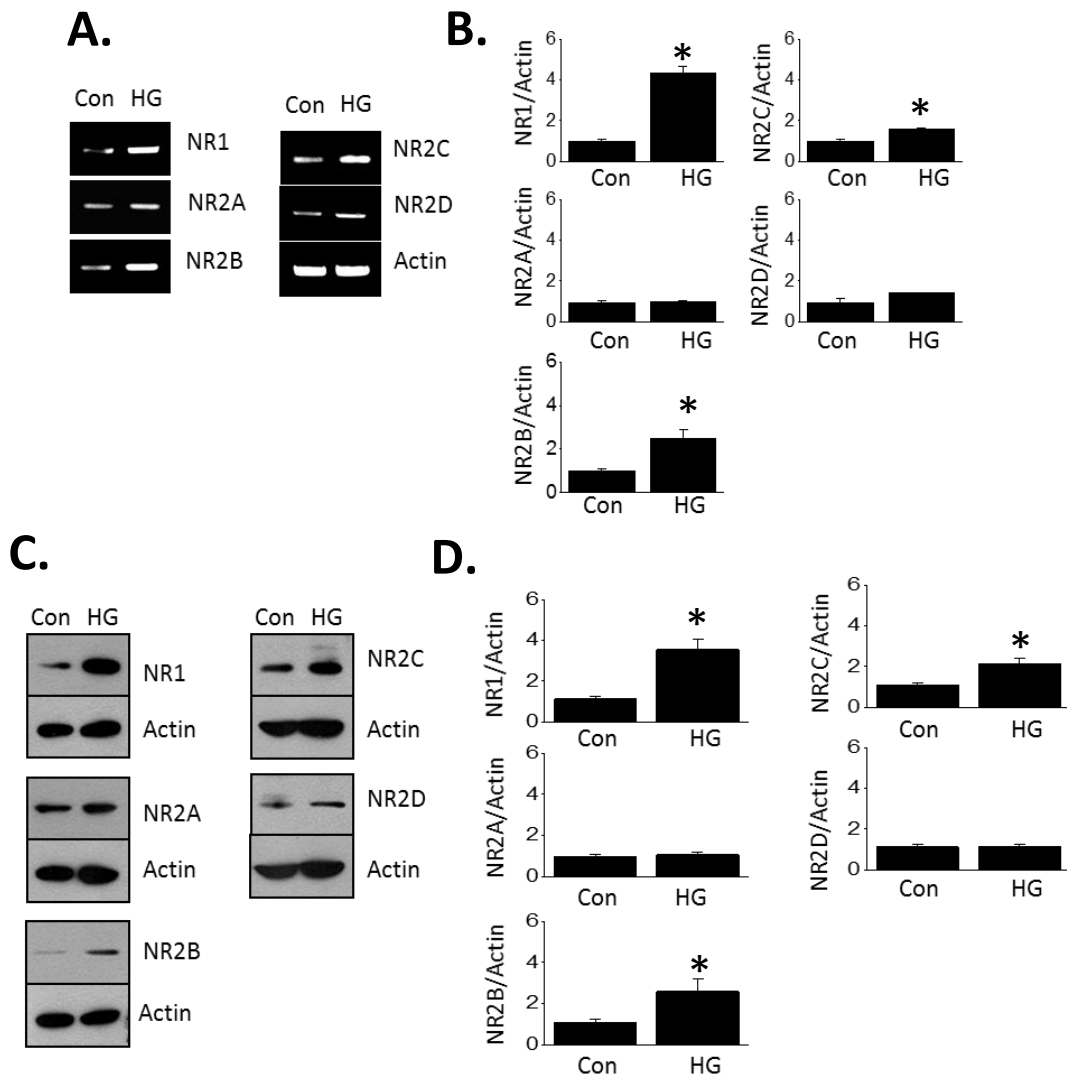


Figure 2. Exposure to high glucose increases expression of NMDA receptor subunits in primary cultures of rat mesangial cells. A: Representative results of RT-PCR showing increased abundance of transcripts encoding NR1, NR2B and NR2C subunits in cells cultured for 24 hr HG medium compared to cells cultured in normal glucose (Con). B: Densitometric analysis of three repetitions of the experiments shown in (A). Bar graphs represent mean  $\pm$  SD. Unpaired student t-test used for statistical analysis ( $P < 0.05$ ). C: Immunoblot analysis showing increased abundance of NMDA receptor subunits in primary cultures of rat mesangial cells cultured in HG. D: Densitometric analysis of three repetitions of the experiments shown in (C). Bar graphs represent mean  $\pm$  SD. Unpaired student t-test used for statistical analysis ( $P < 0.05$ ).

In these experiments we use male Akita mice (D2.B6-Ins2Akita/MatbJ), which are heterozygous for the C96Y mutation in the Ins2 gene [235]. The control mice in our experiments were wild-type DBA/2J mice. We examined expression of NMDA receptor subunits in renal cortex from 12-week old animals. Using RT-PCR, we obtained evidence for increased abundance of transcripts encoding NR1, NR2A, and NR2C subunits (Fig. 3A, B). This pattern was also observed by immunoblot analyses of renal cortex (Fig. 3C, D). The increase in the staining of NMDA receptor subunits in Akita mice is seen throughout the kidney (Fig. 4). Using immunohistochemistry we observed marked increases in the staining of NR1, NR2A and NR2C in most renal tubules, especially near the cortical-medullary boundary (Fig. 4A). Within glomeruli, we observed more modest increases in the staining of NMDA receptor subunits (Fig. 4B).

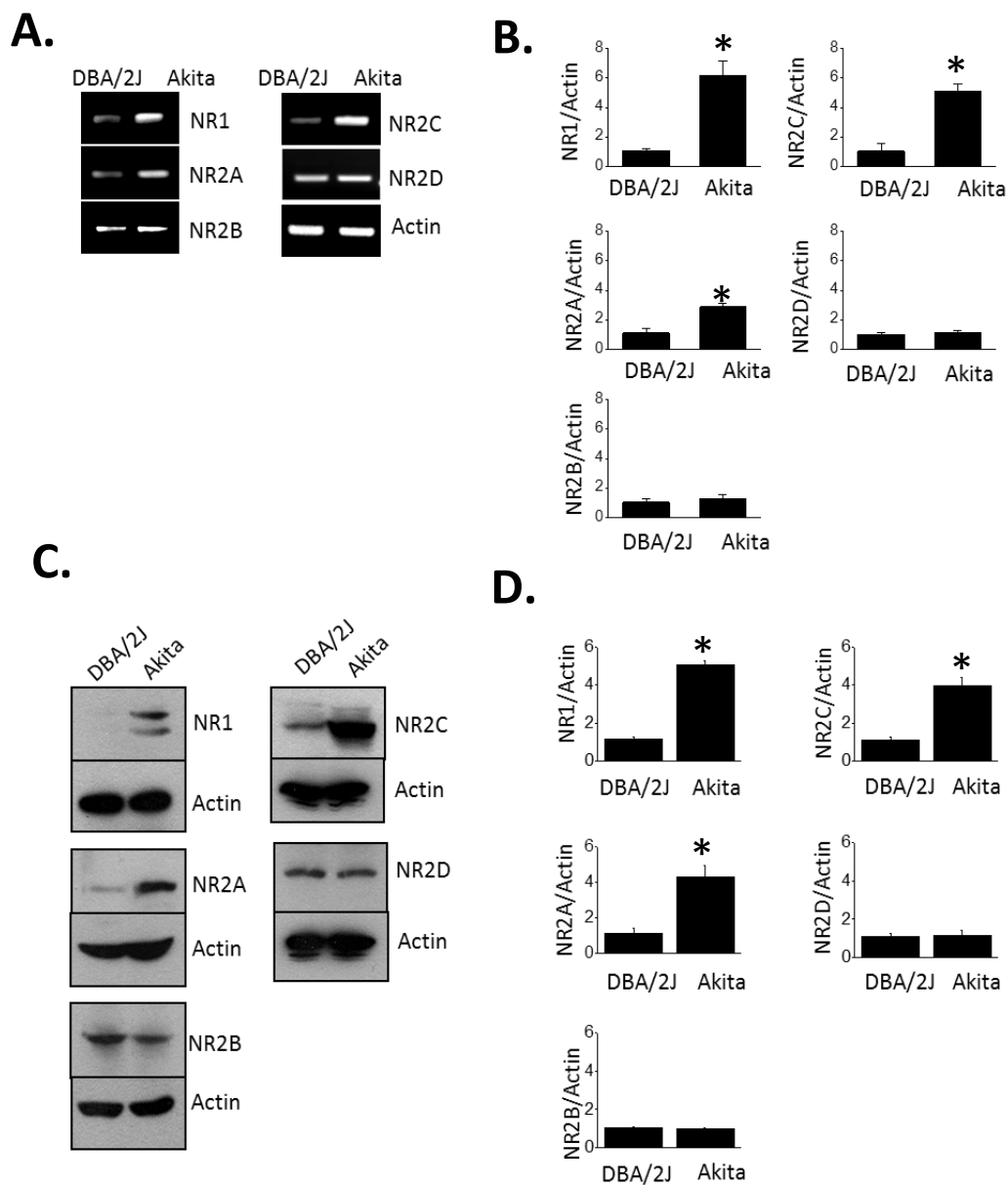


Figure 3. Increased expression of NMDA receptor subunits in renal cortex of Akita mice. A: Representative results of RT-PCR showing increased abundance of transcripts encoding NR1, NR2A, and NR2C subunits in renal cortex in 12 week-old Akita mice compared to 12-week old DBA/2J control mice. B: Densitometric analysis from N = 4 mice per group. Bar graphs represent mean  $\pm$  SD. Unpaired student t-test used for statistical analysis ( $P < 0.01$ ). C: Immunoblot analysis showing increased abundance of NMDA receptor subunits in Akita mice compared to DBA/2J controls. D: Densitometric analysis of analyses from N = 4 mice per group. Bar graphs represent mean  $\pm$  SD. Unpaired student t-test used for statistical analysis ( $P < 0.01$ ).

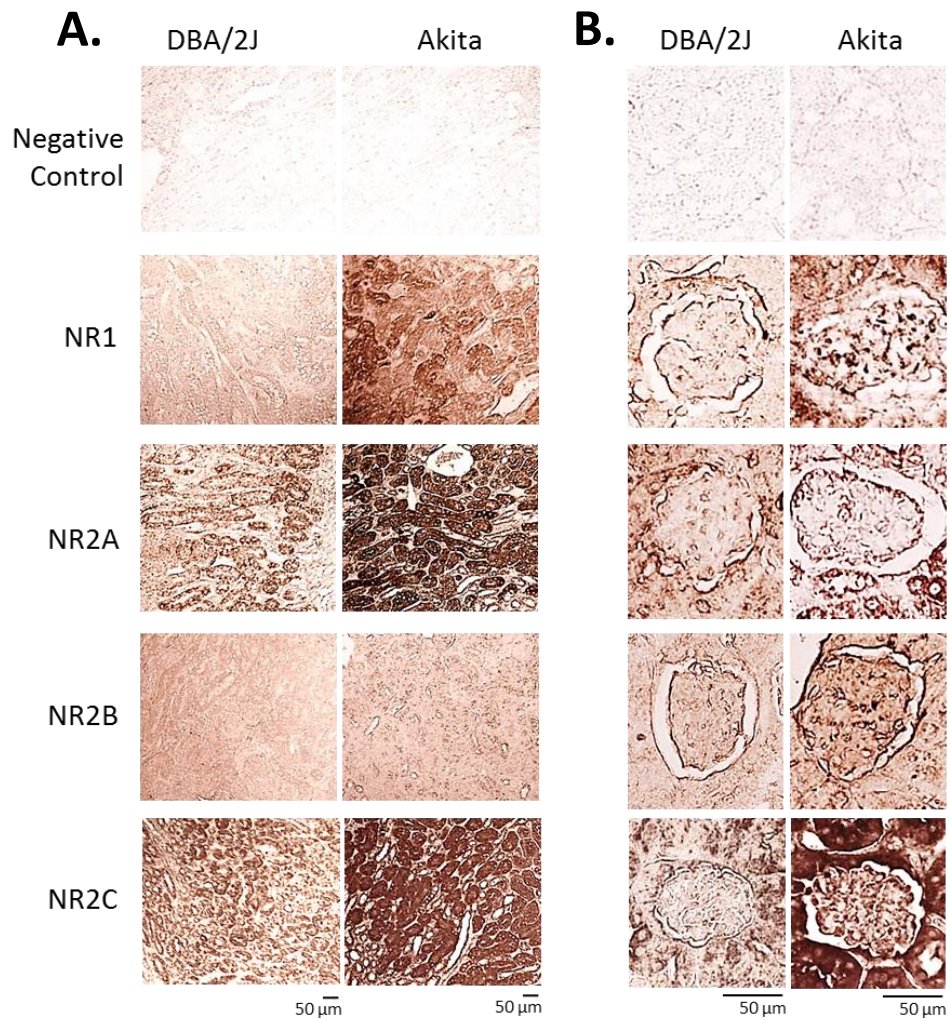


Figure 4. Increased IHC staining of NMDA receptor subunits throughout the kidney of Akita mice. Immunohistochemistry for subunits that were increased based on previous biochemical studies carried out in paraffin sections. A: Note especially large increases in the staining of NR1, NR2A and NR2C in renal tubules. B: Signal in glomeruli for NR1, NR2A and NR2C provides evidence for increase in podocytes of Akita mice. Mice were 12-weeks old when these analyses were carried out. Negative control sections were not exposed to a primary antibody.

Sustained activation of NMDA receptors can drive glomerulosclerosis in mice and rats [220, 221]. Increased numbers of receptors could lead to excessive NMDA receptor activation on cells even if endogenous ligands are not changed. However, there is evidence

that diabetes causes metabolic changes leading to increased levels of circulating agonists [223, 225, 227, 236-240]. To examine if sustained NMDA receptor activation contributes to the progression of diabetic nephropathy, we implanted osmotic minipumps containing the NMDA antagonist MK-801 or saline subcutaneously into Akita mice and DBA/2J controls at 8 weeks of age, an age at which there are very modest increases in urine albumin excretion. The pumps delivered a dose of approximately 0.5 mg/kg/day of MK-801 continuously for 28 days. We observed that Akita mice do not gain weight at the same rate as DBA/2J controls (Fig. 5A). This was seen in both saline- and MK-801- treated animals. In fact, reduced weight was actually greater in MK-801-treated Akita mice than in the saline group. The reason why sustained MK-801 attenuates normal weight gain is not known. In any case, this pattern suggests that MK-801 does not alleviate the primary metabolic consequences of type-1 diabetes, and in other experiments we have observed that 4-weeks of MK-801 treatment had no effect on blood glucose levels or mean arterial blood pressure in either control mice or mice with type-1 diabetes (data not shown).

As with previous reports [235] we observed markedly increased 24-hr urine albumin excretion in 12-week old Akita mice compared to DBA/2J controls (Fig. 5B). This was attenuated in mice that received MK-801 compared to mice that received saline. These data were analyzed using two-way ANOVA. We observed a significant effect of genotype ( $P < 0.0001$ ), and a significant interaction effect between drug treatment and genotype ( $P < 0.05$ ), indicating that the antagonist reduces renal manifestations of diabetes. MK-801 also reduced mesangial expansion in Akita mice, as assessed by computation of mesangial scores from PAS-stained paraffin sections of kidney (Fig. 5C, D). Mesangial expansion is not severe in Akita mice on a DBA/2J background [235] but is nevertheless reduced in

Akita mice that received MK-801 compared to those that received saline, and the effect was significant based on two-way ANOVA ( $P < 0.05$ ). We also observed marked foot process effacement and thickening of the glomerular basement membrane in Akita mice by 12-weeks of age (Fig. 5E, F). Ultrastructure was markedly improved in Akita mice that received MK-801 (Fig. 5E, F). There was a significant interaction effect between the effects of MK-801 and genotype ( $P < 0.05$ ) on GBM thickness, again indicating a therapeutic effect of the drug. MK-801 had no discernible effect on glomerular ultrastructure in DBA/2J controls. The effect of MK-801 can also be seen with scanning EM (Fig. 6). We observed marked foot process flattening and disorganization in Akita mice that received saline (Fig. 6A). There are still some abnormalities in Akita mice that received MK-801, but overall structure is closer to normal. In general, effects of MK-801 on renal structure and ultrastructure were more impressive than effects on albumin excretion.

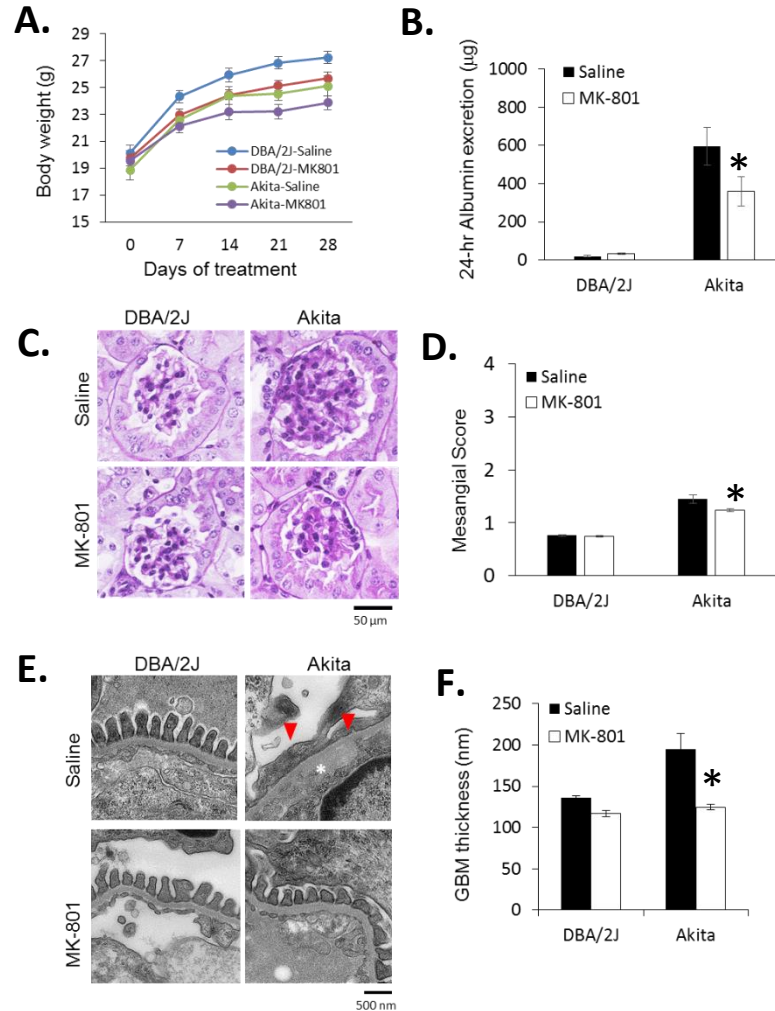


Figure 5. The NMDA antagonist MK-801 reduces progression of nephropathy in Akita mice. A: Reduced weight gain in Akita mice was not alleviated by MK-801. Bar graphs represent mean  $\pm$  SEM in this and all subsequent figures. B: Reduced 24-hr albumin excretion in Akita mice that received MK-801 compared to saline-treated controls. The effect of genotype ( $F = 52.15$ ,  $P < 0.0001$ ), and an interaction effect between drug treatment and genotype ( $F = 5.2$ ,  $P = 0.0283$ ) were significant by two-way ANOVA with  $N = 9-10$  mice per group. C: Representative PAS-stained sections of saline-treated and drug-treated Akita mice and DBA/2J controls. D: Mesangial matrix expansion expressed as mesangial score shows modest increase in Akita mice that received saline. This increase did not occur in Akita mice that received MK-801. An interaction effect between drug and genotype on this outcome is significant ( $F = 5.33$ ,  $P = 0.0396$ ,  $N = 4$  mice per group). E: Representative transmission electron micrographs of mice. Note extensive foot process effacement (red arrowheads) and GBM thickening (asterisks) in Akita mice that received saline. Ultrastructure is markedly improved in Akita mice that were treated with MK-801. F: GBM thickness is increased in Akita mice treated with saline but not in Akita mice that received MK-801. An interaction between the effects of MK-801 and genotype ( $F = 6.22$ ,  $P = 0.0373$ ,  $N = 4$  mice per group) on GBM thickness was significant.

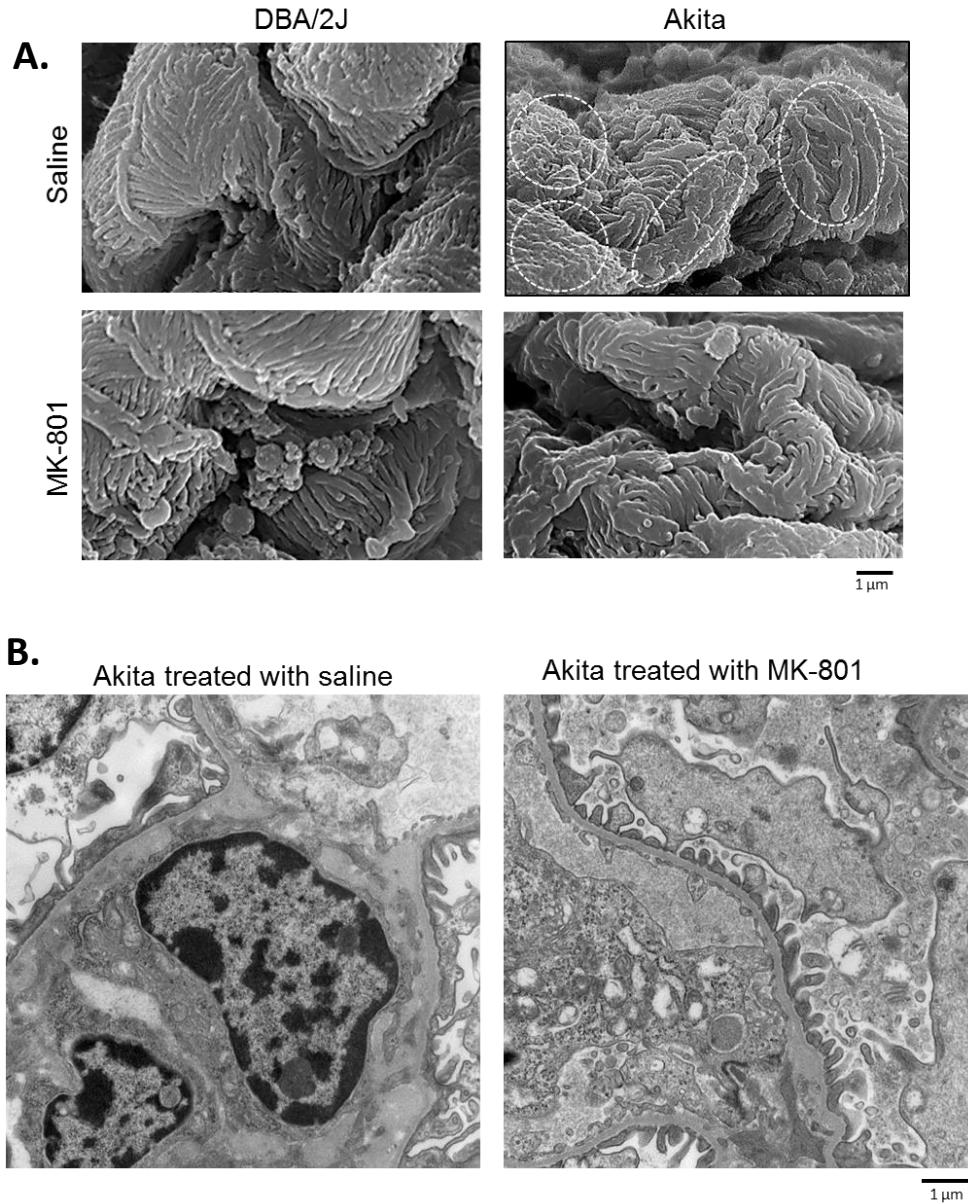


Figure 6. Scanning and transmission EM of glomerular capillary loops in control and Akita mice at 12 weeks of age. A: Scanning EM show marked disorganization of foot processes along surface of glomerular capillary in Akita mice. Note flattening of foot processes, especially in areas within white lines. Foot process morphology is closer to normal in Akita mice that received MK-801. Treatment with MK-801 has no effect on glomeruli in DBA/2J mice. B: Transmission EM of glomeruli from Akita mice at the same magnification for comparison.

MK-801 is a strong NMDA receptor antagonist that produces profound cognitive and behavioral effects [229, 241]. By contrast, memantine is a structurally distinct NMDA receptor antagonist that spares a basal level of NMDA receptor-mediated synaptic transmission while reducing excitotoxicity [229, 241]. It is well tolerated and is in widespread clinical use for moderate-severe Alzheimer's dementia [230-232]. Memantine or saline were applied using osmotic minipumps implanted subcutaneously at 8 weeks of age and delivered at a dose of 0.2 mg/kg/day. As with MK-801, we observed that memantine did not alleviate lower growth rates in Akita mice compared to DBA/2J controls (Fig. 7A), but reduced 24-hr urine albumin excretion in Akita mice (Fig. 7B). The interaction between drug and genotype on albumin excretion was significant ( $P < 0.05$ ). Memantine also caused a trend toward reduction in mesangial matrix expansion (Fig. 7C, D) ( $F = 3.82$ ,  $P = 0.0743$ ) in Akita mice. Memantine improved glomerular ultrastructure in Akita mice (Fig. 7E), with some reduction in the amount of foot process effacement. However, effects of memantine on GBM thickness (Fig. 7F) were not statistically significant. All these experiments (with both memantine and MK-801 treatments) were also performed in low-dose streptozotocin (STZ) induced diabetic mice as another type-1 mouse model of diabetes, which are not shown in this dissertation. But, overall, MK-801 also has some beneficial effects in the low-dose STZ model, even though treatment was started later in the disease process.

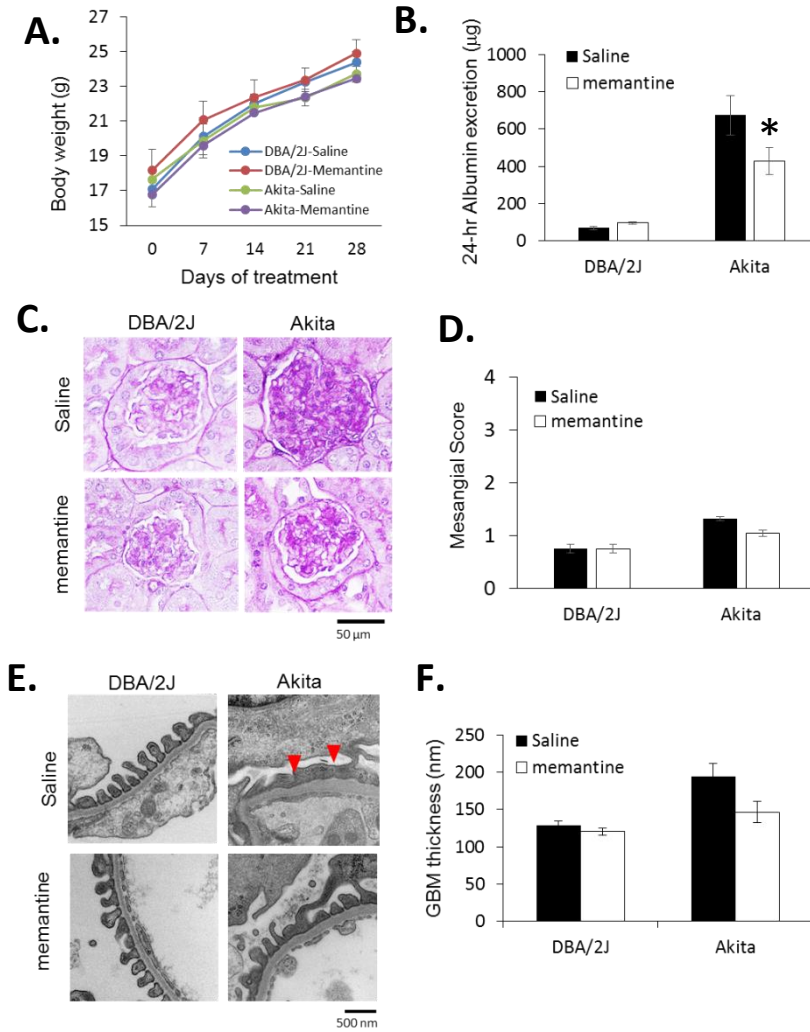


Figure 7. The NMDA antagonist memantine reduces progression of nephropathy in Akita mice. A: Reduced weight gain in Akita mice was not alleviated by memantine. B: Reduced 24-hr albumin excretion in Akita mice that received memantine for 28 days compared to saline-treated controls. The interaction between drug and genotype on albumin excretion was significant ( $F = 4.58$ ,  $P = 0.0403$  with  $N = 10$  mice per group). C: Representative PAS-stained sections of saline-treated and drug-treated Akita mice and DBA/2J controls. D: Mesangial matrix expansion expressed as mesangial score shows modest increase in 12-week old Akita mice that received saline. This increase did not occur in Akita mice that received memantine. Memantine also caused a reduction in mesangial matrix expansion ( $F = 3.82$ ,  $P = 0.0743$ ,  $N = 4$  mice per group) in Akita mice. E: Representative transmission electron micrographs of mice that received memantine or saline. Note reduction in the severity of effacement in Akita mice that received memantine. F: The effect of memantine on GBM thickness, in Akita mice was not statistically significant ( $P > 0.1$ ) by two-way ANOVA with  $N = 4$  mice per group.

### 6.3 Discussion

In this study we have tested the hypothesis that renal NMDA receptors contribute to the progression of diabetic nephropathy in the Akita mouse model of type-1 diabetes. We have observed that elevated glucose causes marked increases in NMDA receptor abundance in two different renal cell types implicated in diabetic nephropathy; that there are marked increases in the abundance of NMDA receptor subunits throughout the kidney of Akita mice; and that sustained inhibition of NMDA receptors *in vivo* using two structurally dissimilar antagonists reduces urine albumin excretion. In addition, MK-801 improved structural and ultrastructural changes that occur in glomeruli of Akita mice during early stages of diabetic nephropathy.

A surprising observation in this study is that all known NMDA receptor subunits and their transcripts can be detected in a widely used immortalized podocyte cell line (MPC-5 cells) and in primary cultures of rat mesangial cells. High glucose caused robust increases in NR1 subunits in both cell types. These cell types differed in terms of which NR2 subunits were upregulated by HG. Nevertheless, the biochemical pattern in both cell types predicts marked increases in functional responses to agonists. The overall pattern in podocytes is similar to that seen in the renal cortex of Akita mice but it should be noted that the biochemical signal in kidney cortex extracts is almost certainly dominated by more robust increases in the expression of NMDA receptor subunits in renal tubules. Increased NMDA receptors were already present by 7 weeks of age in Akita mice, a time at which nephropathy cannot be discerned using light microscopic histological methods and urine albumin excretion is only slightly increased. This suggests that elevated renal NMDA receptors drive the glomerular pathology and are not simply a response to it.

Increased expression of NMDA receptors occurred throughout the kidney of mice with type-1 diabetes, including in cortical and medullary tubules and within glomeruli. Previous studies have shown statistical correlations between serum L-homocysteine and the subsequent appearance of microalbuminuria in patients with diabetes [223, 225, 227, 236]. However, the marked induction of renal NMDA receptors that we and others observe in mouse models of diabetes means that an excessive number of these receptors could be activated even if circulating and locally produced agonists (e.g, HCA and L-quinolinic acid) are present at normal levels. Obviously, any increase in circulating NMDA agonists, which can occur as renal failure progresses [237-240] would cause even more of these receptors to become active.

While many studies of early-stage diabetic nephropathy have focused on glomerular and vascular elements, diabetes produces effects throughout the kidney as a result of hyperfiltration, proximal tubule hyper-reabsorption, alterations in sodium delivery to distal tubules, and marked increases in tubular flow rates [242, 243]. Indeed, in diabetes, there are sustained changes in overall regulatory set-points resulting in marked changes in Na<sup>+</sup> dynamics in diabetic tubules [242, 243]. An intriguing question is whether NMDA receptor activation leads to sustained changes in expression of other transport proteins in a wide range of renal cells in manner reminiscent of biochemical changes in neurons that occur during NMDA receptor-mediated synaptic plasticity [244].

In the CNS, excessive activation of NMDA receptors induces Ca<sup>2+</sup>-overload and oxidative stress, and over time can lead to neurodegeneration [245]. These observations spurred development of several classes of NMDA antagonists, many of which are effective in animal models of neurodegeneration [229, 241]. MK-801 is a non-competitive NMDA

receptor antagonist that can cause nearly complete inhibition of NMDA receptors resulting in cognitive and behavioral deficits, and therefore strong NMDA antagonists are not used clinically. We observed that continuous MK-801 treatment for 28 days reduced nearly every index in diabetic nephropathy. Importantly, a reduction in albumin excretion and improvement in mesangial matrix expansion was observed with memantine, a second structurally distinct NMDA receptor antagonist. Memantine also acts by blocking the NMDA receptor pore, although blockade with this drug is less complete than MK-801. Therefore, synaptic transmission through NMDA receptors is maintained in the presence of memantine, while excessive activation, especially at extrasynaptic receptors, is eliminated [229, 241]. Several clinical studies have shown that memantine can slow the progression of cognitive decline in Alzheimer's disease [230-232]. We observed that memantine also reduced albumin excretion in Akita mice, and also reduced podocyte foot process effacement and mesangial matrix expansion, albeit less than MK-801. Memantine was administered at a dose of 0.2 mg/kg/day. This is less than in the experiments on MK-801, but this dose was chosen to be comparable to the FDA-approved regimen of 20 mg daily that is recommended for treatment of Alzheimer's disease [246]. However, higher doses of memantine are well tolerated and may produce additional benefits for selected patients with Alzheimer's disease [246]. It is possible that higher doses of memantine might produce greater effects in diabetic nephropathy, as we saw with MK-801.

The mechanisms whereby NMDA antagonists could be beneficial to renal function in diabetes are likely to be complex, especially given that NMDA receptors are expressed and up-regulated in many different renal cell types in diabetic animals. NMDA antagonists at the doses used here did not affect systemic mean arterial blood pressure. However,

cortical NMDA receptors have been previously shown to exert a tonic vasodilatory response, especially after glycine infusion, and it is possible that inhibition of these receptors produces hemodynamic effects that help to preserve renal function in the presence of hyperglycemia. NMDA receptors in collecting ducts are upregulated in response to osmotic challenge [218], and perhaps this is relevant in the context of polyuria that occurs in diabetes.

As mentioned previously, sustained application of NMDA to immortalized mouse podocytes induce  $\text{Ca}^{2+}$  influx, oxidative stress and changes in expression of slit diaphragm proteins [66]. If this occurs *in vivo*, one would expect glomerulosclerosis and glomerular dysfunction, as is seen in mouse models of hyperhomocysteinemia [220, 221]. With continuing loss of renal function, circulating NMDA agonists such as HCA, guanadinosuccinate, and L-quinolinic acid may increase, thereby producing a positive feedback loop driving renal pathology.

In summary, we have observed that hyperglycemia and diabetes cause marked increases in the expression of renal NMDA receptors throughout the kidney, and that sustained treatment with NMDA antagonists reduces the progression of nephropathy in a mouse model of type-1 diabetes. One of the agents tested here, memantine, is well tolerated and in widespread clinical use for other conditions. It is possible that other clinically used drugs in this class, such as dextromethorphan, might also be useful. In this regard, the present experiments were carried out in a mouse model of type-1 diabetes in which there is quite minimal  $\beta$ -cell function. However, there is evidence that patients with type-2 diabetes have improved insulin secretion and glycemic control after treatment with dextromethorphan, in part due to effects on NMDA receptors on pancreatic islets [247,

248]. In addition, a large number of NMDA antagonists that bind to sites on NR1 subunits have been discovered [249]. Many of those have poor ability to cross the blood-brain barrier. While that would limit their usefulness for most neurological conditions, it could represent a strategy to strongly inhibit peripheral NMDA receptors without producing cognitive dysfunction.

## 7. CONCLUSIONS

In this dissertation, I have shown that mouse and rat podocyte TRPC6 channels are activated in response to ATP and 20-HETE. Activation of podocyte TRPC6 channels by ATP and 20-HETE requires generation of ROS, G protein signaling, and podocin (Fig. 1). 20-HETE- and ATP-evoked activation of TRPC6 channels are abolished by treatments that inhibit or knockdown TRPC6 and podocin. I have also shown that ATP and 20-HETE upregulate steady-state cell surface expression of TRPC6 channels in podocytes.

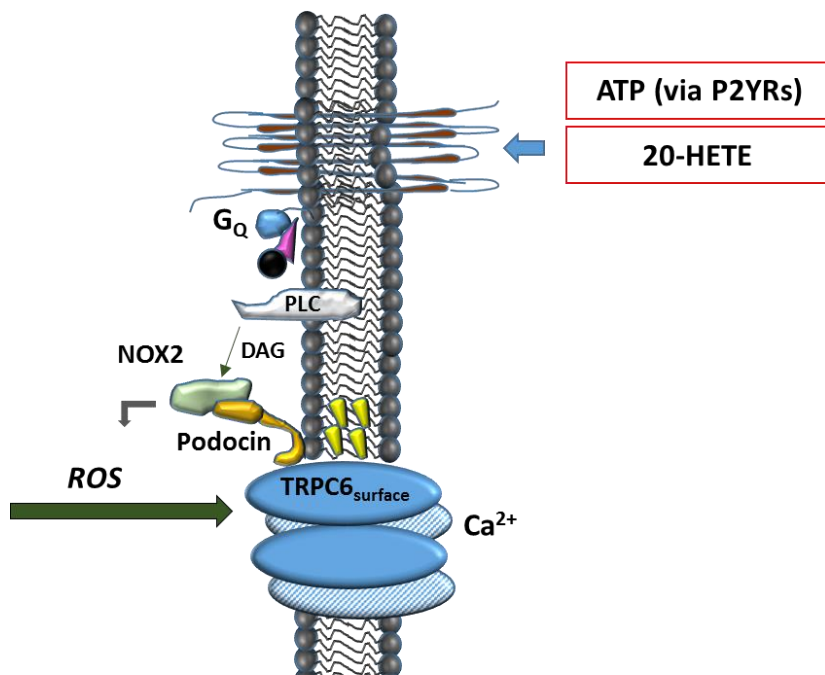


Figure 1. Chemical stimuli ATP and 20-HETE activate mouse and rat podocyte TRPC6 channels. Activation of podocyte TRPC6 channels by ATP and 20-HETE requires generation of ROS, G protein signaling, and podocin.

Large qualitative changes in the behavior of podocyte cationic channels with the properties of TRPC6 occur in distinctly different models of acquired nephrotic syndromes, including the chronic PAN model of secondary FSGS in rats, and *in vitro* models in which immortalized mouse podocytes were exposed to serum or plasma from patients with relapsed recurrent FSGS, or to recombinant glomerular “permeability factors” (TNF and suPAR) implicated in primary FSGS. In most of these *in vitro* and *in vivo* models, TRPC6 currents are dramatically increased in response to the mechanical stimulus, but are diminished in response to chemical stimuli, a phenomenon that closely correlates with the loss of podocin in the cells. I also observed that these changes in TRPC6 gating properties were reduced in serum taken from patients who were in a remission from their disease.

In the last chapter of this dissertation, I demonstrated that renal NMDA receptors contribute to the progression of diabetic nephropathy in the Akita mouse model of type-1 diabetes. Moreover, elevated external glucose caused marked increases in NMDA receptor abundance in podocytes and mesangial cells, both of which are implicated in diabetic nephropathy. There are marked increases in the abundance of NMDA receptor subunits throughout the kidney of Akita mice, and sustained inhibition of NMDA receptors *in vivo* using two structurally dissimilar antagonists (MK-801 and memantine) significantly reduced urine albumin excretion. In addition, MK-801 significantly improved structural and ultrastructural changes that occur in glomeruli of Akita mice during early stages of diabetic nephropathy.

These results suggest possible therapeutic strategies for treatment of these devastating kidney disease. It is possible that small-molecule TRPC6 inhibitors could be useful for treatment of all forms of FSGS, not just the rare subset of patients who have

mutations in the *TRPC6* gene, but also patients with mutations in *NPHS2*, and patients with primary or secondary acquired forms of FSGS. Similarly small molecule NMDA antagonists might be useful to reduce renal complications of diabetes in humans, which accounts for a large portion of patients currently requiring dialysis for survival. One such molecule, memantine, is already in widespread clinical use for patients with dementias. Additional studies are needed by the results of these studies provide a strong rationale to continue this line of research.

## REFERENCES

1. Eaton DC, Pooler J. *Vander's Renal Physiology, 7th Edition*. McGraw-Hill Education, Placed Published: 2009.
2. Somlo S, Mundel P. Getting a foothold in nephrotic syndrome. *Nat Genet* 2000;24(4):333-335
3. Kerjaschki D. Caught flat-footed: podocyte damage and the molecular bases of focal glomerulosclerosis. *J Clin Invest* 2001;108(11):1583-1587
4. K/DOQI clinical practice guidelines for chronic kidney disease: evaluation, classification, and stratification. *Am J Kidney Dis* 2002;39(2 Suppl 1):S1-266
5. Remuzzi G, Bertani T. Pathophysiology of progressive nephropathies. *N Engl J Med* 1998;339(20):1448-1456
6. Nath KA. The tubulointerstitium in progressive renal disease. *Kidney Int* 1998;54(3):992-994
7. Remuzzi G, Ruggenti P, Perico N. Chronic renal diseases: renoprotective benefits of renin-angiotensin system inhibition. *Ann Intern Med* 2002;136(8):604-615
8. Hales CN. Suicide of the nephron. *Lancet* 2001;357(9250):136-137
9. Nath KA. Reshaping the interstitium by platelet-derived growth factor. Implications for progressive renal disease. *Am J Pathol* 1996;148(4):1031-1036
10. Burton CJ, Combe C, Walls J, *et al*. Secretion of chemokines and cytokines by human tubular epithelial cells in response to proteins. *Nephrol Dial Transplant* 1999;14(11):2628-2633
11. Muntner P, Coresh J, Smith JC, *et al*. Plasma lipids and risk of developing renal dysfunction: the atherosclerosis risk in communities study. *Kidney Int* 2000;58(1):293-301
12. Fried LF, Orchard TJ, Kasiske BL. Effect of lipid reduction on the progression of renal disease: a meta-analysis. *Kidney Int* 2001;59(1):260-269
13. Remuzzi G. Cigarette smoking and renal function impairment. *Am J Kidney Dis* 1999;33(4):807-813
14. Orth SR, Ogata H, Ritz E. Smoking and the kidney. *Nephrol Dial Transplant*

2000;15(10):1509-1511

15. Pinto-Sietsma SJ, Mulder J, Janssen WM, *et al.* Smoking is related to albuminuria and abnormal renal function in nondiabetic persons. *Ann Intern Med* 2000;133(8):585-591
16. Ritz E, Orth SR. Nephropathy in patients with type 2 diabetes mellitus. *N Engl J Med* 1999;341(15):1127-1133
17. Fored CM, Ejerblad E, Lindblad P, *et al.* Acetaminophen, aspirin, and chronic renal failure. *N Engl J Med* 2001;345(25):1801-1808
18. Rexrode KM, Buring JE, Glynn RJ, *et al.* Analgesic use and renal function in men. *Jama* 2001;286(3):315-321
19. Krop JS, Coresh J, Chambless LE, *et al.* A community-based study of explanatory factors for the excess risk for early renal function decline in blacks vs whites with diabetes: the Atherosclerosis Risk in Communities study. *Arch Intern Med* 1999;159(15):1777-1783
20. Freedman BI, Soucie JM, Stone SM, *et al.* Familial clustering of end-stage renal disease in blacks with HIV-associated nephropathy. *Am J Kidney Dis* 1999;34(2):254-258
21. Freedman BI, Soucie JM, Chapman A, *et al.* Racial variation in autosomal dominant polycystic kidney disease. *Am J Kidney Dis* 2000;35(1):35-39
22. Rosenberg ME KC. *The Kidney Physiology and Pathophysiology*. Williams & Wilkins, Placed Published: 2000.
23. Saran R, Li Y, Robinson B, *et al.* US Renal Data System 2014 Annual Data Report: Epidemiology of Kidney Disease in the United States. *Am J Kidney Dis* 2015;66(1 Suppl 1):Svii, S1-305
24. Haas M, Spargo BH, Coventry S. Increasing incidence of focal-segmental glomerulosclerosis among adult nephropathies: a 20-year renal biopsy study. *Am J Kidney Dis* 1995;26(5):740-750
25. Andreoli SP. Racial and ethnic differences in the incidence and progression of focal segmental glomerulosclerosis in children. *Adv Ren Replace Ther* 2004;11(1):105-109

26. Jefferson JA, Shankland SJ. The Pathogenesis of Focal Segmental Glomerulosclerosis. *Advances in Chronic Kidney Disease* 2014;21(5):408-416
27. Conlon PJ, Butterly D, Albers F, *et al.* Clinical and pathologic features of familial focal segmental glomerulosclerosis. *Am J Kidney Dis* 1995;26(1):34-40
28. Winn MP, Conlon PJ, Lynn KL, *et al.* Clinical and genetic heterogeneity in familial focal segmental glomerulosclerosis. International Collaborative Group for the Study of Familial Focal Segmental Glomerulosclerosis. *Kidney Int* 1999;55(4):1241-1246
29. Savin VJ, Sharma R, Sharma M, *et al.* Circulating factor associated with increased glomerular permeability to albumin in recurrent focal segmental glomerulosclerosis. *N Engl J Med* 1996;334(14):878-883
30. Wei C, Trachtman H, Li J, *et al.* Circulating suPAR in two cohorts of primary FSGS. *J Am Soc Nephrol* 2012;23(12):2051-2059
31. Wei C, El Hindi S, Li J, *et al.* Circulating urokinase receptor as a cause of focal segmental glomerulosclerosis. *Nat Med* 2011;17(8):952-960
32. McCarthy ET, Sharma M, Savin VJ. Circulating permeability factors in idiopathic nephrotic syndrome and focal segmental glomerulosclerosis. *Clin J Am Soc Nephrol* 2010;5(11):2115-2121
33. Suranyi MG, Guasch A, Hall BM, *et al.* Elevated levels of tumor necrosis factor-alpha in the nephrotic syndrome in humans. *Am J Kidney Dis* 1993;21(3):251-259
34. Bakr A, Shokeir M, El-Chenawi F, *et al.* Tumor necrosis factor-alpha production from mononuclear cells in nephrotic syndrome. *Pediatr Nephrol* 2003;18(6):516-520
35. Leroy S, Guignon V, Bruckner D, *et al.* Successful anti-TNFalpha treatment in a child with posttransplant recurrent focal segmental glomerulosclerosis. *Am J Transplant* 2009;9(4):858-861
36. Bitzan M, Babayeva S, Vasudevan A, *et al.* TNFalpha pathway blockade ameliorates toxic effects of FSGS plasma on podocyte cytoskeleton and beta3 integrin activation. *Pediatr Nephrol* 2012;27(12):2217-2226
37. Coroneos E, Petrussevska G, Varghese F, *et al.* Focal segmental glomerulosclerosis with acute renal failure associated with alpha-interferon therapy. *Am J Kidney Dis* 1996;28(6):888-892

38. D'Agati V. The many masks of focal segmental glomerulosclerosis. *Kidney Int* 1994;46(4):1223-1241
39. Graham BL, Jr., Rubin J, Files JC, *et al.* Focal glomerulosclerosis in Hodgkin's disease necessitating peritoneal dialysis. *South Med J* 1989;82(9):1187-1189
40. Mazbar SA, Schoenfeld PY, Humphreys MH. Renal involvement in patients infected with HIV: experience at San Francisco General Hospital. *Kidney Int* 1990;37(5):1325-1332
41. Rennke HG, Klein PS. Pathogenesis and significance of nonprimary focal and segmental glomerulosclerosis. *Am J Kidney Dis* 1989;13(6):443-456
42. Kaplan JM, Kim SH, North KN, *et al.* Mutations in ACTN4, encoding alpha-actinin-4, cause familial focal segmental glomerulosclerosis. *Nat Genet* 2000;24(3):251-256
43. Fogo A, Hawkins EP, Berry PL, *et al.* Glomerular hypertrophy in minimal change disease predicts subsequent progression to focal glomerular sclerosis. *Kidney Int* 1990;38(1):115-123
44. Fogo A, Bruijn JA, Cohen AH, *et al.* *Fundamentals of Renal Pathology*. Springer New York, Placed Published: 2007.
45. Kitiyakara C, Eggers P, Kopp JB. Twenty-one-year trend in ESRD due to focal segmental glomerulosclerosis in the United States. *Am J Kidney Dis* 2004;44(5):815-825
46. Reiser J, Pixley FJ, Hug A, *et al.* Regulation of mouse podocyte process dynamics by protein tyrosine phosphatases rapid communication. *Kidney Int* 2000;57(5):2035-2042
47. Shih NY, Li J, Karpitskii V, *et al.* Congenital nephrotic syndrome in mice lacking CD2-associated protein. *Science* 1999;286(5438):312-315
48. Michaud JL, Lemieux LI, Dube M, *et al.* Focal and segmental glomerulosclerosis in mice with podocyte-specific expression of mutant alpha-actinin-4. *J Am Soc Nephrol* 2003;14(5):1200-1211
49. Roselli S, Gribouval O, Boute N, *et al.* Podocin localizes in the kidney to the slit diaphragm area. *Am J Pathol* 2002;160(1):131-139
50. Schwarz K, Simons M, Reiser J, *et al.* Podocin, a raft-associated component of the glomerular slit diaphragm, interacts with CD2AP and nephrin. *J Clin Invest* 2001;108(11):1621-1629

51. Huber TB, Schermer B, Muller RU, *et al.* Podocin and MEC-2 bind cholesterol to regulate the activity of associated ion channels. *Proc Natl Acad Sci U S A* 2006;103(46):17079-17086
52. Boute N, Gribouval O, Roselli S, *et al.* NPHS2, encoding the glomerular protein podocin, is mutated in autosomal recessive steroid-resistant nephrotic syndrome. *Nat Genet* 2000;24(4):349-354
53. Pedersen SF, Owsianik G, Nilius B. TRP channels: an overview. *Cell Calcium* 2005;38(3-4):233-252
54. Nilius B, Voets T. Diversity of TRP channel activation. *Novartis Found Symp* 2004;258:140-149; discussion 149-159, 263-146
55. Clapham DE. TRP channels as cellular sensors. *Nature* 2003;426(6966):517-524
56. Reiser J, Polu KR, Moller CC, *et al.* TRPC6 is a glomerular slit diaphragm-associated channel required for normal renal function. *Nat Genet* 2005;37(7):739-744
57. Winn MP, Conlon PJ, Lynn KL, *et al.* A mutation in the TRPC6 cation channel causes familial focal segmental glomerulosclerosis. *Science* 2005;308(5729):1801-1804
58. Heeringa SF, Möller CC, Du J, *et al.* A Novel *TRPC6* Mutation That Causes Childhood FSGS. *PLoS ONE* 2009;4(11):e7771
59. Schlondorff J, Del Camino D, Carrasquillo R, *et al.* TRPC6 mutations associated with focal segmental glomerulosclerosis cause constitutive activation of NFAT-dependent transcription. *Am J Physiol Cell Physiol* 2009;296(3):7
60. Moller CC, Wei C, Altintas MM, *et al.* Induction of TRPC6 channel in acquired forms of proteinuric kidney disease. *J Am Soc Nephrol* 2007;18(1):29-36
61. Krall P, Canales CP, Kairath P, *et al.* Podocyte-Specific Overexpression of Wild Type or Mutant *Trpc6* in Mice Is Sufficient to Cause Glomerular Disease. *PLoS ONE* 2010;5(9):e12859
62. Wang Z, Wei X, Zhang Y, *et al.* NADPH Oxidase-derived ROS Contributes to Upregulation of TRPC6 Expression in Puromycin Aminonucleoside-induced Podocyte Injury. *Cellular Physiology and Biochemistry* 2009;24(5-6):619-626
63. Hofmann T, Obukhov AG, Schaefer M, *et al.* Direct activation of human TRPC6 and TRPC3 channels by diacylglycerol. *Nature* 1999;397(6716):259-263

64. Anderson M, Kim EY, Hagmann H, *et al.* Opposing effects of podocin on the gating of podocyte TRPC6 channels evoked by membrane stretch or diacylglycerol. *Am J Physiol Cell Physiol* 2013;305(3):C276-289
65. Kim EY, Anderson M, Dryer SE. Insulin increases surface expression of TRPC6 channels in podocytes: role of NADPH oxidases and reactive oxygen species. *Am J Physiol Renal Physiol* 2012;302(3):F298-307
66. Kim EY, Anderson M, Dryer SE. Sustained activation of N-methyl-D-aspartate receptors in podocytes leads to oxidative stress, mobilization of transient receptor potential canonical 6 channels, nuclear factor of activated T cells activation, and apoptotic cell death. *Mol Pharmacol* 2012;82(4):728-737
67. Anderson M, Roshanravan H, Khine J, *et al.* Angiotensin II activation of canonical transient receptor potential-6 (TRPC6) channels in rat podocytes requires generation of reactive oxygen species. *Journal of Cellular Physiology* 2013;n/a-n/a
68. Roshanravan H, Dryer SE. ATP acting through P2Y receptors causes activation of podocyte TRPC6 channels: Role of podocin and reactive oxygen species. *American Journal of Physiology - Renal Physiology* 2014
69. Liu BC, Song X, Lu XY, *et al.* High glucose induces podocyte apoptosis by stimulating TRPC6 via elevation of reactive oxygen species. *Biochim Biophys Acta* 2013;1833(6):1434-1442
70. Inoue R, Jensen LJ, Jian Z, *et al.* Synergistic activation of vascular TRPC6 channel by receptor and mechanical stimulation via phospholipase C/diacylglycerol and phospholipase A2/omega-hydroxylase/20-HETE pathways. *Circ Res* 2009;104(12):1399-1409
71. Storch U, Mederos y Schnitzler M, Gudermann T. G protein-mediated stretch reception. *Am J Physiol Heart Circ Physiol* 2012;302(6):H1241-1249
72. Reidy K, Kang HM, Hostetter T, *et al.* Molecular mechanisms of diabetic kidney disease. *J Clin Invest* 2014;124(6):2333-2340
73. Lim A. Diabetic nephropathy - complications and treatment. *Int J Nephrol Renovasc Dis* 2014;7:361-381
74. Alicic RZ, Tuttle KR. Novel therapies for diabetic kidney disease. *Adv Chronic Kidney Dis* 2014;21(2):121-133

75. Schwartz MM, Lewis EJ, Leonard-Martin T, *et al.* Renal pathology patterns in type II diabetes mellitus: relationship with retinopathy. The Collaborative Study Group. *Nephrol Dial Transplant* 1998;13(10):2547-2552
76. Huang W, Gallois Y, Bouby N, *et al.* Genetically increased angiotensin I-converting enzyme level and renal complications in the diabetic mouse. *Proc Natl Acad Sci U S A* 2001;98(23):13330-13334
77. Rudberg S, Rasmussen LM, Bangstad HJ, *et al.* Influence of insertion/deletion polymorphism in the ACE-I gene on the progression of diabetic glomerulopathy in type 1 diabetic patients with microalbuminuria. *Diabetes Care* 2000;23(4):544-548
78. Benz K, Amann K. Endothelin in diabetic renal disease. *Contrib Nephrol* 2011;172:139-148
79. Brownlee M. Biochemistry and molecular cell biology of diabetic complications. *Nature* 2001;414(6865):813-820
80. Beckerman P, Susztak K. Sweet debate: fructose versus glucose in diabetic kidney disease. *J Am Soc Nephrol* 2014;25(11):2386-2388
81. Lanasa MA, Ishimoto T, Cicerchi C, *et al.* Endogenous fructose production and fructokinase activation mediate renal injury in diabetic nephropathy. *J Am Soc Nephrol* 2014;25(11):2526-2538
82. Prevention CfDca. *Centers for Disease Control and Prevention, Annual Number (in Thousands) of New Cases of Diagnosed Diabetes Among Adults Aged 18–79 Years, United States, 1980–2011.* <http://www.cdc.gov/diabetes/statistics/incidence/fig1.htm>.
83. Sheetz MJ, King GL. Molecular understanding of hyperglycemia's adverse effects for diabetic complications. *Jama* 2002;288(20):2579-2588
84. Craven PA, Davidson CM, DeRubertis FR. Increase in diacylglycerol mass in isolated glomeruli by glucose from de novo synthesis of glycerolipids. *Diabetes* 1990;39(6):667-674
85. Bank N, Aynedjian HS. Role of EDRF (nitric oxide) in diabetic renal hyperfiltration. *Kidney Int* 1993;43(6):1306-1312
86. Dunn MJ. Prostaglandin I<sub>2</sub> and the kidney. *Arch Mal Coeur Vaiss* 1989;82 Spec No 4:27-31

87. Williams B, Schrier RW. Glucose-induced protein kinase C activity regulates arachidonic acid release and eicosanoid production by cultured glomerular mesangial cells. *J Clin Invest* 1993;92(6):2889-2896
88. Garcia-Garcia PM, Getino-Melian MA, Dominguez-Pimentel V, *et al.* Inflammation in diabetic kidney disease. *World J Diabetes* 2014;5(4):431-443
89. Pickup JC. Inflammation and activated innate immunity in the pathogenesis of type 2 diabetes. *Diabetes Care* 2004;27(3):813-823
90. Kim EY, Choi KJ, Dryer SE. Nephrin binds to the COOH terminus of a large-conductance Ca<sup>2+</sup>-activated K<sup>+</sup> channel isoform and regulates its expression on the cell surface. *Am J Physiol Renal Physiol* 2008;295(1):F235-246
91. Savin VJ, Terreros DA. Filtration in single isolated mammalian glomeruli. *Kidney Int* 1981;20(2):188-197
92. Kim EY, Anderson M, Wilson C, *et al.* NOX2 interacts with podocyte TRPC6 channels and contributes to their activation by diacylglycerol: essential role of podocin in formation of this complex. *American Journal of Physiology - Cell Physiology* 2013;305(9):C960-C971
93. Eckstein F, Cassel D, Levkovitz H, *et al.* Guanosine 5'-O-(2-thiodiphosphate). An inhibitor of adenylate cyclase stimulation by guanine nucleotides and fluoride ions. *Journal of Biological Chemistry* 1979;254(19):9829-9834
94. Kim EY, Roshanravan H, Dryer SE. Syndecan-4 ectodomain evokes mobilization of podocyte TRPC6 channels and their associated pathways: An essential role for integrin signaling. *Biochim Biophys Acta* 2015;1853(10 Pt A):2610-2620
95. Huang Y, Border WA, Yu L, *et al.* A PAI-1 mutant, PAI-1R, slows progression of diabetic nephropathy. *J Am Soc Nephrol* 2008;19(2):329-338
96. Pavenstadt H, Kriz W, Kretzler M. Cell biology of the glomerular podocyte. *Physiol Rev* 2003;83(1):253-307
97. Höhne M, Ising C, Hagmann H, *et al.* Light Microscopic Visualization of Podocyte Ultrastructure Demonstrates Oscillating Glomerular Contractions. *The American Journal of Pathology* 2013;182(2):332-338
98. Peti-Peterdi J, Sipos A. A high-powered view of the filtration barrier. *J Am Soc Nephrol* 2010;21(11):1835-1841

99. Kriz W, Shirato I, Nagata M, *et al.* The podocyte's response to stress: the enigma of foot process effacement. *Am J Physiol Renal Physiol* 2013;304(4):F333-347
100. Holstein-Rathlou NH, Wagner AJ, Marsh DJ. Tubuloglomerular feedback dynamics and renal blood flow autoregulation in rats. *Am J Physiol* 1991;260(1 Pt 2):F53-68
101. Holstein-Rathlou NH. Oscillations and chaos in renal blood flow control. *J Am Soc Nephrol* 1993;4(6):1275-1287
102. Komlosi P, Bell PD, Zhang ZR. Tubuloglomerular feedback mechanisms in nephron segments beyond the macula densa. *Curr Opin Nephrol Hypertens* 2009;18(1):57-62
103. Singh P, Thomson SC. Renal homeostasis and tubuloglomerular feedback. *Curr Opin Nephrol Hypertens* 2010;19(1):59-64
104. Ren Y, D'Ambrosio MA, Garvin JL, *et al.* Possible mediators of connecting tubule glomerular feedback. *Hypertension* 2009;53(2):319-323
105. Ren Y, Garvin JL, Liu R, *et al.* Possible mechanism of efferent arteriole (Ef-Art) tubuloglomerular feedback. *Kidney Int* 2007;71(9):861-866
106. Schnermann J. Maintained tubuloglomerular feedback responses during acute inhibition of P2 purinergic receptors in mice. *American Journal of Physiology - Renal Physiology* 2011;300(2):F339-F344
107. Schnermann J, Briggs JP. Tubuloglomerular feedback: mechanistic insights from gene-manipulated mice. *Kidney Int* 2008;74(4):418-426
108. Peti-Peterdi J. Calcium wave of tubuloglomerular feedback. *Am J Physiol Renal Physiol* 2006;291(2):F473-480
109. Dale N. Dynamic ATP signalling and neural development. *J Physiol* 2008;586(10):2429-2436
110. Li A, Banerjee J, Leung CT, *et al.* Mechanisms of ATP release, the enabling step in purinergic dynamics. *Cell Physiol Biochem* 2011;28(6):1135-1144
111. Toma I, Bansal E, Meer EJ, *et al.* Connexin 40 and ATP-dependent intercellular calcium wave in renal glomerular endothelial cells. *Am J Physiol Regul Integr Comp Physiol* 2008;294(6):R1769-1776

112. Dietrich A, Gudermann T. TRPC6. In: Flockerzi V, Nilius B, eds. *Transient Receptor Potential (TRP) Channels*. Springer Berlin Heidelberg 2007, 125-141.
113. Dryer SE, Reiser J. TRPC6 channels and their binding partners in podocytes: role in glomerular filtration and pathophysiology. *American Journal of Physiology - Renal Physiology* 2010;299(4):F689-F701
114. Fischer KG, Saueressig U, Jacobshagen C, *et al.* Extracellular nucleotides regulate cellular functions of podocytes in culture. *Am J Physiol Renal Physiol* 2001;281(6):F1075-1081
115. Ilatovskaya DV, Palygin O, Levchenko V, *et al.* Pharmacological characterization of the P2 receptors profile in the podocytes of the freshly isolated rat glomeruli. *Am J Physiol Cell Physiol* 2013;305(10):C1050-1059
116. von Kügelgen I, Wetter A. Molecular pharmacology of P2Y-receptors. *Naunyn-Schmiedeberg's Archives of Pharmacology* 2000;362(4-5):310-323
117. El-Tayeb A, Qi A, Nicholas RA, *et al.* Structural Modifications of UMP, UDP, and UTP Leading to Subtype-Selective Agonists for P2Y2, P2Y4, and P2Y6 Receptors. *Journal of Medicinal Chemistry* 2011;54(8):2878-2890
118. Tian D, Jacobo SM, Billing D, *et al.* Antagonistic regulation of actin dynamics and cell motility by TRPC5 and TRPC6 channels. *Sci Signal* 2010;3(145):ra77
119. Jung S, Mühle A, Schaefer M, *et al.* Lanthanides Potentiate TRPC5 Currents by an Action at Extracellular Sites Close to the Pore Mouth. *Journal of Biological Chemistry* 2003;278(6):3562-3571
120. Bailey MA, Turner CM, Hus-Citharel A, *et al.* P2Y Receptors Present in the Native and Isolated Rat Glomerulus. *Nephron Physiology* 2004;96(3):p79-p90
121. Vallon V, Rieg T. Regulation of renal NaCl and water transport by the ATP/UTP/P2Y2 receptor system. *American Journal of Physiology - Renal Physiology* 2011;301(3):F463-F475
122. Vonend O, Stegbauer J, Sojka J, *et al.* Noradrenaline and extracellular nucleotide cotransmission involves activation of vasoconstrictive P2X(1,3)- and P2Y6-like receptors in mouse perfused kidney. *Br J Pharmacol* 2005;145(1):66-74
123. Lehrmann H, Thomas J, Kim SJ, *et al.* Luminal P2Y2 Receptor-Mediated

- Inhibition of Na<sup>+</sup> Absorption in Isolated Perfused Mouse CCD. *Journal of the American Society of Nephrology* 2002;13(1):10-18
124. Shirley DG, Bailey MA, Unwin RJ. In vivo stimulation of apical P2 receptors in collecting ducts: evidence for inhibition of sodium reabsorption. *American Journal of Physiology - Renal Physiology* 2005;288(6):F1243-F1248
125. Rieg T, Bunday RA, Chen Y, *et al.* Mice lacking P2Y<sub>2</sub> receptors have salt-resistant hypertension and facilitated renal Na<sup>+</sup> and water reabsorption. *The FASEB Journal* 2007;21(13):3717-3726
126. Pochynyuk O, Bugaj V, Rieg T, *et al.* Paracrine Regulation of the Epithelial Na<sup>+</sup> Channel in the Mammalian Collecting Duct by Purinergic P2Y<sub>2</sub> Receptor Tone. *Journal of Biological Chemistry* 2008;283(52):36599-36607
127. Pochynyuk O, Rieg T, Bugaj V, *et al.* Dietary Na<sup>+</sup> inhibits the open probability of the epithelial sodium channel in the kidney by enhancing apical P2Y<sub>2</sub>-receptor tone. *The FASEB Journal* 2010;24(6):2056-2065
128. Kishore B, Nelson R, Miller RL, *et al.* P2Y<sub>2</sub> receptors and water transport in the kidney. *Purinergic Signalling* 2009;5(4):491-499
129. Praetorius HA, Leipziger J. Intrarenal Purinergic Signaling in the Control of Renal Tubular Transport. *Annual Review of Physiology* 2010;72(1):377-393
130. Potthoff SA, Stegbauer J, Becker J, *et al.* P2Y<sub>2</sub> receptor deficiency aggravates chronic kidney disease progression. *Frontiers in Physiology* 2013;4
131. Homolya L, Watt WC, Lazarowski ER, *et al.* Nucleotide-regulated Calcium Signaling in Lung Fibroblasts and Epithelial Cells from Normal and P2Y<sub>2</sub> Receptor (-/-) Mice. *Journal of Biological Chemistry* 1999;274(37):26454-26460
132. Ito O, Roman RJ. Regulation of P-450 4A activity in the glomerulus of the rat. *Am J Physiol* 1999;276(6 Pt 2):R1749-1757
133. Ito O, Roman RJ. Role of 20-HETE in elevating chloride transport in the thick ascending limb of Dahl SS/Jr rats. *Hypertension* 1999;33(1 Pt 2):419-423
134. Ito O, Alonso-Galicia M, Hopp KA, *et al.* Localization of cytochrome P-450 4A isoforms along the rat nephron. *Am J Physiol* 1998;274(2 Pt 2):F395-404
135. Omata K, Abraham NG, Schwartzman ML. Renal cytochrome P-450-arachidonic

acid metabolism: localization and hormonal regulation in SHR. *Am J Physiol* 1992;262(4 Pt 2):F591-599

136. Carroll MA, Sala A, Dunn CE, *et al.* Structural identification of cytochrome P450-dependent arachidonate metabolites formed by rabbit medullary thick ascending limb cells. *J Biol Chem* 1991;266(19):12306-12312

137. Escalante B, Erlj D, Falck JR, *et al.* Effect of cytochrome P450 arachidonate metabolites on ion transport in rabbit kidney loop of Henle. *Science* 1991;251(4995):799-802

138. Ma YH, Gebremedhin D, Schwartzman ML, *et al.* 20-Hydroxyeicosatetraenoic acid is an endogenous vasoconstrictor of canine renal arcuate arteries. *Circ Res* 1993;72(1):126-136

139. Fan F, Sun C-W, Maier KG, *et al.* 20-Hydroxyeicosatetraenoic Acid Contributes to the Inhibition of K<sup>+</sup> Channel Activity and Vasoconstrictor Response to Angiotensin II in Rat Renal Microvessels. *PLoS ONE* 2013;8(12):e82482

140. Schnermann J. Concurrent activation of multiple vasoactive signaling pathways in vasoconstriction caused by tubuloglomerular feedback: a quantitative assessment. *Annu Rev Physiol* 2015;77:301-322

141. Lange A, Gebremedhin D, Narayanan J, *et al.* 20-Hydroxyeicosatetraenoic acid-induced vasoconstriction and inhibition of potassium current in cerebral vascular smooth muscle is dependent on activation of protein kinase C. *J Biol Chem* 1997;272(43):27345-27352

142. Obara K, Koide M, Nakayama K. 20-Hydroxyeicosatetraenoic acid potentiates stretch-induced contraction of canine basilar artery via PKC alpha-mediated inhibition of K<sub>Ca</sub> channel. *Br J Pharmacol* 2002;137(8):1362-1370

143. Muthalif MM, Benter IF, Karzoun N, *et al.* 20-Hydroxyeicosatetraenoic acid mediates calcium/calmodulin-dependent protein kinase II-induced mitogen-activated protein kinase activation in vascular smooth muscle cells. *Proc Natl Acad Sci U S A* 1998;95(21):12701-12706

144. Sun CW, Falck JR, Harder DR, *et al.* Role of tyrosine kinase and PKC in the vasoconstrictor response to 20-HETE in renal arterioles. *Hypertension* 1999;33(1 Pt 2):414-418

145. Randriamboavonjy V, Busse R, Fleming I. 20-HETE-induced contraction of small coronary arteries depends on the activation of Rho-kinase. *Hypertension* 2003;41(3 Pt 2):801-806
146. Alonso-Galicia M, Maier KG, Greene AS, *et al.* Role of 20-hydroxyeicosatetraenoic acid in the renal and vasoconstrictor actions of angiotensin II. *Am J Physiol Regul Integr Comp Physiol* 2002;283(1):R60-68
147. Zhang F, Wang MH, Krishna UM, *et al.* Modulation by 20-HETE of phenylephrine-induced mesenteric artery contraction in spontaneously hypertensive and Wistar-Kyoto rats. *Hypertension* 2001;38(6):1311-1315
148. Parmentier JH, Muthalif MM, Saeed AE, *et al.* Phospholipase D activation by norepinephrine is mediated by 12(s)-, 15(s)-, and 20-hydroxyeicosatetraenoic acids generated by stimulation of cytosolic phospholipase a2. tyrosine phosphorylation of phospholipase d2 in response to norepinephrine. *J Biol Chem* 2001;276(19):15704-15711
149. Carroll MA, Balazy M, Huang D-D, *et al.* Cytochrome P450-derived renal HETEs: Storage and release. *Kidney International* 1997;51(6):1696-1702
150. Graham S, Gorin Y, Abboud HE, *et al.* Abundance of TRPC6 protein in glomerular mesangial cells is decreased by ROS and PKC in diabetes. *Am J Physiol Cell Physiol* 2011;301(2):C304-315
151. Ge Y, Murphy SR, Lu Y, *et al.* Endogenously produced 20-HETE modulates myogenic and TGF response in microperfused afferent arterioles. *Prostaglandins & Other Lipid Mediators* 2013;102–103(0):42-48
152. Zoccali C, Mallamaci F, Grassi G. *20-Hydroxyeicosatetraenoic acid, a far-reaching autacoid in chronic kidney disease: hypertension and beyond.* *J Hypertens.* 2015 Sep;33(9):1764-6. doi: 10.1097/HJH.0000000000000678., Placed Published.
153. Eid S, Maalouf R, Jaffa AA, *et al.* 20-HETE and EETs in Diabetic Nephropathy: A Novel Mechanistic Pathway. *PLoS ONE* 2013;8(8):e70029
154. Williams JM, Murphy S, Burke M, *et al.* 20-HETE: A NEW TARGET FOR THE TREATMENT OF HYPERTENSION. *Journal of cardiovascular pharmacology* 2010;56(4):336-344
155. Klawitter J, Klawitter J, McFann K, *et al.* Bioactive lipid mediators in polycystic

kidney disease. *J Lipid Res* 2013;55(6):1139-1149

156. McGiff JC, Quilley J. 20-HETE and the kidney: resolution of old problems and new beginnings. *Am J Physiol* 1999;277(3 Pt 2):R607-623

157. Eid S, Abou-Kheir W, Sabra R, *et al.* Involvement of renal cytochromes P450 and arachidonic acid metabolites in diabetic nephropathy. *J Biol Regul Homeost Agents* 2013;27(3):693-703

158. Eid AA, Gorin Y, Fagg BM, *et al.* Mechanisms of Podocyte Injury in Diabetes: Role of Cytochrome P450 and NADPH Oxidases. *Diabetes* 2009;58(5):1201-1211

159. Benter IF, Yousif MH, Canatan H, *et al.* Inhibition of Ca<sup>2+</sup>/calmodulin-dependent protein kinase II, RAS-GTPase and 20-hydroxyeicosatetraenoic acid attenuates the development of diabetes-induced vascular dysfunction in the rat carotid artery. *Pharmacol Res* 2005;52(3):252-257

160. Luo P, Zhou Y, Chang HH, *et al.* Glomerular 20-HETE, EETs, and TGF-beta1 in diabetic nephropathy. *Am J Physiol Renal Physiol* 2009;296(3):F556-563

161. Regner KR, Zuk A, Van Why SK, *et al.* Protective effect of 20-HETE analogues in experimental renal ischemia reperfusion injury. *Kidney Int* 2009;75(5):511-517

162. Hoff U, Lukitsch I, Chaykovska L, *et al.* Inhibition of 20-HETE synthesis and action protects the kidney from ischemia/reperfusion injury. *Kidney Int* 2011;79(1):57-65

163. Graham S, Ding M, Sours-Brothers S, *et al.* Downregulation of TRPC6 protein expression by high glucose, a possible mechanism for the impaired Ca<sup>2+</sup> signaling in glomerular mesangial cells in diabetes. *American Journal of Physiology - Renal Physiology* 2007;293(4):F1381-F1390

164. Leca N. Focal segmental glomerulosclerosis recurrence in the renal allograft. *Adv Chronic Kidney Dis* 2014;21(5):448-452

165. Horinouchi I, Nakazato H, Kawano T, *et al.* In situ evaluation of podocin in normal and glomerular diseases. *Kidney Int* 2003;64(6):2092-2099

166. Babayeva S, Miller M, Zilber Y, *et al.* Plasma from a case of recurrent idiopathic FSGS perturbs non-muscle myosin IIA (MYH9 protein) in human podocytes. *Pediatr Nephrol* 2011;26(7):1071-1081

167. Doublier S, Musante L, Lupia E, *et al.* Direct effect of plasma permeability

- factors from patients with idiopathic FSGS on nephrin and podocin expression in human podocytes. *Int J Mol Med* 2005;16(1):49-58
168. Blasi F, Sidenius N. The urokinase receptor: focused cell surface proteolysis, cell adhesion and signaling. *FEBS Lett* 2010;584(9):1923-1930
169. Fujimoto K, Imura J, Atsumi H, *et al.* Clinical significance of serum and urinary soluble urokinase receptor (suPAR) in primary nephrotic syndrome and MPO-ANCA-associated glomerulonephritis in Japanese. *Clin Exp Nephrol* 2015;19(5):804-814
170. Spinale JM, Mariani LH, Kapoor S, *et al.* A reassessment of soluble urokinase-type plasminogen activator receptor in glomerular disease. *Kidney Int* 2015;87(3):564-574
171. Harita Y, Ishizuka K, Tanego A, *et al.* Decreased glomerular filtration as the primary factor of elevated circulating suPAR levels in focal segmental glomerulosclerosis. *Pediatr Nephrol* 2014;29(9):1553-1560
172. Verschueren P, Lensen F, Lerut E, *et al.* Benefit of anti-TNFalpha treatment for nephrotic syndrome in a patient with juvenile inflammatory bowel disease associated spondyloarthritis complicated with amyloidosis and glomerulonephritis. *Ann Rheum Dis* 2003;62(4):368-369
173. Raveh D, Shemesh O, Ashkenazi YJ, *et al.* Tumor necrosis factor-alpha blocking agent as a treatment for nephrotic syndrome. *Pediatr Nephrol* 2004;19(11):1281-1284
174. Bustos C, Gonzalez E, Muley R, *et al.* Increase of tumour necrosis factor alpha synthesis and gene expression in peripheral blood mononuclear cells of children with idiopathic nephrotic syndrome. *Eur J Clin Invest* 1994;24(12):799-805
175. Drewe E, McDermott EM, Powell RJ. Treatment of the nephrotic syndrome with etanercept in patients with the tumor necrosis factor receptor-associated periodic syndrome. *N Engl J Med* 2000;343(14):1044-1045
176. Bertani T, Abbate M, Zoja C, *et al.* Tumor necrosis factor induces glomerular damage in the rabbit. *Am J Pathol* 1989;134(2):419-430
177. Koyama A, Fujisaki M, Kobayashi M, *et al.* A glomerular permeability factor produced by human T cell hybridomas. *Kidney Int* 1991;40(3):453-460
178. Diamond JR, Karnovsky MJ. Focal and segmental glomerulosclerosis following a

- single intravenous dose of puromycin aminonucleoside. *Am J Pathol* 1986;122(3):481-487
179. Mampaso FM, Egido J, Martinez-Montero JC, *et al.* Interstitial mononuclear cell infiltrates in experimental nephrosis: effect of PAF antagonist. *Nephrol Dial Transplant* 1989;4(12):1037-1044
180. Jemal I, Soriano S, Conte AL, *et al.* G protein-coupled receptor signalling potentiates the osmo-mechanical activation of TRPC5 channels. *Pflugers Arch* 2014;466(8):1635-1646
181. Shen B, Wong CO, Lau OC, *et al.* Plasma membrane mechanical stress activates TRPC5 channels. *PLoS One* 2015;10(4):e0122227
182. Wei C, Moller CC, Altintas MM, *et al.* Modification of kidney barrier function by the urokinase receptor. *Nat Med* 2008;14(1):55-63
183. Mas-Moruno C, Rechenmacher F, Kessler H. Cilengitide: the first anti-angiogenic small molecule drug candidate design, synthesis and clinical evaluation. *Anticancer Agents Med Chem* 2010;10(10):753-768
184. Schordan S, Schordan E, Endlich K, *et al.* AlphaV-integrins mediate the mechanoprotective action of osteopontin in podocytes. *Am J Physiol Renal Physiol* 2011;300(1):F119-132
185. Brenner BM, Troy JL, Daugharty TM. The dynamics of glomerular ultrafiltration in the rat. *J Clin Invest* 1971;50(8):1776-1780
186. Sachs N, Sonnenberg A. Cell-matrix adhesion of podocytes in physiology and disease. *Nat Rev Nephrol* 2013;9(4):200-210
187. Salmon AH, Toma I, Sipos A, *et al.* Evidence for restriction of fluid and solute movement across the glomerular capillary wall by the subpodocyte space. *Am J Physiol Renal Physiol* 2007;293(6):F1777-1786
188. DeCaen PG, Delling M, Vien TN, *et al.* Direct recording and molecular identification of the calcium channel of primary cilia. *Nature* 2013;504(7479):315-318
189. Schwartz F, Duka A, Triantafyllidi E, *et al.* Serial analysis of gene expression in mouse kidney following angiotensin II administration. *Physiol Genomics* 2003;16(1):90-98

190. McCarthy ET, Sharma R, Sharma M, *et al.* TNF-alpha increases albumin permeability of isolated rat glomeruli through the generation of superoxide. *J Am Soc Nephrol* 1998;9(3):433-438
191. Alachkar N, Wei C, Arend LJ, *et al.* Podocyte effacement closely links to suPAR levels at time of posttransplantation focal segmental glomerulosclerosis occurrence and improves with therapy. *Transplantation* 2013;96(7):649-656
192. Bock ME, Price HE, Gallon L, *et al.* Serum soluble urokinase-type plasminogen activator receptor levels and idiopathic FSGS in children: a single-center report. *Clin J Am Soc Nephrol* 2013;8(8):1304-1311
193. Meijers B, Poesen R, Claes K, *et al.* Soluble urokinase receptor is a biomarker of cardiovascular disease in chronic kidney disease. *Kidney Int* 2015;87(1):210-216
194. Hayek SS, Sever S, Ko YA, *et al.* Soluble Urokinase Receptor and Chronic Kidney Disease. *N Engl J Med* 2015;373(20):1916-1925
195. Schlondorff D. Are serum suPAR determinations by current ELISA methodology reliable diagnostic biomarkers for FSGS? *Kidney Int* 2014;85(3):499-501
196. Trachtman H, Reiser J. suPAR is the circulating factor in some but not all FSGS. *Nat Rev Nephrol* 2014;10(10):610
197. Nip J, Rabbani SA, Shibata HR, *et al.* Coordinated expression of the vitronectin receptor and the urokinase-type plasminogen activator receptor in metastatic melanoma cells. *J Clin Invest* 1995;95(5):2096-2103
198. Tarui T, Mazar AP, Cines DB, *et al.* Urokinase-type plasminogen activator receptor (CD87) is a ligand for integrins and mediates cell-cell interaction. *J Biol Chem* 2001;276(6):3983-3990
199. Savin VJ, Sharma M, Zhou J, *et al.* Renal and Hematological Effects of CLCF-1, a B-Cell-Stimulating Cytokine of the IL-6 Family. *J Immunol Res* 2015;2015:714964
200. Sharma M, Zhou J, Gauchat JF, *et al.* Janus kinase 2/signal transducer and activator of transcription 3 inhibitors attenuate the effect of cardiotrophin-like cytokine factor 1 and human focal segmental glomerulosclerosis serum on glomerular filtration barrier. *Transl Res* 2015;166(4):384-398
201. Enocsson H, Wettero J, Skogh T, *et al.* Soluble urokinase plasminogen activator

- receptor levels reflect organ damage in systemic lupus erythematosus. *Transl Res* 2013;162(5):287-296
202. Musetti C, Quaglia M, Cena T, *et al.* Circulating suPAR levels are affected by glomerular filtration rate and proteinuria in primary and secondary glomerulonephritis. *J Nephrol* 2015;28(3):299-305
203. Nijenhuis T, Sloan AJ, Hoenderop JGJ, *et al.* Angiotensin II Contributes to Podocyte Injury by Increasing TRPC6 Expression via an NFAT-Mediated Positive Feedback Signaling Pathway. *The American Journal of Pathology* 2011;179(4):1719-1732
204. Streuli CH, Akhtar N. Signal co-operation between integrins and other receptor systems. *Biochem J* 2009;418(3):491-506
205. Bouaouina M, Blouin E, Halbwachs-Mecarelli L, *et al.* TNF-induced beta2 integrin activation involves Src kinases and a redox-regulated activation of p38 MAPK. *J Immunol* 2004;173(2):1313-1320
206. Holstein-Rathlou NH, Marsh DJ. A dynamic model of renal blood flow autoregulation. *Bull Math Biol* 1994;56(3):411-429
207. Muller-Deile J, Schiffer M. The podocyte power-plant disaster and its contribution to glomerulopathy. *Front Endocrinol (Lausanne)* 2014;5:209
208. Pezzolesi MG, Poznik GD, Mychaleckyj JC, *et al.* Genome-wide association scan for diabetic nephropathy susceptibility genes in type 1 diabetes. *Diabetes* 2009;58(6):1403-1410
209. Johnson SA, Spurney RF. Twenty years after ACEIs and ARBs: emerging treatment strategies for diabetic nephropathy. *Am J Physiol Renal Physiol* 2015;309(10):F807-820
210. Ruggenti P, Cravedi P, Remuzzi G. Mechanisms and treatment of CKD. *J Am Soc Nephrol* 2012;23(12):1917-1928
211. Jahr CE, Stevens CF. Calcium permeability of the N-methyl-D-aspartate receptor channel in hippocampal neurons in culture. *Proc Natl Acad Sci U S A* 1993;90(24):11573-11577
212. Mayer ML, Westbrook GL. Permeation and block of N-methyl-D-aspartic acid

- receptor channels by divalent cations in mouse cultured central neurones. *J Physiol* 1987;394:501-527
213. Paoletti P, Bellone C, Zhou Q. NMDA receptor subunit diversity: impact on receptor properties, synaptic plasticity and disease. *Nat Rev Neurosci* 2013;14(6):383-400
214. Rastaldi MP, Armelloni S, Berra S, *et al.* Glomerular podocytes contain neuron-like functional synaptic vesicles. *Faseb j* 2006;20(7):976-978
215. Anderson M, Suh JM, Kim EY, *et al.* Functional NMDA receptors with atypical properties are expressed in podocytes. *Am J Physiol Cell Physiol* 2011;300(1):C22-32
216. Dryer SE. Glutamate receptors in the kidney. *Nephrology Dialysis Transplantation* 2015
217. Deng A, Thomson SC. Renal NMDA receptors independently stimulate proximal reabsorption and glomerular filtration. *Am J Physiol Renal Physiol* 2009;296(5):F976-982
218. Sproul A, Steele SL, Thai TL, *et al.* N-methyl-D-aspartate receptor subunit NR3a expression and function in principal cells of the collecting duct. *Am J Physiol Renal Physiol* 2011;301(1):F44-54
219. Lau A, Tymianski M. Glutamate receptors, neurotoxicity and neurodegeneration. *Pflugers Arch* 2010;460(2):525-542
220. Zhang C, Yi F, Xia M, *et al.* NMDA receptor-mediated activation of NADPH oxidase and glomerulosclerosis in hyperhomocysteinemic rats. *Antioxid Redox Signal* 2010;13(7):975-986
221. Zhang C, Hu JJ, Xia M, *et al.* Protection of podocytes from hyperhomocysteinemia-induced injury by deletion of the gp91phox gene. *Free Radic Biol Med* 2010;48(8):1109-1117
222. Kundu S, Pushpakumar SB, Tyagi A, *et al.* Hydrogen sulfide deficiency and diabetic renal remodeling: role of matrix metalloproteinase-9. *American Journal of Physiology - Endocrinology and Metabolism* 2013;304(12):E1365-E1378
223. Hoogeveen EK, Kostense PJ, Jager A, *et al.* Serum homocysteine level and protein intake are related to risk of microalbuminuria: the Hoorn Study. *Kidney Int* 1998;54(1):203-209

224. Jager A, Kostense PJ, Nijpels G, *et al.* Serum homocysteine levels are associated with the development of (micro)albuminuria: the Hoorn study. *Arterioscler Thromb Vasc Biol* 2001;21(1):74-81
225. Cho EH, Kim EH, Kim WG, *et al.* Homocysteine as a risk factor for development of microalbuminuria in type 2 diabetes. *Korean Diabetes J* 2010;34(3):200-206
226. Ukinc K, Ersoz HO, Karahan C, *et al.* Methyltetrahydrofolate reductase C677T gene mutation and hyperhomocysteinemia as a novel risk factor for diabetic nephropathy. *Endocrine* 2009;36(2):255-261
227. Feng Y, Shan MQ, Bo L, *et al.* Association of homocysteine with type 1 diabetes mellitus: a meta-analysis. *Int J Clin Exp Med* 2015;8(8):12529-12538
228. Mtiraoui N, Ezzidi I, Chaieb M, *et al.* MTHFR C677T and A1298C gene polymorphisms and hyperhomocysteinemia as risk factors of diabetic nephropathy in type 2 diabetes patients. *Diabetes Res Clin Pract* 2007;75(1):99-106
229. Lipton SA. Paradigm shift in NMDA receptor antagonist drug development: molecular mechanism of uncompetitive inhibition by memantine in the treatment of Alzheimer's disease and other neurologic disorders. *J Alzheimers Dis* 2004;6(6 Suppl):S61-74
230. Reisberg B, Doody R, Stoffler A, *et al.* A 24-week open-label extension study of memantine in moderate to severe Alzheimer disease. *Arch Neurol* 2006;63(1):49-54
231. Peskind ER, Potkin SG, Pomara N, *et al.* Memantine treatment in mild to moderate Alzheimer disease: a 24-week randomized, controlled trial. *Am J Geriatr Psychiatry* 2006;14(8):704-715
232. Tariot PN, Farlow MR, Grossberg GT, *et al.* Memantine treatment in patients with moderate to severe Alzheimer disease already receiving donepezil: a randomized controlled trial. *Jama* 2004;291(3):317-324
233. Kim EY, Suh JM, Chiu YH, *et al.* Regulation of podocyte BK(Ca) channels by synaptopodin, Rho, and actin microfilaments. *Am J Physiol Renal Physiol* 2010;299(3):F594-604
234. Kim EY, Choi K-J, Dryer SE. Nephrin binds to the COOH terminus of a large-conductance Ca<sup>2+</sup>-activated K<sup>+</sup> channel isoform and regulates its expression on the cell

- surface. *American Journal of Physiology - Renal Physiology* 2008;295(1):F235-F246
235. Gurley SB, Mach CL, Stegbauer J, *et al.* *Influence of genetic background on albuminuria and kidney injury in Ins2+/C96Y (Akita) mice*, Placed Published: 2010.
236. Jager A, Kostense PJ, Nijpels G, *et al.* Serum Homocysteine Levels Are Associated With the Development of (Micro)albuminuria: The Hoorn Study. *Arteriosclerosis, Thrombosis, and Vascular Biology* 2001;21(1):74-81
237. Oxenkrug GF. Metabolic syndrome, age-associated neuroendocrine disorders, and dysregulation of tryptophan-kynurenine metabolism. *Ann N Y Acad Sci* 2010;1199:1-14
238. Favennec M, Hennart B, Caiazzo R, *et al.* The kynurenine pathway is activated in human obesity and shifted toward kynurenine monooxygenase activation. *Obesity (Silver Spring)* 2015;23(10):2066-2074
239. D'Hooge R, Raes A, Lebrun P, *et al.* N-methyl-D-aspartate receptor activation by guanidinosuccinate but not by methylguanidine: behavioural and electrophysiological evidence. *Neuropharmacology* 1996;35(4):433-440
240. Levi A, Cohen E, Levi M, *et al.* Elevated serum homocysteine is a predictor of accelerated decline in renal function and chronic kidney disease: A historical prospective study. *Eur J Intern Med* 2014;25(10):951-955
241. Chen HS, Lipton SA. The chemical biology of clinically tolerated NMDA receptor antagonists. *J Neurochem* 2006;97(6):1611-1626
242. Blantz RC, Singh P. Glomerular and tubular function in the diabetic kidney. *Adv Chronic Kidney Dis* 2014;21(3):297-303
243. Vallon V. The proximal tubule in the pathophysiology of the diabetic kidney. *American Journal of Physiology - Regulatory, Integrative and Comparative Physiology* 2011;300(5):R1009-R1022
244. Park P, Volianskis A, Sanderson TM, *et al.* NMDA receptor-dependent long-term potentiation comprises a family of temporally overlapping forms of synaptic plasticity that are induced by different patterns of stimulation. *Philos Trans R Soc Lond B Biol Sci* 2014;369(1633):20130131
245. Hardingham GE, Bading H. Synaptic versus extrasynaptic NMDA receptor signalling: implications for neurodegenerative disorders. *Nat Rev Neurosci* 2010;11(10):682-696

246. Bassil N, Thaipisuttikul P, Grossberg GT. Memantine ER, a once-daily formulation for the treatment of Alzheimer's disease. *Expert Opin Pharmacother* 2010;11(10):1765-1771
247. Marquard J, Otter S, Welters A, *et al.* Characterization of pancreatic NMDA receptors as possible drug targets for diabetes treatment. 2015;21(4):363-372
248. Marquard J, Stirban A, Schliess F, *et al.* Effects of dextromethorphan as add-on to sitagliptin on blood glucose and serum insulin concentrations in individuals with type 2 diabetes mellitus: a randomized, placebo-controlled, double-blinded, multiple crossover, single-dose clinical trial. *Diabetes Obes Metab* 2016;18(1):100-103
249. Jansen M, Dannhardt G. Antagonists and agonists at the glycine site of the NMDA receptor for therapeutic interventions. *Eur J Med Chem* 2003;38(7-8):661-670